



# ALISO CANYON NATURAL GAS DISASTER Air Quality Monitoring and Modeling

TECHNICAL REPORT:  
Exposure Modeling, Ambient Monitoring and  
Identification of Fugitive Emissions

October 30, 2018

Prepared by GIS HEAL Labs for Los Angeles County Department of Public Health

# CONTENTS

CONTENTS .....	2
Contributors .....	4
Acknowledgments .....	4
Executive Summary .....	5
<b>Data .....</b>	<b>5</b>
<b>Analysis of blowout data collected with SNAQ monitors .....</b>	<b>6</b>
<b>Air model development for the Aliso Canyon disaster .....</b>	<b>6</b>
<b>Ultra-fine-particle and PM<sub>2.5</sub> measurements .....</b>	<b>6</b>
<b>Pre-injection monitoring .....</b>	<b>7</b>
Section I. Introduction .....	10
Section II. Data .....	11
<b>Air Monitoring During the Aliso Canyon Disaster .....</b>	<b>11</b>
<b>Air Monitoring After the Aliso Canyon Disaster .....</b>	<b>11</b>
<b>Meteorological Data .....</b>	<b>12</b>
SECTION III. Analysis of air quality data collected with SNAQ monitors .....	12
<b>Overview .....</b>	<b>12</b>
<b>Results.....</b>	<b>12</b>
SECTION IV. Develop methane air model for the Aliso Canyon natural gas disaster .....	13
<b>Overview .....</b>	<b>13</b>
<b>Model Inputs .....</b>	<b>14</b>
<b>Model results.....</b>	<b>15</b>
SECTION V. Ultra-fine-particle and PM <sub>2.5</sub> measurements .....	17
<b>Ultrafine particles .....</b>	<b>17</b>
<b>Particle measurements and measurement sites .....</b>	<b>17</b>
<b>Wind Direction.....</b>	<b>18</b>
<b>Ultrafine PM concentrations and their relationships with wind direction.....</b>	<b>18</b>
<b>Discussion.....</b>	<b>21</b>
SECTION VI. Pre-injection monitoring.....	21
<b>Monitoring Techniques .....</b>	<b>21</b>
<b>Methods .....</b>	<b>22</b>
<b>Monitoring Results.....</b>	<b>23</b>
SECTION VII. Ancillary analyses and source identification .....	23
<b>Particle Data .....</b>	<b>23</b>
<b>Spectral analysis of particle data .....</b>	<b>24</b>
<b>SCAQMD Trigger Samples.....</b>	<b>25</b>
<b>Ancillary analysis of methane from Argos Scientific.....</b>	<b>25</b>
SECTION VIII. Summary of findings .....	28
<b>Analysis of blowout data collected with SNAQ boxes during Aliso Canyon disaster .....</b>	<b>28</b>
<b>Air model development for the Aliso Canyon disaster .....</b>	<b>28</b>

<b>Ultra-fine-particle and PM<sub>2.5</sub> measurements (after blowout/prior to reinjection)</b> .....	<b>29</b>
<b>Pre-injection monitoring (after blowout/prior to reinjection)</b> .....	<b>29</b>
<b>Ancillary analyses and source identification (after blowout/prior to reinjection)</b> .....	<b>29</b>
REFERENCES .....	31
APPENDIX A. Tables and Figures.....	33
Table 1. Measurement periods, locations, general observations and peak events .....	34
Table 2. Summary of monitoring methods used for collection of air quality between 09/06/16 – 06/13/16.....	35
Table 3. Results of VOC, ammonia, and formaldehyde monitoring Sept 6-13, 2016.....	36
Table 3 (cont). Results of VOC, ammonia, and formaldehyde monitoring Sept 6-13, 2016. ....	37
Table 4. Correlation table of detected compounds during pre-injection monitoring .....	38
Table 5: Summa Canister trigger samples of selected VOCs collected after the well was sealed (Table 5 continues on next page ;see note below§) .....	39

## Contributors

Bernard Beckerman, *GIS HEAL Labs*

Michael Jerrett, *GIS HEAL Labs, University of California at Los Angeles and Berkeley*

Diane Garcia-Gonzales, *GIS HEAL Labs*

Suzanne Paulson, *University of California at Los Angeles*

Dilhara Rangasinghe, *University of California at Los Angeles*

David Carruthers, *Cambridge Environmental Research Consultants, UK*

Chetan Lad, *Cambridge Environmental Research Consultants, UK*

Roderic Jones, *University of Cambridge, UK*

Olalekan Popoola, *University of Cambridge, UK*

## Acknowledgments

The research team is grateful to the community members who hosted the air monitoring equipment to make this project possible. This project was supported by administrative and technical resources from the Toxicology and Environmental Assessment Branch of the Environmental Health Division in the Los Angeles County Department of Public Health.

## Executive Summary

Related to the aftermath of the blowout at Well Standard Sesnon 25 (SS-25) in the Aliso Canyon Natural Gas Storage Facility on October 23, 2015, the Los Angeles Department of Public Health (DPH) led additional environmental monitoring efforts and analyses. DPH tasked Geographical Information Systems Health Exposure Analysis Laboratories (GIS HEAL Labs) and its academic partners to conduct these analyses with three main objectives:

1. Develop an air dispersion model to support future study of exposures and related health impacts that occurred during the blowout at Well SS-25; and
2. Collect data for future comparative analyses on ambient background levels of airborne particulates (also referred to as particulate matter) and organic compounds (also referred to as air toxics) when the natural gas field was not in operation; and
3. Identify whether the nearby community may be impacted by hazardous airborne exposures from the oil and gas industry that are not attributable to normal operations (e.g. residual off-gassing, abandoned wells).

This work was motivated by air quality monitoring results collected both during and after the blowout. Specifically, the motivation came from air monitors deployed during the blowout by University of California at Los Angeles (UCLA) researchers, Argos Scientific (a non-governmental organization), and Southern California Air Quality Monitoring District (SCAQMD)/ California Air Resource Board (CARB). These monitors showed transient elevations in concentrations of air toxics including benzene, airborne particles, and methane when winds were arriving from the north, which was the direction of Well SS-25 and associated operations. In some instances, these elevations were compared to control sites that were not in the downwind direction, with control sites generally showing lower levels or different temporal patterns in the ambient concentrations.

During the time when the facility was not withdrawing or injecting natural gas and after Well SS-25 was permanently plugged with cement, air monitoring results also indicated similar elevated concentrations when winds were coming from the north. Concerns were compounded by reports of suspected residual off-gassing from the ground and into the atmosphere; as well as the presence of buried and plugged or abandoned oil wells in and around the Porter Ranch community (data available at [www.conservation.ca.gov/dog](http://www.conservation.ca.gov/dog)). The concerns from these wells were that they produced uncharacterized fugitive emissions that may impact the community and, thus, merited further investigation.

## Data

During the active blowout, as Well SS-25 was releasing methane, air monitoring data were collected from both government agency monitors, and an additional network of monitors placed by GIS HEAL Labs, researchers at UCLA, and by Argos Scientific ([www.argos-sci.com](http://www.argos-sci.com)). After Well SS-25 was permanently plugged on February 18, 2016, monitoring of the community continued. Agency monitors continued to operate, researchers at UCLA continued their

independent monitoring efforts, and the Argos Scientific monitor continued to gather data. In addition, between September 6 and 13, 2016, DPH began a supplemental monitoring campaign was conducted in the Porter Ranch community. During this monitoring period, the following air toxics were assessed at nine locations throughout the Porter Ranch community: 77 volatile organic compounds (VOCs), formaldehyde, and ammonia.

### **Analysis of data collected with SNAQ and Argos Scientific monitors during the blowout**

During the blowout, UCLA researchers used Sensor Networks for Air Quality (SNAQ) monitors to collect gaseous air quality data (carbon monoxide, nitrogen oxide, total volatile organic compounds and carbon dioxide) at six locations. Large fluctuations in contaminant gas concentration were observed over the period. Analysis of the data collected with the SNAQ monitors, when compared to agency methane monitors, suggest that the monitors were characterizing air quality levels consistent with levels attributable to the blowout. Shortly after the well was plugged, a continued analysis of the Argos Scientific methane data suggested that there were continued, albeit lesser, methane sources to the north, northeast, south and east.

### **Air model development for the Aliso Canyon disaster data collected during the blowout**

In support of future studies aimed at assessing the health impacts of the Aliso Canyon gas blowout on the Porter Ranch and nearby communities, researchers tested the utility of using the Atmospheric Dispersion Modeling Systems (ADMS) modeling software to estimate likely air pollution dispersion. The modeling was conducted over the period January 14, 2016 to February 12, 2016 using hourly methane measurements from eight agency monitoring sites across Porter Ranch. Good correlation was observed between the modeled data and observed methane levels. This effort suggests that the model parameters developed by researchers regarding the source release and dispersive process were correctly attributed to the Well SS-25 blowout. Further work would need to focus on expanding the modeling to cover the entire period of the blowout and integrate known, or estimated, emission rates at the SS-25 wellhead.

### **Ultra-fine-particle and PM<sub>2.5</sub> measurements post blowout (pre-injection)**

Between March 2016 and February 2017, post blowout and prior to re-injection of the natural gas storage field, UCLA researchers measured ultrafine particulate (UFP) number concentration (with aerodynamic diameter of 100 nanometers or less) and average particle size, as well as some measurements of PM<sub>2.5</sub> (particulate matter with an aerodynamic diameter less than or equal to 2.5 microns) number concentrations. Concentrations of UFP in the Porter Ranch neighborhoods were within the ranges commonly observed for urbanized areas of the Los Angeles area. UFP levels, however, displayed an unusual diurnal pattern, peaking in the afternoon rather than the morning when the atmosphere is more stable. The reasons for this are not known but possible explanations include unknown local sources or photochemical reactions of gaseous pollutants that causes ultrafine particle formation.

UFP concentrations were highest when the winds were easterly and southerly. Winds from northerly directions brought considerably lower concentrations on average but had more peak events than when winds arrived from the east and south. In comparison to UFP, fewer

measurements of PM<sub>2.5</sub> were taken due to equipment availability. The highest concentrations were observed when winds came only from the southerly directions, but during sampling periods for which there were northerly and easterly winds (which were few), highest concentrations came from these directions.

### **Air toxic measurements post blowout (pre-injection monitoring)**

Monitoring was conducted while the storage field was not pressurized (post blow out and prior to re-injection) between September 6 – 13, 2016. Data collected during this period serves as a baseline for future analyses, when the storage facility is returned to normal operation. Samples were collected continuously over a 5-day period, between September 6 to September 11, 2016, to assess average concentrations of VOCs, formaldehyde, and ammonia in ambient air. Due to logistical reasons, two samples were collected two days after the earlier deployment (September 8 – 13, 2016). Results of the monitoring suggest levels of these organic compounds and ammonia are not at levels that pose a health risk above those generally experienced by the general population of California. The correlation analysis of the collected data does not appear to suggest sources that are notably correlated with methane: it is the preferred indicator of a source associated with the oil and gas here. Overall, the correlation patterns based on this short-term pre-injection monitoring do not assist in the identification of any specific fugitive sources.

Results from Summa Canisters trigger samples collected between March 4, 2016 and November 14, 2016 by SCAQMD are presented to expand on the pre-injection monitoring of VOCs. In general, most reported contaminants were below levels of health concern. In total, there were 21 of 40 samples that detected benzene; of these, the average benzene level was 2.2 ppb, which is above typical ambient background levels in Los Angeles. On only one occasion did the concentration exceed the reference level (REL) of 8 parts per billion (ppb), when a benzene concentration of 13 ppb was detected in July 2016. In nearly all cases, samples were triggered in the hours between 6:00 and 9:00 am or near midnight.

## **Ancillary analyses and source identification of emissions during the pre-injection period**

The ancillary analysis used particle count collected from UCLA and methane data collected at the Argos Scientific monitoring location post blowout and prior to re-injection (pre-injection). Particle count data used in this analysis were collected in early to mid-September 2016 at two locations, one in Porter Ranch Estates and the other in the Highlands neighborhood. The goal of the analysis of the particle data was to assess if regular events occur within a week period that produced elevations in particle count. When juxtaposed with meteorological conditions, the data suggest a possible—yet undefined—process to the north that may be causing these transient elevations ( $>1.5 \times 10^{-6} / \text{ft}^3$ ) in particle concentration. Elevations were happening during the evening and early morning. The reasons for this are not entirely clear. A formal analysis of the periodicity suggest that the particle data are not sufficiently regular to identify a regular repeated event. Given these results and the potential

confounding of observed particulate levels from combustion sources, methane was the most obvious contaminant associated with a gas and oil well field to be studied further.

Analyses of the methane data spanned the period June 1, 2016 through September 30, 2016. It was hypothesized that, if unique natural gas production based sources are responsible for elevated ambient contaminant levels, these would be identified through the outliers in the observed distribution of ambient methane (99<sup>th</sup> percentile and greater). Machine learning methods (Expectation-Maximization clustering algorithm) were used to identify factors/patterns associated with source locations. The analysis did not identify a specific source; but two patterns were identified: (1) In the evening to early morning, a fugitive emission source from the north contributes to elevated levels of methane; and (2) A source from the southeast to southwest elevates ambient levels of methane between 8:00 am and 10:00 am. The results provide evidence to corroborate the hypothesis that fugitive emissions, unrelated to regular operations, were reaching the community. It should be noted that these northerly emissions happened during late night/early morning, i.e., times when Summa Canister Trigger samples were collected. These results lend support to the hypothesis that the nearby community may have been impacted by fugitive emissions (post blowout and pre re-injection) from the north during overnight and early morning hours. In total, these findings along with continued symptom reports to DPH warrant further investigation and dedication of resources to long-term environmental and health monitoring in surrounding communities.

This page has been intentionally left blank

## Section I. Introduction

The Los Angeles County Department of Public Health (DPH) tasked Geographical Information Systems Health Exposure Analysis Laboratories (GIS HEAL Labs) with conducting several analyses to better understand exposures to airborne particulates and organic compounds occurring during and after the massive gas release (also referred to as ‘blowout’ or ‘natural gas disaster’) of Well Standard Sesnon (SS-25) at the Aliso Canyon Natural Gas Storage Facility. As part of these analyses, three tasks included:

1. Developing an air dispersion model to support future study of exposures and related health impacts that occurred during the blowout at Well SS-25 (see Section IV);
2. Collecting data for future comparative analyses on ambient background levels of airborne particulates (also referred to as particulate matter) and organic compounds (also referred to as air toxics) when the natural gas field was not in operation (see Section V, VI); and
3. Identifying whether the nearby community may be impacted by hazardous airborne exposures from the oil and gas industry that are not attributable to normal operations (e.g. residual off-gassing, abandoned wells; see Section VII).

This work was motivated by air quality monitoring results collected both during and after the blowout. Specifically, air monitors deployed during the blowout by University of California at Los Angeles (UCLA) researchers, Argos Scientific (a non-governmental organization), and Southern California Air Quality Monitoring District (SCAQMD)/ California Air Resource Board (CARB) showed brief elevations in concentrations of air toxics including benzene, particles, and methane when winds were arriving from the north, or from the direction of Well SS-25 and associated operations. During the time when the facility was not withdrawing or injecting natural gas and after Well SS-25 was permanently plugged with cement (henceforth referred to as the ‘pre-injection’ period), air monitoring results also indicated similar elevated concentrations when winds were coming from the north. Concerns were compounded by reports of suspected residual off-gassing from the ground and into the atmosphere; as well as the presence of buried and plugged or abandoned oil wells in and around the Porter Ranch community (data available at [www.conservation.ca.gov/dog](http://www.conservation.ca.gov/dog)) as shown in Figure 1. Historical wells across the nation have been known to contribute to ambient methane emissions (Brandt, et al., 2014). The concerns from these wells were that they produced uncharacterized fugitive emissions that may impact the community and, thus, merited further investigation.

In early May 2016 (three months after Well SS-25 was permanently sealed), DiSCmini particle monitors were deployed at residential locations in two housing developments closest to the Aliso Canyon Natural Gas Storage Facility, namely Porter Ranch Estates and the Highlands

Estates. These types of monitors can measure very small (ultrafine and small accumulation mode) particles (less than 0.1  $\mu\text{m}$  in aerodynamic diameter). These results suggest particle concentrations within the Porter Ranch community were generally low, with infrequent “high” elevations in particle concentrations ( $\sim 100,000$  particles/ $\text{cm}^3$ ) occurring every several days. These episodic particle monitoring elevations lasted 15-40 minutes, occurring when the wind came from the northeast to northwest during the mid-to-late evening hours. In combination with data collected during the Aliso Canyon gas disaster of elevated particle readings, and data collected after the gas disaster showing methane levels periodically spike for short periods (10-45 minutes) above background levels at several locations in the community, these findings merited further investigation.

## Section II. Data

### Air Monitoring During the Aliso Canyon Gas Disaster

Throughout the approximately four months that Well SS-25 leaked methane and other air toxic emissions, air monitoring data were collected from air monitors set up by several interested stakeholders including government agencies, GIS HEAL Labs and researchers at the UCLA, and Argos Scientific ([www.argos-sci.com](http://www.argos-sci.com)). CARB and SCAQMD agencies evaluated air emissions from eight air monitoring sites in the Porter Ranch community (**Figure 2**). GIS HEAL Labs and UCLA researchers installed six SNAQ monitors during the gas disaster in the Porter Ranch community and at sites immediately adjacent to it (**Figure 3**). Argos Scientific placed an air monitor in the Highland Estates to collect methane data during and after the gas disaster from late January 2016 to present (as of October 2018).

### Air Monitoring After the Aliso Canyon Disaster

Air monitoring continued after Well SS-25 was permanently plugged on February 18, 2016 and the Aliso Canyon Storage Facility was not injecting or withdrawing natural gas (the ‘pre-injection’ period) by all groups, including CARB and AQMD agencies, GIS HEAL Labs, and Argos Scientific. Five of eight CARB/SCAQMD monitoring sites {Site: 1, 2, 5, 7, 8} were taken out of operation in late July 2016 after several months of methane level readings consistent with typical ambient air for the region. DPH worked with GIS HEAL Labs on air monitoring at nine locations throughout the Porter Ranch community over 5 days during a seven-day period (September 6-13, 2017) for having detailed air toxics data that could be used to compare with ambient air quality data in the future when the field resumed operations and increased storage capacity. GIS HEAL Labs collected data on 77 different volatile organic compounds (VOCs), as well as formaldehyde and ammonia (see Table 3 for full list). Argos Scientific also continued to operate a continuous methane monitor in the Highland Estates community.

## Meteorological Data

Meteorological data was collected from two locations. For modeling analyses conducted during the period of the Aliso Canyon gas disaster, meteorology was collected from ARB site #5 and from a citizen science station, DW4339 Porter Ranch Station (CA) located at latitude: 34.29735, longitude: -118.54529. During the period of monitoring after the gas disaster, meteorological data was obtained from instrumentation co-located with the methane monitor run by Argos Scientific. As an additional meteorological data source and as a means of data assurance, data were also collected from a citizen science crowd-sourcing weather website, [www.wunderground.com](http://www.wunderground.com) from station KCANORTH13 in the northern part of the Porter Ranch community. Data from KCANORTH13 were like data collected from other sites. The meteorological locations yielding primary data collection, namely wind speed and wind direction, were used for the analyses described in this technical report.

## SECTION III. Analysis of air quality data collected during the active blowout

### Overview

This section summarizes work related to the network deployment of portable SNAQ air quality sensors in Porter Ranch, California from January 15, 2016 through February 20, 2016. The SNAQ monitor is a small portable air quality monitor that collects a variety of air contaminants. The monitors were powered by a conventional 120V supply and data was logged on internal memory via USB. In this report, results are presented for particulate matter (PM), carbon monoxide (CO), carbon dioxide (CO<sub>2</sub>), nitrogen oxide (NO), total VOCs (TVOC), and particulate size species (PM<sub>1.0</sub>, PM<sub>2.5</sub> and PM<sub>10</sub>).<sup>1</sup> In addition, the data collected by the SNAQ monitors are presented with co-temporal methane and local meteorological data as a comparative tool to understand the observed results.

### Results

Data collected with the SNAQ monitors are presented in **Figure 4** for gas concentrations (CO, NO, TVOCs or CO<sub>2</sub>) and are presented in **Figure 5** for PM concentrations. Large fluctuations in all gas concentrations and PM concentrations were observed over the period (**Figures 4 and 5**). There appears to be periodic, short-time scale (few minutes) spikes in

---

<sup>1</sup> PM<sub>1.0</sub> is particulate matter with an aerodynamic diameter of up to 1.0 µm. PM<sub>2.5</sub> is particulate matter with an aerodynamic diameter of up to 2.5 µm, referred to as the fine particle fraction (which per definition includes PM<sub>1.0</sub>). PM<sub>10</sub> is particulate matter with an aerodynamic diameter of up to 10 µm, referred to as coarse particles (which per definition includes PM<sub>1.0</sub> and PM<sub>2.5</sub>).

concentrations of PM, CO, and TVOC, while CO<sub>2</sub> and NO show longer time scale increases in concentrations. The elevated PM concentrations observed on January 20, 29 and 30 along with stable atmospheric conditions provide evidence that this was a build-up of pollution during this time. This kind of build-up of pollution is also reflected in some of the gas measurements, notably CO concentrations (**Figure 4**).

Methane (CH<sub>4</sub>) data from SCAQMD Site #4 (**Figure 2**) in proximity of one of the SNAQ monitors (SNAQ14 [**Figure 3**]) shows evidence of the ongoing blowout in the sharp peaks of elevated methane up to 65 ppmV occurring during January 27, 2016 and February 11, 2016 (**Figure 6**). The sharp decline in methane concentrations after February 11, 2016 denotes the plugging of Well SS-25 with mud, with confirmation of permanent plugging with cement from the state regulatory agency declared on February 18, 2016 (shaded in gray on **Figure 6**). Polar bivariate plots indicate wind speed and wind direction as Well SS-25 was leaking (**Figure 7a**) and after Well SS-25 was plugged (**Figure 7b**). The periodically high methane readings (> 10 ppmv) observed in the top panel of **Figure 6** combined with wind data from the polar bivariate plot (**Figure 7a**) revealed that the methane elevated concentrations were coming from the northwest, which is consistent with the direction of Well SS-25 to the air monitoring site SNAQ14. After Well SS-25 was plugged, there were periodic elevations in methane concentrations but at much lower concentrations than observed during the blowout of approximately 3 to 6 ppmV (**Figure 6**) source attribution analysis using the polar bivariate plot (**Figure 7b**) of methane data collected after the well was plugged shows that there are potentially multiple sources for these smaller elevations of methane coming from several different wind directions including the north, northeast, south and east.

## SECTION IV. Develop methane air model for the Aliso Canyon natural gas disaster

### Overview

Researchers developed a model to estimate methane exposure during the Aliso Canyon natural gas blowout that could be used to predict methane concentrations at locations in the Porter Ranch community where monitoring data had not been collected. This modeling framework could be applied to predict what people could have potentially been exposed to during the active blowout and used for future health effects assessments. The model was developed for the period January 14, 2016 to February 12, 2016. This period likely underestimates the extreme range in methane exposure during the entire period of the natural gas blowout that began on October 23, 2015 since the model timeframe did not include

November 2015, when methane concentrations were at their highest. Data collected prior to January 14, 2016 was not usable for this kind of validation modeling study.

Hourly methane measurements from eight SCAQMD/CARB air monitoring sites throughout the Porter Ranch community were compared to an exposure model produced by the Atmospheric Dispersion Modeling Systems version 5.2 (ADMS). The ADMS model was chosen because it includes the ability to use high-resolution modeled airflow over complex terrain. For this study area, this is essential, as there is a significant amount of complex topography at the base of mountain terrain. **Figure 8** shows the locations of the SCAQMD/CARB air monitoring sites and the location of Well SS-25 located approximately 2 to 3 km to the north of those sites in hilly terrain. Note that **Figure 8** shows the same locations as **Figure 2** with the addition of site-numbers designated by the CARB.

### Model Inputs

The Well SS-25 location was modeled as a ground-level point source with a 1 meter diameter and modeled as an ambient passive release. Terrain height inputs to the model were derived from the Shuttle Radar Topography Mission 1-arc second [SRTM30] dataset (Becker et al., 2009), from which 60 meter resolution height data were generated for the 15 kilometer x 15 kilometer domain shown in **Figure 9**. Hourly averaged wind speed, wind direction and temperature from meteorological station DW4339 in Porter Ranch.<sup>2</sup> A wind rose of modeled wind speeds and directions is also shown in **Figure 9**. In the absence of cloud cover data, a value 3 oktas (1/4 coverage or scattered clouds) was used for all hours; the use of a fixed value is expected to lead to underestimates in the variation in atmospheric stability. A surface roughness of 0.5 meters was assumed for the modeling domain along with a site latitude of 34.3°. For the model runs we have assumed a nominal constant emission rate of 1 grams per second (g/s) at the Well SS-25 site, since the rate of emission is unknown, and no other sources of emissions are considered. Thus, if the model is performing well, and if Well SS-25 is the dominant source, we would expect to see reasonable correlation between the model and measurements but would not expect the modeled values to reflect actual concentration values. As only a unit emission rate was used (1 g/s) when the actual emission rate was much larger, but unknown, the modeled values will reflect the relative variability of the pollutant concentration, but not its actual value. To derive actual values, the actual or estimated emission rate would need to be known.

**Figure 10** shows time series of measured methane concentrations at eight SCAQMD/CARB air monitoring locations from January 14, 2016 (the start date of the meteorological data from the methane monitoring site numbered 5436) until February 11, 2016

---

<sup>2</sup> DW4339 Porter Ranch Station (CA) at latitude: 34.29735, longitude: -118.54529. Data available for download at: [http://mesowest.utah.edu]

inclusive (when the monitoring indicates the plugging of the well).<sup>3</sup> The time series plot shows the intermittent nature of the traces are consistent with varying emissions and meteorological conditions (wind speed, wind direction and stability). The air monitoring sites 5435, 5436 and 5433 show the largest impact consistent with the prevailing wind direction from Well SS-25 during the period.

## Model results

**Figures 11 and 12** show polar bivariate plots where methane time series are shown as functions of wind speed and wind direction for measured and modeled methane concentrations across the eight locations for the study period. The model produces results that are comparable to measurements at those sites, particularly for sites 5435 and 5436 located closest to Well SS-25; these findings support that the main source of methane observed at those sites comes from the Well SS-25 blowout.

Time series and polar bivariate plots were plotted by atmospheric stability for monitoring sites 5436, 5435 and 5433 (**Figures 13, 14, and 15**, respectively), to further illuminate the relationship between the measured methane concentrations, modeled concentrations, and the meteorological conditions. The polar bivariate plots in the bottom-right quadrants show that both the measured and modeled methane concentrations are higher during stable night time meteorological conditions for all three sites. The modeled methane concentrations appear to capture the measured methane concentration peaks in the polar bivariate plots, especially at sites 5436 and 5435 located closest to Well SS-25. However, the time series plots of modeled methane concentrations over time do not appear to align closely with the measured concentrations over time, which may indicate a variable release rate for methane over the monitoring period. **Figures 16 and 17** are time series plots comparing measured methane concentration to modeled concentrations for the time periods Jan. 27-29, 2016 and Feb. 9-11, 2016, respectively. These were time-periods when methane concentrations were elevated at the three identified sites (5436, 5435, 5433). These figures show that the modeled methane concentrations (shown in red bars) do not coincide well with the measured methane concentrations (shown in blue bars) even during times when measured methane concentrations peak. This suggests more site-specific data may be necessary to model some of the observed variability in ambient methane levels.

One limitation of the presented ADMS model is that the only available meteorological data within the study area (during the time of the blowout) was at site 5436, the site closest to Well SS-25. **Figure 18** shows a scatter plot of the ADMS model's input wind speed and the model's calculated wind speed at site 5436 to indicate the efficiency of the ADMS model. The

---

<sup>3</sup> State agencies confirmed permanent plugging of Well SS-25 on February 18, 2016.

difference between the model's input wind speed and the model's output wind speed provides an indication of the modeling efficacy. The most accurate model would show input and modeled wind speed data plotted the same way and overlapping ideally; however, **Figure 18** shows that the modeled wind speed is typically higher than the input wind speed. Additionally, there are also directional changes in wind (direction is indicated by the angle of the arrowed-shaped plot points), which suggest that the complex terrain is having a large impact on the wind flow at air monitoring site 5436. An example of how terrain affects the wind pattern can be seen in Appendix B (**Figure B1**). **Figure B1** represents the wind field flow for a single hour on February 11, 2016 using meteorological data collected at CARB/SCAQMD Air Monitoring Site #5 (**Figure 2**). During this hour, the observed deviations from straight-line wind flow indicate the tendency for the air mass flowing across the local terrain to drift to the east under northerly prevailing wind conditions.

In view of these discrepancies, the model was re-run with adjusting the upwind wind speeds using a systematic approach, so that modeled winds at air monitoring site 5436 corresponded more closely to the measured winds. This was achieved using an iterative approach to optimize the model inputs. **Figure 19** compares the modeled output wind speeds for the original and adjusted wind speeds run, against the measured wind speeds at 5436. The agreement between modeled and measured wind speeds is generally improved for the adjusted wind speeds. The polar bivariate plots based on the modeling estimates using the adjusted wind speeds (**Figure 20**) indicate better model performance based on better correlation with the measured methane data (**Figure 11**), specifically at sites 5435 and 5436. Further refinement of the model would require improving the meteorological inputs, such as including cloud cover information; detailed back-trajectory of wind flow; or the availability of suitable upwind meteorological measurements, along with detailed information about other sources of methane emissions in the area.

Results reported in this section suggest that modeling the methane emissions using the ADMS dispersion model is a viable option to address a retrospective exposure assessments of the Porter Ranch community, to emissions from the SS-25 Well blowout, for future health studies. The results of the modeling confirm that the assumptions regarding the source release, dispersion process, and meteorological conditions were reasonable with respect to the blowout. For future exposure reconstruction efforts, we will need to focus on expanding the predictive model to cover the entire period of the blowout and integrate measured (or estimated) methane emission rates at the SS-25 wellhead.

## SECTION V. Pre-injection monitoring of Ultra-fine-particle and PM<sub>2.5</sub> measurements

### Ultrafine particles

Ultrafine particles (UFP) are defined as particles smaller than or equal to 0.1 µm in diameter. UFP are emitted to the atmosphere primarily from combustion sources and as pollutant gases are oxidized and form lower volatility condensable products. Also, it is possible to generate UFP by evaporating larger particles, although this source is much less common. UFP have lifetimes of tens of minutes in the atmosphere, as they quickly collide with other particles and become incorporated into the gas phase. There are no regulatory standards for UFP, although there are numerous studies in the literature suggesting they may have unique toxicity based on their small size and ability to translocate to organs outside of the lungs, as well as epidemiological studies indicating that exposure to fresh combustion emissions (of which UFP are both a major component and a tracer) results in elevated incidence of many adverse health outcomes (Franck, et al., 2011; Oberdörster, 2000; Valavanidis, et al., 2008).

Scientists at GIS HEAL Labs and others from UCLA, collected ambient UFP and PM<sub>2.5</sub> concentration levels in Porter Ranch Estates (PRE) and the Highlands neighborhood. These data were collected during various time periods between March 2016 and February 2017 to characterize ambient levels of particulates when the storage facility was operating at reduced intensity. It was expected that conclusions from this monitoring and subsequent analysis would be more qualitative than quantitative. They would create a better understanding of the likely variability in particulate levels, not related to storage activities, and help identify a potential need for future monitoring efforts to characterize fugitive emissions from the Aliso Canyon Storage Facility.

### Particle measurements and measurement sites

Continuous UFP number concentration and average particle size measurements were made at three locations in the Porter Ranch neighborhood intermittently at 11 separate time periods between March 2016 and February 2017, as well as some measurements of PM<sub>2.5</sub> number concentration (**Table 1**). The monitoring locations included one site in the PRE neighborhood on the 19000 block of Crystal Hills Drive and two sites in the Highlands neighborhood: Highlands 1 (H1) on the 19000 block of Kilfinan Street and Highlands 2 (H2) on the 19000 block of Kilfinan Street.<sup>4</sup> Ultrafine particle measurements were made with DiSCminis

---

<sup>4</sup> For privacy considerations, addresses have been partially redacted, i.e. referred to as their 1000<sup>th</sup> block to respect Porter Ranch residents' identity.

(Testo, Germany) and PM<sub>2.5</sub> number concentrations measurements (0.5 – 2.5 µm) were made with a Dylos 1100 (Dylos, Riverside, CA, USA).

All outdoor monitors were placed in residential backyards. The PRE site is in the interior of a quiet, residential neighborhood. The H2 site borders the open space on the North side of the community of Porter Ranch inside another quiet, residential neighborhood. The H1 site, on the other hand, was located along a busy road which led to high narrow spikes in UFP concentrations characteristic of nearby vehicle emissions. Since the main objective of this monitoring was to evaluate UFP concentrations believed to be coming from the Aliso Canyon Natural Gas Storage Facility and not due to local traffic, therefore measurements at H1 were discontinued.

In addition to the monitoring measurements, residents living at the property of the PRE site maintained a log of local events likely to produce high particulate matter concentrations, including dates and timings of visits from gardening crews sanitation/recycling/yard waste collection and special events such as backyard barbecues. Data associated with these recorded events in the field log that would have resulted in elevations of UFP from these other emission sources were excluded from the data presented below, as they would confound the ability to understand emission sources related to oil and gas wells.

### **Wind Direction**

Meteorological data recorded at the Argos Scientific measurement site in the Highlands neighborhood was used in the analysis of data for the March 2016 to December 2016 period (refer to Meteorological Data on page 12). A meteorological station in Chatsworth to the south of Porter Ranch (Station ID: EW9895) was used in the analysis of data for the January 2017 to February 2017 period. The data collection sites PRE and H2 are located close to the foot of the mountains; and local topography is known to influence local wind patterns. Due to the local topography, the wind direction may be shifted from general flow patterns; this will add uncertainty to any assessment reported here.

Apart from the early January 2017 period, winds during all measurement periods were predominantly easterly or southerly. Southerly winds tend to carry particle pollutants from urban, high-traffic areas into the San Fernando Valley. To the east of Porter Ranch is the low density residential neighborhoods of Granada Hills that also does not have obvious sources of high particle pollution emissions such as heavy traffic.

### **Ultrafine Particle (UFP) concentrations and their relationships with wind direction**

**Average UFP concentrations.** Table 1 shows average UFP concentrations for the measurement periods. Concentrations are also plotted as a function of wind direction shown in Figures 24-26. For measurements made at the PRE site, average concentrations during periods

of predominantly southerly or easterly winds were 5,000 – 10,000 particles per cubic centimeter (particles/cm<sup>3</sup>) of air. For measurements made at the H2 site during the sampling period from late January 2017 to February 2017, average concentrations during periods of predominantly southerly winds were 7,100 particles/cm<sup>3</sup>. The only period of sampling when there were predominantly northerly winds was at the PRE site during a 3-day period in January, during which UFP concentrations were markedly lower, averaging 2,900 particles/cm<sup>3</sup>.

Porter Ranch is a relatively low-density suburban, relatively affluent neighborhood in greater Los Angeles, comprising of single family homes and no obvious sources of high concentrations of UFPs other than traffic and episodic use of small engines (such as gas-powered lawnmowers) and domestic sources such as outdoor grilling. Affluent areas tend to have newer, cleaner vehicle fleets, and residential areas have fewer light and medium duty diesel trucks than more urbanized, mixed use areas. The 24-hour average UFP concentrations at the PRE site are at least as high and sometimes higher than average concentrations found in other affluent neighborhoods of Los Angeles, such as Santa Monica and West Los Angeles that have even more dense land use development, where daytime concentrations away from freeways and major roadways are typically well below 10,000 particles/cm<sup>3</sup>, sometimes as low as 2,000 – 6,000 particles/cm<sup>3</sup> (Choi, 2013).

The hourly averaged UFP concentrations for Porter Ranch indicate a diurnal trend, with concentrations peaking during the afternoon and lowest during the early morning hours. An example of this diurnal trend is shown in **Figure 21**, for the monitoring period from September 2 to September 11, 2016. Peak hourly averages range from 15,000 – 28,000 particles/cm<sup>3</sup> with an increasing trend from 13:00PM to 18:00PM (1:00 PM to 5:00 PM) (**Figure 21** and **Table 1**). This contrasts with the typical pattern for more urban parts of Los Angeles, in which UFP and other primary air pollutants peak in the morning when emissions are high and there is less atmospheric mixing compared to the afternoon. **Figure 22** shows a more typical pattern of UFP concentrations from an air monitoring site in Encino, which is due south of Porter Ranch in the southern part of the San Fernando Valley. The Encino site is located 20 meters from the edge of the 101 Freeway and is expected to have higher UFP concentrations than any of the Porter Ranch sites at any time of day. It should be noted that the site was upwind of the freeway for some of the sampling period; this would attenuate concentration levels compared to a downwind scenario.

Unlike typical conditions in the urbanized parts of Los Angeles where concentrations are lowest in the afternoon, conditions in Porter Ranch are the opposite with highest concentrations observed in the afternoon. The reasons for the unexpected pattern in Porter Ranch are unknown. Possible explanations include unknown local sources and photochemical reactions of gaseous pollutants that cause particles to form.

**High Concentration Ultrafine Particle Concentration Events.** Short-duration, high UFP concentration events were observed (**Table 1**). The duration of the events ranged from approximately 5 to 15 minutes with peak concentrations 6 or more times that of background concentrations. Events were associated with all wind directions. The high UFP concentration events were usually associated with smaller UFPs (less than 100 nm), which is very commonly observed in UFP data and consistent with either nearby sources of combustion particles or photochemical reactions of gaseous pollutants.

**Filtering.** **Figure 23** shows a representative UFP concentration time series collected at the PRE site during September 3 to September 5, 2016. To investigate the wind directions associated with peak UFP concentration events, the peak events were filtered from the concentration time series. We identified peak events (**Figure 23**: red stars) as concentrations that were one standard deviation above the local background. The background (**Figure 21**: magenta line) was defined by a smoothing function with a two-hour window. The standard deviation, that was used as the threshold to identify peak events as described above, was calculated as a running standard deviation with a two-hour window.

**Wind Direction Dependence of Ultra Fine Particle Concentrations.** UFP concentration-wind roses, for several (3 to 5-day) time periods, are shown in **Figures 24 –26**.<sup>5</sup> Two plots are shown for each time-period; with the plots on the left utilizing all measured UFP concentration data during this time and the plots on the right showing only peak UFP concentration events.

**Concentration-Wind Roses.** During most time periods of air monitoring for UFP, the wind direction was predominantly southerly (i.e. from west/southwest to east/southeast) (**Figures 24-26**). Although peak UFP concentration events occurred during both northerly and southerly winds, peak UFP events associated with southerly winds were generally higher in magnitude than peak UFP events associated with northerly winds. Overall, however, there were more peak events coming from the north.

**Wind Direction Dependence of PM<sub>2.5</sub> Particle Concentrations.** PM<sub>2.5</sub> concentration-wind direction roses are shown in **Figures 27 and 28** for two separate time periods of air monitoring, one that overlaps the time period for UFP concentration air monitoring (September 2 to September 6, 2016) and another from January 28 to January 30, 2017. the PM<sub>2.5</sub> instrument is an inexpensive optical particle counter that reports measurements in particles per cubic foot (particles/ft<sup>3</sup>), which are notably different units than reported for the UFP

---

<sup>5</sup> **Reading Concentration-Wind Direction Roses**

The plots show measured concentrations of UFP or PM<sub>2.5</sub> particles (colors), and wind direction with the direction of the wedges. Only the length of the wedges is important; the length of each wedge shows the percent of all winds arriving from that direction, indicated by the circular scale and percentage labels. The widths of the color bars and wedges are not important.

concentrations. For the air monitoring conducted in September 2016, the highest  $PM_{2.5}$  concentrations occurred when winds came from the northeast and east/southeast, with the PM originating either from the mountains to the north or the residential areas to the east (**Figure 27**). the air monitoring conducted in January 2017, the highest  $PM_{2.5}$  concentrations occurred when winds came from the northwest (**Figure 28**). Winds from southerly directions yielded the highest  $PM_{2.5}$  concentrations, with the PM originating from the urbanized areas to the southeast.

## Discussion

UFP and  $PM_{2.5}$  concentrations in two Porter Ranch neighborhoods were measured during several pre-injection time periods spanning from May 2016 to February 2017. During this time, the Aliso Canyon wells were not pressurized. During almost all measurement periods, winds were predominantly from southerly directions. Overall, concentrations of UFP in the Porter Ranch neighborhoods were at the higher end of the range commonly observed for urbanized areas of the Los Angeles area. In addition, they were higher than expected given the suburban land use with predominantly single-family homes and low traffic density. The UFP concentrations display an unusual diurnal pattern, with concentrations peaking in the afternoon when atmospheric mixing is usually more vigorous, rather than in the morning when the atmosphere is more stable, as is observed elsewhere in urbanized areas in Los Angeles. UFP concentrations were highest when the winds came from easterly, followed by southerly directions. Although UFP concentrations were considerably lower in magnitude when winds came northerly (as opposed to southerly), there were more frequent peak UFP concentration events with northerly winds. Air monitoring of  $PM_{2.5}$  concentrations show mixed results. Highest  $PM_{2.5}$  concentrations overall were observed when winds came only from the southerly directions since that is the predominant wind direction during the monitoring period. When there were northerly and easterly winds, the highest  $PM_{2.5}$  concentrations came from these directions.

Given the unusual diurnal patterns in UFP and indications of peak concentrations of particulates are being more often observed from only a few directions, more monitoring is needed to better understand the causes of these unexpected patterns.

## SECTION VI. Pre-injection monitoring of air toxics

### Monitoring Techniques

Integrated outdoor ambient air samples were collected over a 5-day period during September 6 through September 11, 2016. Due to logistical reasons, two samples were collected two days after the earlier deployment (September 8 – 13, 2016). Samples were

collected from nine residential locations around the Porter Ranch community and tested for 79 different pollutants (see Table 3 for full list) with known or suspected associations to oil and natural gas development and storage and/or posed as a particular health concern. The chemical category and test method that were analyzed for each sample, collection media, preservation, and holding time is summarized in **Table 2**. This pre-injection monitoring is meant to serve as a baseline for possible future analyses, for example, after the Aliso Canyon Natural Gas Storage facility resumes injecting natural gas into the field.

## Methods

Standard ambient air sampling protocol procedures were followed. One duplicate sample was obtained for each media type outlined in Table 2. Three equipment blanks were collected for the Radiello Cartridge and the Ogawa Sampler. Nitrile gloves were worn during the deployment and collection of the sampling media and were disposed of as municipal waste at the completion of sampling at each location. Each sample container was marked in the field with the sampling location ID and date and time of sample deployment and collection. An entry was made on a chain-of-custody form for each sample that is submitted to the laboratory for analysis. The Summa Canisters and Radiello cartridges were submitted to ALS Environmental in Simi Valley for analysis and the Ogawa Samplers were shipped to RTI International in North Carolina for analysis. The Radiello cartridges were securely packed in a cooler and stored on blue ice to be chilled to approximately 4 degrees Celsius in preparation for delivery to the appropriate laboratory. The samples were analyzed on the standard laboratory turnaround time and in accordance with standard QA/QC protocol.

Available health-based standards were compiled to compare with measured concentrations of target pollutants. These include the Reference Exposure Levels (REL) and Reference Concentrations (RfC) from the Office of Environmental Health Hazard Assessment (OEHHA) (Cal/EPA, 2016), Integrated Risk Information System/Environmental Protection Agency (IRIS/EPA) (US EPA, 2016), designed to address long-term exposures (up to a lifetime) in a residential setting and are protective of sensitive populations such as children. Strong correlations with methane, our preferred indicator of an unidentified source associated with the oil and gas industry, can help identify possible common emissions sources. For example, air pollutants with strong correlations to methane suggest co-emissions from a common source, in this case, from Well SS-25. We had hypothesized that if the collected data was characterizing a source associated with a well-field fugitive emission, then we might expect to see methane correlated with benzene and toluene.

## Monitoring Results

Average, minimum and maximum concentrations of speciated VOCs, ammonia, and formaldehyde are presented in **Table 3** along with several health-based standards. Results suggest that exposure levels of the monitored VOCs were at levels below health-based reference levels. As with similar monitoring conducted earlier in the year; acrolein levels were elevated and above the OEHHA REL of  $0.35 \text{ ug/m}^3$  with a mean value of  $0.79 \text{ ug/m}^3$  (min: 0.48, max: 1.1). In context, the measured mean concentrations of acrolein were below average ambient air in the United States, which are typically seen in the range of  $1.2\text{--}8.0 \text{ ug/m}^3$ ; levels have likely come down in recent years compared to earlier periods when levels were likely to be higher, so we are unable to conclude definitively that levels observed in this study are lower than contemporaneous averages in the United States (ATSDR, 2007; Seaman, Bennett, and Cahill, 2007).

The data do not appear to suggest chemicals that are notably correlated with methane during the pre-injection timeframe (**Table 4**: correlations of  $|0.5|$  and higher are highlighted for illustration). Methane has a weak correlation with acetone. Benzene is most strongly correlated with acetone, ethanol, and toluene but negatively correlated with formaldehyde. Formaldehyde, in general, appears to be negatively correlated with indicators of both combustion by-products and fossil fuels. These patterns of correlation do not assist in the identification of a unique source, outside of combustion sources.

## SECTION VII. Ancillary analyses and source identification during the pre-injection period

Particle count and continuous methane monitoring data was used in this analysis to identify evidence suggesting that there were specific fugitive emission sources associated the Aliso Canyon Storage Facility, or other sources within the general area during the pre-injection timeframe, that could impact the Porter Ranch community post-blowout. In addition to particle data collected by GIS HEAL Labs and methane data collected by Argos Scientific, this analysis uses SCAQMD trigger data to provide additional context to the results presented in this section.

### Particle Data

Particle count data used in this analysis were collected over the pre-injection period in early to mid-September 2016 at two locations using the Dylos instrument, one in Porter Ranch Estates (PRE) and the other in the Highlands neighborhood (H2). Their locations are described in more detail in the previous section, Section V. The time-series of these data are presented in

**Figure 29.** In PRE, the data appear to show diurnal variation throughout the data with a few spikes above 1,000,000 particles/ft<sup>3</sup>. At the H2 location, general levels were much lower but abnormally high spikes occurred on multiple occasions. Moderate spikes occurred at the PRE location during prevailing conditions with winds coming out of the south during daylight hours. At H2, each of the large spikes was during times of still air or was just immediately preceded by low velocity winds coming from the northeast.

**Figure 30** illustrates the diurnal dependency relationship of ambient PM<sub>2.5</sub> at both sites, over the early to mid-September period. Exaggerated concentration elevations in the data are not seen during mid-day hours, and even appear to drop or are low during rush-hours.

There are insufficient data to make good statistical inference based on these data, but the results collected at the Highlands location, when put into context of the co-temporal meteorological conditions suggest a possible, yet undefined, process to the north that may be causing these transient elevations ( $>1.5 \times 10^{-6}$  /ft<sup>3</sup>) in particle concentration. To potentially confound the transient events, the data collected at PRE are suggestive of a regular process causing elevations in particles as is seen by both the periodicity in **Figure 29** and the general patterns seen in **Figure 30** showing measured concentrations as a function of time of day. This plot appears to show that elevations are only happening during the evening and early morning it is not clear whether this is a function of changes due to: regular diurnal changes in boundary layer height; sources that are specific to the evening/early-morning hours; or a combination of both.

Two peaks appear during much of the days on which data were collected at PRE: an early morning peak and an early evening peak. Looking at the time-series figure (**Figure 29**), the general patterns are apparent with a sharp elevation in particle after the mid-day minimums, followed by a decrease in particles and then another elevation. The second elevation in particles mentioned happens in the morning hours and appear to have a steeper gradient than the elevations observed in the evenings; this is most clearly illustrated on days September 7-11 where after a gradual decrease in particle levels a very sharp spike is observed. As the monitoring took place over the Labor Day holiday weekend in September 2016, and did not occur over multiple weeks, it is also unclear whether this may be due to the normal activity pattern of residents attributable to motor vehicle travel habits and other combustion activities, such as grilling and wood burning fire place usage.

### **Spectral analysis of particle data**

A more formal analysis of these fluctuations in these time series data was conducted by estimating the spectrogram for each of the two time-series. The spectrogram is a representation of the frequencies (i.e., the number of times in a day that an event happens)

that define the repeating characteristics in the observed data. The analysis was conducted with both the raw and detrended data, **Figure 31** and **Figure 32**.

Results suggest that the data are not sufficiently regular to identify a repeated specific low frequency event. Ideally, the Fast Fourier Transform analysis presented here would clearly demarcate a specific periodicity in the data (a narrow tall peak). We can see that there is region of elevated spectral density at low frequencies (1-10 events per day) which are likely indicative of both within and between day variability at low frequencies, and variation in the length of time that an elevated event took place, **Figure 33** through **Figure 36**. In the case of PRE, detrending using the Daniell smoothing kernel appeared to better identify a smaller range of potential low frequency peaks (**Figure 34**), but the estimated spectral densities were still too elevated to identify a unique peak. In the case of the Highlands, the detrending did not appreciably alter the estimated spectrogram (**Figure 36**).

### **SCAQMD Trigger Samples**

Trigger samples were also taken by SCAQMD at two locations in the Porter Ranch community after the leaking SS-25 well was permanently plugged. Trigger samples are short-term Summa Canister samples that were collected when ambient air contaminant levels exceeded a predefined threshold, in this case either 5 parts per million (ppm) ppm methane or 35 ppm TVOCs.

Results from SCAQMD's trigger samples for methane and benzene are presented in Table 5. Benzene is presented here as it is toxic chemical of concern, unlike methane which in this context is a marker of emissions from the oil and gas industry and not typically associated with immediate health impacts. In general, most reported contaminants are below levels of health concern. Between March 4, 2016 and November 14, 2016, 21 of 40 trigger samples that detected benzene; of these, the average benzene level was 2.2 parts per billion (ppb) (below the REL of 8.0 ppb). In nearly all cases, samples were triggered in the hours between 6:00 and 9:00 am or near midnight. There was one trigger sample, on July 29, 2016, with a benzene concentration of 13 ppb which exceeds the health-based REL of 8 ppb. Two additional trigger samples taken at the Highlands Community Pool Parking Lot on September 30, 2016 (also in the early morning) detected benzene at levels approaching the REL at 7.5ppb and 7.1 ppb.

### **Ancillary analysis of methane from Argos Scientific**

Given the potential strong confounding of observed particulate levels from combustion sources, methane would be the obvious contaminant most likely associated with a gas and oil well field. While methane has been collected at Site #4 through at least the end of 2016, data published through the California Air Resources Board Air Quality Management and Information Systems (AQMIS) is available at a 1-hour averaged resolution. Results from the particulate data

analyses suggest that events are taking place on a much shorter time scale, and as such, a more highly resolved data source was necessary to understand the events of concern. For this reason, data from the Argos Scientific methane monitor located on the 19000 Block of Kilfinan Street<sup>6</sup> was used for the following analysis as data are available at a 5-minute resolution with co-temporal meteorological data.

Analyses using the Argos Scientific methane data are for data collected over the period June 1 through September 30, 2016 (**Figure 37**). This date range was selected as it captured several months that were not confounded by long periods of moderate to heavy rain. Wind conditions over the same period are illustrated in **Figure 38**. The average level methane level over this period is 2.3 ppm. The analysis that follows investigates the outliers in this dataset to determine whether there appears to be some pattern indicating sources which may be contributing to the observed variability.

The following figure looks at observed methane levels as a function of the time of day (**Figure 39**). The black line represents the long-term average expected fluctuation of methane by hour of day; this was estimated using local polynomial regression fit by least squares. The predicted fluctuation follows the expected diurnal pattern with a constant source. Concentrations are higher when the boundary layer is lowest (evening through early morning). When the boundary layer increases as temperatures rise in the morning, concentrations decrease because of a greater mixing volume.

It was hypothesized that, if unique natural gas production-based sources are responsible for elevated ambient contaminant levels, these would be identified through the outliers in the observed distribution of ambient methane. Outliers, here are identified as those observations in the 99th percentile or greater. In **Figure 40** of the outlier data, there is one distinct pattern that is immediately apparent, very few outliers are found between the hours of noon and 7:00 pm. Two other clusters of outliers are found, one between 9:00 pm and 6:00 am, and the other centered around 9:00 am. These findings are in line with the time at which Summa Canister trigger samples were collected. These patterns are seen on multiple days; and are not just a product of single unique events. Most outliers are below 4 ppm (**Figure 41**).

As a means of trying to establish the factors that identify possible source locations, an unsupervised machine learning method called Expectation-Maximization (EM) clustering algorithm was employed<sup>7</sup>. In applying this method, a dataset consisting of concentration, wind

---

<sup>6</sup> Addresses have been partially redacted, i.e. referred to as their 1000<sup>th</sup> block to respect the Porter Ranch resident's identity.

<sup>7</sup> This method is used to identify latent variables or groups to which the data may represent. For example, if you collected data representing the weight, fur coarseness, and shoulder height of a group of adult mammalian pets, but hid information about the kind of pet and applied the EM clustering algorithm, you might expect to see three groups well represented; these would likely be predictive of dogs, cats, and rodents/rabbits. This seems intuitive

direction, wind-speed, and hour of day was first input into the EM Clustering algorithm. However, initial runs of the EM algorithm, which included wind speed did not produce stable groups. As there is a random component to the method, ideally, there would be little to no change in group/cluster assignments. This was not the case when wind speed was included, so it was removed from the final analysis. To note, wind-direction and hour of day are not linear measures, but cyclical measures. For this reason, these variables underwent a polar transformation into Cartesian space so that times of day near midnight and direction to the north would not be bifurcated by the conventional numbering systems they use. The transformations are described below in the set of equations **Eq. 1**, where  $r$  is the radius and  $\theta$  is the angle. Naturally there is no defined radius for wind-direction and time, but a value of 100 was used to sufficiently create distance across the circle which defines the variable's space in the Cartesian plane:

$$\begin{cases} x = r \cos \theta \\ y = r \sin \theta \end{cases} \quad \text{Eq. 1}$$

In the case of time of day, where the concern was that times before midnight (23:00 – 23:59) would numerically be dissimilar to hours in the morning (midnight=0:00-01:00), the day's 24 hours, not 12, were imagined sitting on a clock so that instead of 6 o'clock at the bottom, 12 o'clock sat there instead.  $\theta$  represents the angle of the hour hand from midnight (6:00 am =  $90^\circ$ , 12:00 pm= $180^\circ$ , 6:00 pm= $270^\circ$ ). In total, there were five variables input into the EM Clustering algorithm. As with many clustering methodologies, the initialization parameters can significantly alter the cluster assignments. For this reason, several initialization methods were investigated, specifically: EM (Biernacki et al. 2003), Rnd/Rnd+ (Maitra 2009), and SVD (Maitra 2001).

Results of the EM clustering are presented in **Figure 42**, these are plots of wind direction against hour of day color coded by their group assignment. Note, that the number and color coding are not necessarily stable across the different initialization methods. After testing multiple iterations of the algorithm using different numbers of clusters, using only three clusters produced the most justifiable results, evaluated using the log-likelihood.

**The pattern of methane concentrations that emerges from the analysis suggests there are two sources:**

1. From the North, during later in the evening to early morning, and
2. From the South-East to South-West, during between 8:00 to 10:00 in the morning.

because dogs tend to have coarser fur, and rodents/rabbits are shorter at the shoulder than either cats or dogs. What makes this powerful is that this method can be extended to high dimensional data.

Much of the instability in the cluster assignments between the different initialization methods are attributable to the methane concentration. **Figure 43**, illustrates the distribution of concentrations against hour of day and wind direction. In the lower left hand corner of the plot, there is clearly a group of higher concentrations that may be creating some instability in the cluster assignments. This instability in group assignment is observed in all the resulting group assignment using the four different initialization methods, **Figure 42**. However, the EM method is the only one which appears to inexplicably mix observations with wind coming from both Northerly and Southerly directions. In both the Rnd and Rnd+ instances, the mixing of Northerly and Southerly observations in a cluster appears to be driven more by time of day as these observations are on the fringes based on wind direction.

These findings do not specifically identify a source for the observed elevations in ambient methane from the Argos Scientific monitor. They do, however, provide evidence to corroborate the hypothesis that fugitive emissions, unrelated to regular operations, are reaching the community.

## **SECTION VIII. Summary of findings**

### **Analysis of blowout data collected with SNAQ and Argos Scientific monitors during Aliso Canyon disaster**

Large fluctuations in contaminant gas concentration are observed for both contaminant gas and PM. There is evidence of pronounced periodic short-time scale events of PM, CO, and TVOC compared to the other gas measurements. There were also several short-term episodic spikes associated with stable atmospheric conditions. An ancillary analysis of the Argos Scientific methane monitor shortly after the well was sealed, suggests there are multiple sources of methane (north, northeast, south and east).

### **Air model development for the Aliso Canyon disaster**

The ADMS modeling systems was used to estimate the variability of ambient methane in the Porter Ranch community associated with the Well SS-25 natural gas well blowout. Using methane and meteorological data collected at agency monitoring sites in the Porter Ranch community, the ADMS model was fit with parameters representing a constant rate of release from the well head. Due to limited meteorological data and the complexity of terrain, an iterative approach was employed to back-calculate the modeled wind-field. Results of the modeling confirm that the model assumptions regarding the emission source and dispersion

process have been correctly attributed to the Well SS-25 blowout, though further refinement of the model would improve estimates.

### **Pre-injection UFP and PM<sub>2.5</sub> measurements**

Particles measured within the community were higher than expected given the low population and traffic density, although within the upper end of the range observed elsewhere in Los Angeles. Unusual diurnal patterns were also observed where peaks in concentration happened in the afternoon when atmospheric mixing is usually more vigorous, rather than the morning when the atmosphere is more stable, as is usually observed in urbanized areas in Los Angeles. While the highest concentrations were observed when winds were from the South, a higher number of peak events occurred when winds were northerly.

### **Pre-injection air toxics monitoring**

Five-day integrated ambient air quality samples were collected at nine locations throughout the Porter Ranch community between September 6-13, 2016. During that period, data on VOCs, formaldehyde, and ammonia were collected with Summa Canisters, Radiello Cartridges and Ogawa samplers, respectively. Aside from the expected elevation of acrolein, which is common in California, the results did not find air contaminant levels that exceeded published health standards. There did not appear to be a correlation pattern in the integrated sample that was suggestive of a unique source. The pre-injection data collected serve as a baseline comparison for future analyses.

### **Ancillary analyses and source identification pre-injection**

An analysis was conducted to ascertain potential sources of fugitive exposures to the Porter Ranch community using particle data collected September 3-13, 2016, trigger samples collected between March 4, 2016 and November 14, 2016, and methane collected from June 1, 2016 through September 30, 2016. During this period, several peak episodes of methane and particles were observed during evening to early morning hours when winds were gently coming from a northerly direction. An analysis of the periodicity in the data was unable to identify a specific spectral signature. Methane data were collected from the Argos Scientific monitor and an analysis of the extreme outliers was conducted. Few outliers were identified mid-day; however, two clusters of outliers were initially identified, one between 9:00 pm and 6:00 am, and the other centered around 9:00 am. These findings agree with the time at which Summa Canister trigger samples were collected, which showed continued evidence of potential fugitive emissions occurring during the early morning hours. A clustering analysis using the EM Clustering algorithm was conducted on the dataset of outliers, looking for patterns based on wind-direction, wind-speed, hour of day and methane concentration. Results of the analysis, define two major clusters, characterized by wind direction and time of day: one cluster from

the north during late-night early-morning hours and the other from the south between the hours of 8:00 am and 10:00 am. An initial review of data of collected at the Argos Scientific location through the summer of 2017 suggest these patterns continue. These results lend support to the hypothesis that the community may have been impacted by fugitive emissions (post blowout) from the north during overnight and early morning hours. In total, these findings along with continued symptom reports to DPH warrant further investigation and dedication of resources to long-term environmental and health monitoring in surrounding communities.

## REFERENCES

Agency for Toxic Substances and Disease Control (ATSDR). 2007. Toxicological profile for acrolein. U.S. DEPARTMENT OF HEALTH AND HUMAN SERVICES. Public Health Service. Agency for Toxic Substances and Disease Registry. August 2007.  
<https://www.atsdr.cdc.gov/toxprofiles/tp124.pdf> [accessed March 8, 2017].

Becker, J. J., D. T. Sandwell, W. H. F. Smith, J. Braud, B. Binder, J. Depner, D. Fabre, J. Factor, S. Ingalls, S-H. Kim, R. Ladner, K. Marks, S. Nelson, A. Pharaoh, R. Trimmer, J. Von Rosenberg, G. Wallace, P. Weatherall., Global Bathymetry and Elevation Data at 30 Arc Seconds Resolution: SRTM30\_PLUS, *Marine Geodesy*, 32:4, 355-371, 2009.

Biernacki C, Celeux G, Govaert G. 2003. Choosing starting values for the EM algorithm for getting the highest likelihood in multivariate Gaussian mixture models. *Computational Statistics and Data Analysis*, 413, 561–575.

Brandt, A.R., Heath, G.A., Kort, E.A., O'sullivan, F., Pétron, G., Jordaan, S.M., Tans, P., Wilcox, J., Gopstein, A.M., Arent, D. and Wofsy, S., 2014. Methane leaks from North American natural gas systems. *Science*, 343(6172), pp.733-735.

Cal/EPA 2016. Office of Environmental Health and Hazard Assessment, Chronic Reference Exposure Levels to address long-term exposures. <http://oehha.ca.gov/air/general-info/oehha-acute-8-hour-and-chronic-reference-exposure-level-rel-summary>.

Choi, W.S., M. He, V. Barbesant, K. Kozawa, S. Mara, A.M. Winer, and S.E. Paulson. 2013. 'Neighborhoods, roadways, and airports: Air quality benefits of emissions reductions from mobile sources', *Atmospheric Environment*, 80: 300-21.

Franck, U., Odeh, S., Wiedensohler, A., Wehner, B. and Herbarth, O., 2011. The effect of particle size on cardiovascular disorders—The smaller the worse. *Science of the Total Environment*, 409(20), pp.4217-4221.

Maitra R. 2001. Clustering massive datasets with applications to software metrics and tomography. *Technometrics*, 43(3), 336–346.

Maitra R. 2009. Initializing Partition-Optimization Algorithms. *IEEE/ACM Transactions on Computational Biology and Bioinformatics*, 6, 144–157. doi:<http://doi.ieeecomputersociety.org/10.1109/TCBB.2007.70244>.

Oberdörster, G., 2000. Pulmonary effects of inhaled ultrafine particles. *International archives of occupational and environmental health*, 74(1), pp.1-8.

Seaman V., Bennett D., Cahill T., 2007. Origin, occurrence, and source emission rate of acrolein in residential indoor air. Environmental Science Technology. Oct 15;41 (20): 6940-6.

US EPA. United States Environmental Protection Agency. Integrated Risk Information System (IRIS). 2016. <https://cfpub.epa.gov/ncea/iris/search/index.cfm>.

Valavanidis, A., Fiotakis, K. and Vlachogianni, T., 2008. Airborne particulate matter and human health: toxicological assessment and importance of size and composition of particles for oxidative damage and carcinogenic mechanisms. Journal of Environmental Science and Health, Part C, 26(4), pp.339-362.

## APPENDIX A. Tables and Figures

Table 1. Measurement periods, locations, general observations and peak events

Location	Measurement Period	Average Concentration (St. Dev.)	Max. Hourly Avg. Concentration	Event [UFP] elevation relative to background /Event duration/Wind direction during events
H2 indoor	3/10/16-3/14/16		3500 /cm <sup>3</sup>	Winds mostly northerly. 10 min. wide peak event 6 x the baseline.
PRE outdoor	5/5/16-5/9/16	8700/cm <sup>3</sup> (18000) /cm <sup>3</sup>	25000/cm <sup>3</sup>	Winds mostly calm, turning north. 10 min. wide peak event 6 x the baseline.
PRE outdoor	5/17/16-5/20/16	5100/cm <sup>3</sup> (3100)/cm <sup>3</sup>	25000 /cm <sup>3</sup>	Winds from SW
PRE outdoor	5/27/16-6/4/16	9800/cm <sup>3</sup> (5400)/cm <sup>3</sup>	25000/cm <sup>3</sup>	Winds mostly calm, E/SE, some N. 7 min. wide peak 9 x baseline
PRE outdoor	6/14/16-6/22/16	7600/cm <sup>3</sup> (4630)/cm <sup>3</sup>	25000/cm <sup>3</sup>	Winds mostly southerly
H1 outdoor	7/11/16-7/17/16		20000/cm <sup>3</sup>	Winds calm SE/NE/N Sharp narrow (2 min) peaks, 10x baseline
PRE outdoor	6/30/16-7/05/16	9800/cm <sup>3</sup> (5000)/cm <sup>3</sup>	28000/cm <sup>3</sup>	Winds S/SE 1 broad (38 min) peak, 6 x baseline
PRE outdoor	7/11/16-7/19/16	8400/cm <sup>3</sup> (8900)/cm <sup>3</sup>	25000/cm <sup>3</sup>	Winds calm SE/NE/N Broad (1.5 hr) peak, 1.5 x baseline
PRE outdoor	9/2/16-9/11/16	8100/cm <sup>3</sup> (4500)/cm <sup>3</sup>	25000/cm <sup>3</sup>	Winds E/SE/NE
PRE outdoor	1/28/17-1/30/17	2800/cm <sup>3</sup> (2700)/cm <sup>3</sup>	10000/cm <sup>3</sup>	Winds from N 9 min. wide peaks 2.5 x baseline
H2 outdoor	1/30/17-2/2/17	7200/cm <sup>3</sup> (2700)/cm <sup>3</sup>	15000/cm <sup>3</sup>	Winds from SE Broad (1 h) peaks 2 x baseline

Table 2. Summary of monitoring methods used for collection of air quality between 09/06/16 – 09/13/16.

Laboratory Analysis	Collection Media	Preservation	Holding Time
VOCs, EPA TO-15 Low Level	6-Liter Summa Canister, batch certified, fitted with a 5-day flow controller	None	30 days
Formaldehyde, EPA TO-11A	DNPH Radiello Cartridge	4° Celsius before and after collection	60 days
Ammonia, Ion Chromatography	Ogawa Sampler	None	14 days

Table 3. Results of VOC, ammonia, and formaldehyde monitoring Sept 6-13, 2016. Available health-based standards are provided in the "Note" column.

<b>Compounds</b>	<b>Mean (ug/m3)</b>	<b>Min</b>	<b>Max</b>	<b>Detects /Non- Detects</b>	<b>Note</b>
1,1-Dichloroethane (1,1-DCA)	ND	0	0	0/10	
1,1-Dichloroethene (1,1-DCE)	ND	0	0	0/10	
1,1,1-Trichloroethane (TCA)	ND	0	0	0/10	
1,1,2-Trichloroethane	ND	0	0	0/10	
1,1,2-Trichlorotrifluoroethane	0.52	0.44	0.56	10/0	
1,1,2,2-Tetrachloroethane	ND	0	0	0/10	
1,2-Dibromo 3-Chloropropane	ND	0	0	0/10	
1,2-Dibromoethane	ND	0	0	0/10	
1,2-Dichloro-1,1,2,2-tetrafluoroethane	ND	0	0	0/10	
1,2-Dichlorobenzene	ND	0	0	0/10	
1,2-Dichloroethane	ND	0	0	0/10	
1,2-Dichloroethane-d4	481.80	475	492	0/10	calibration gas
1,2-Dichloropropane	ND	0	0	0/10	
1,2,4-Trichlorobenzene	ND	0	0	0/10	
1,2,4-Trimethylbenzene	0.45	0.38	0.52	2/8	RfC 0.06 mg/m3
1,3-Butadiene	ND	0	0	0/10	
1,3-Dichlorobenzene	ND	0	0	0/10	
1,3,5-Trimethylbenzene	ND	0	0	0/10	
1,4-Dichlorobenzene	0.43	0.23	0.76	3/7	REL 0.8 mg/m3 (OEHHA)
1,4-Dioxane	ND	0	0	0/10	
2-Butanone (MEK)	1.28	0.87	2.3	10/0	RfC 5 mg/m3
2-Hexanone	0.48	0.48	0.48	1/9	
2-Propanol (Isopropyl Alcohol)	2.20	1.2	5.9	7/3	REL 3200 ug/m3 (OEHHA)
3-Chloro-1-propene (Allyl Chloride)	ND	0	0	0/10	
4-Bromofluorobenzene	528.20	520	533	10/0	calibration gas
4-Ethyltoluene	ND	0	0	0/10	
4-Methyl-2-pentanone	ND	0	0	0/10	
Acetone	13.50	10	19	10/0	toxicity not assessed for inhalation route
Acetonitrile	ND	0	0	0/10	
Acrolein	0.79	0.48	1.1	2/8	REL 0.35 ug/m3 (OEHHA)
Acrylonitrile	ND	0	0	0/10	
alpha-Pinene	0.45	0.45	0.45	1/9	minor effects at 450 mg/m3
Ammonia	4.35	1.34	6.89	10/0	REL 200 ug/m3 (OEHHA)
Benzene	0.56	0.49	0.7	10/0	REL 3 ug/m3 (OEHHA)
Benzyl Chloride	ND	0	0	0/10	
Bromodichloromethane	ND	0	0	0/10	
Bromoform	ND	0	0	0/10	
Bromomethane	ND	0	0	0/10	
Carbon Disulfide	ND	0	0	0/10	
Carbon Tetrachloride	0.44	0.37	0.47	9/1	REL 40 ug/m3 (OEHHA)
Chlorobenzene	ND	0	0	0/10	
Chloroethane	ND	0	0	0/10	
Chloroform	0.34	0.27	0.54	5/5	REL 150 ug/m3 (OEHHA)
Chloromethane	ND	0	0	0/10	
cis-1,2-Dichloroethene	ND	0	0	0/10	
cis-1,3-Dichloropropene	ND	0	0	0/10	
Cyclohexane	ND	0	0	0/10	
d-Limonene	0.53	0.53	0.53	1/9	not assessed for inhalation route
Dibromochloromethane	ND	0	0	0/10	
Dichlorodifluoromethane	1.92	1.7	2.1	10/0	not assessed for inhalation route

\*(Table 3 continues the following page)

Table 3 (cont). Results of VOC, ammonia, and formaldehyde monitoring Sept 6-13, 2016. Available health-based standards are provided in the "Note" column.

<b>Compounds</b>	<b>Mean (ug/m3)</b>	<b>Min</b>	<b>Max</b>	<b>Detects/Non-Detects</b>	<b>Note</b>
<i>Methylene Chloride</i>	0.50	0.46	0.53	4/6	
<i>Ethanol</i>	9.53	7.5	13	10/0	REL 1900mg/m3 (OEHHA)
<i>Ethyl Acetate</i>	1.68	1	4.8	9/1	
<i>Ethylbenzene</i>	ND	0	0	0/10	
<i>Formaldehyde</i>	4.73	4.2	5.9	10/2	REL 9 ug/m3 (OEHHA)
<i>Hexachlorobutadiene</i>	ND	0	0	0/10	
<i>Isopropylbenzene (Cumene)</i>	ND	0	0	0/10	
<i>m,p-Xylenes</i>	1.04	0.75	1.2	4/6	REL 700 ug/m3 (OEHHA)
<i>Methane</i>	3.70	2.9	5.4	10/0	
<i>Methyl Methacrylate</i>	ND	0	0	0/10	
<i>Methyl tert-Butyl Ether</i>	ND	0	0	0/10	
<i>n-Butyl Acetate</i>	ND	0	0	0/10	
<i>n-Heptane</i>	ND	0	0	0/10	
<i>n-Hexane</i>	0.49	0.41	0.53	3/7	REL 7000 ug/m3 (OEHHA)
<i>n-Nonane</i>	ND	0	0	0/10	
<i>n-Octane</i>	ND	0	0	0/10	
<i>n-Propylbenzene</i>	ND	0	0	0/10	
<i>Naphthalene</i>	ND	0	0	0/10	
<i>o-Xylene</i>	0.40	0.38	0.42	2/8	REL 700 ug/m3 (OEHHA)
<i>Propene</i>	0.88	0.47	1.5	5/5	REL 3000 ug/m3 (OEHHA)
<i>Styrene</i>	ND	0	0	0/10	
<i>Tetrachloroethene</i>	ND	0	0	0/10	
<i>Tetrahydrofuran (THF)</i>	ND	0	0	0/10	
<i>Toluene</i>	1.36	1.1	2.1	10/0	REL 300 ug/m3 (OEHHA)
<i>Toluene-d8</i>	510.10	504	519	10/0	calibration gas
<i>trans-1,2-Dichloroethene</i>	ND	0	0	0/10	
<i>trans-1,3-Dichloropropene</i>	ND	0	0	0/10	
<i>Trichloroethene (TCE)</i>	ND	0	0	0/10	
<i>Trichlorofluoromethane (CFC 11)</i>	1.07	0.94	1.1	10/0	not assessed for inhalation route
<i>Vinyl Acetate</i>	2.20	2.2	2.2	1/9	REL 200 ug/m3 (OEHHA)
<i>Vinyl Chloride</i>	ND	0	0	0/10	

Table 4. Correlation table of detected compounds during pre-injection monitoring

	1 : 1,1,2-...	2 : 2-Buta...	3 : Aceton...	4 : Ammoni...	5 : Benzen...	6 : Dichlo...	7 : Ethano...	8 : Formal...	9 : Methan...	10 : Toluen...	11 : Trichl...
1:1,1,2-Trichlorotrifluoroethane		-0.01	-0.12	-0.39	0.03	0.88	0.20	0.09	-0.35	0.24	0.88
2:2-Butanone (MEK)	-0.01		0.88	0.34	0.49	0.22	0.21	-0.64	0.20	0.14	0.28
3:Acetone	-0.12	0.88		0.26	0.74	0.22	0.39	-0.79	0.43	0.45	0.20
4:Ammonia	-0.39	0.34	0.26		0.19	-0.31	0.54	-0.01	-0.30	0.12	-0.32
5:Benzene	0.03	0.49	0.74	0.19		0.35	0.68	-0.56	0.29	0.89	0.21
6:Dichlorodifluoromethane (CFC 12)	0.88	0.22	0.22	-0.31	0.35		0.35	-0.10	-0.25	0.51	0.83
7:Ethanol	0.20	0.21	0.39	0.54	0.68	0.35		-0.11	-0.05	0.79	0.33
8:Formaldehyde	0.09	-0.64	-0.79	-0.01	-0.56	-0.10	-0.11		-0.31	-0.31	-0.13
9:Methane	-0.35	0.20	0.43	-0.30	0.29	-0.25	-0.05	-0.31		0.05	0.00
10:Toluene	0.24	0.14	0.45	0.12	0.89	0.51	0.79	-0.31	0.05		0.29
11:Trichlorofluoromethane (CFC 11)	0.88	0.28	0.20	-0.32	0.21	0.83	0.33	-0.13	0.00	0.29	

Table 5: Summa Canister trigger samples of selected VOCs collected after the well was sealed (Table 5 continues on next page; see note belows)

Location	Date	Time	Methane (ppmv)	Benzene (ppbv)
	Acute RELs (ppb):		NA	8
Castlebay	3/4/16	7:07	4	3.8
Castlebay	3/15/16	10:33	4	0.2
Highlands	3/17/16	7:10	2	0.2
Highlands	3/18/16	6:28	3	0.4
Castlebay	3/18/16	6:32	3	0.3
Castlebay	4/2/16	7:55	3	0.2
Highlands	4/7/16	7:11	NA	NA
Castlebay	4/7/16	8:24	3	0.3
Highlands	4/7/16	7:13	2	0.6
Highlands	6/17/16	7:40	NA	NA
Highlands	6/17/16	7:46	2	1.2
Highlands	6/19/16	22:23	3	<0.1
Highlands	6/23/16	9:50	NA	NA
Highlands	6/23/16	9:50	NA	NA
Highlands	7/1/16	7:02	3	NA
Highlands	7/10/16	22:00	NA	NA
Highlands	7/15/16	7:18	3	0.7
Highlands	7/29/16	6:42	4	13
Highlands	8/16/16	6:33	3	<0.1
Highlands	8/19/16	7:14	3	<0.1
Highlands	8/19/16	7:15	3	NA
Highlands	8/19/16	7:11	3	0.7
Highlands	8/26/16	7:25	3	0.3
Highlands	9/2/16	6:34	NA	NA
Highlands	9/11/16	8:23	NA	NA
Highlands	9/23/16	6:50	3	1.9
Highlands	9/23/16	6:49	NA	NA
Highlands	9/26/16	**	NA	NA
Highlands	9/27/16	13:35	2	0.1
Highlands	9/30/16	6:15	2	7.5
Highlands	9/30/16	6:59	3	7.1
Highlands	9/30/16	6:15	NA	NA

\* Chronic REL in place of acute REL

\*\* Illegible handwriting

§ Data were transcribed from scanned paper reports. Each of the sampling events did not necessarily measure for all compounds. Compounds reported in Table 5 represent VOCs most likely to be characteristic of oil and gas activities. "NA" represents not measured, "<0.1" represents measured concentrations below detection or quantification limits. Original data can be found at [<http://www.aqmd.gov/home/news-events/community-investigations/aliso-canyon-update/air-sampling/air-monitoring-activities/grab-sample-data>]

Table 5 (cont): Summa Canister trigger samples of selected VOCs collected after the well was sealed (see note belows)

Location	Date	Time	Methane (ppmv)	Benzene (ppbv)
	Acute RELs (ppb):		NA	8
Highlands	10/3/16	13:20 **	NA	NA
Highlands	10/3/16	4:20	3	NA
Highlands	10/3/16	4:22	2	NA
Highlands	11/5/16	12:38	3	NA
Highlands	11/5/16	12:39	2	NA
Highlands	11/5/16	12:40	2	NA
Highlands	11/14/16	13:55	3	NA

\* Chronic REL in place of acute REL

\*\* Illegible handwriting

§ Data were transcribed from scanned paper reports. Each of the sampling events did not necessarily measure for all compounds. Compounds reported in Table 5 represent VOCs most likely to be characteristic of oil and gas activities. "NA" represents not measured, "<0.1" represents measured concentrations below detection or quantification limits. Original data can be found at [<http://www.aqmd.gov/home/news-events/community-investigations/aliso-canyon-update/air-sampling/air-monitoring-activities/grab-sample-data>]

## **APPENDIX B. Supplemental Materials**

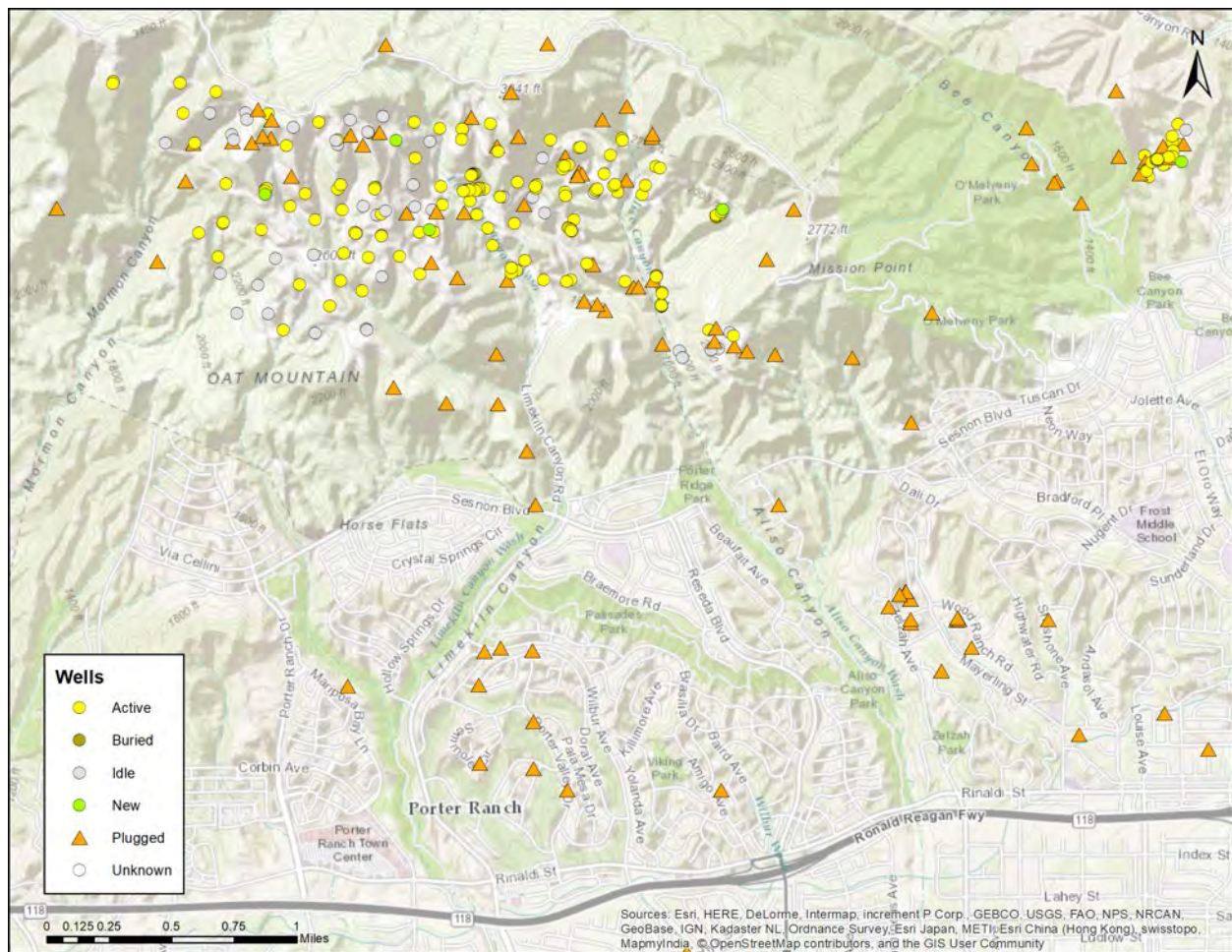


Figure 1. Map of buried and abandoned (plugged) wells

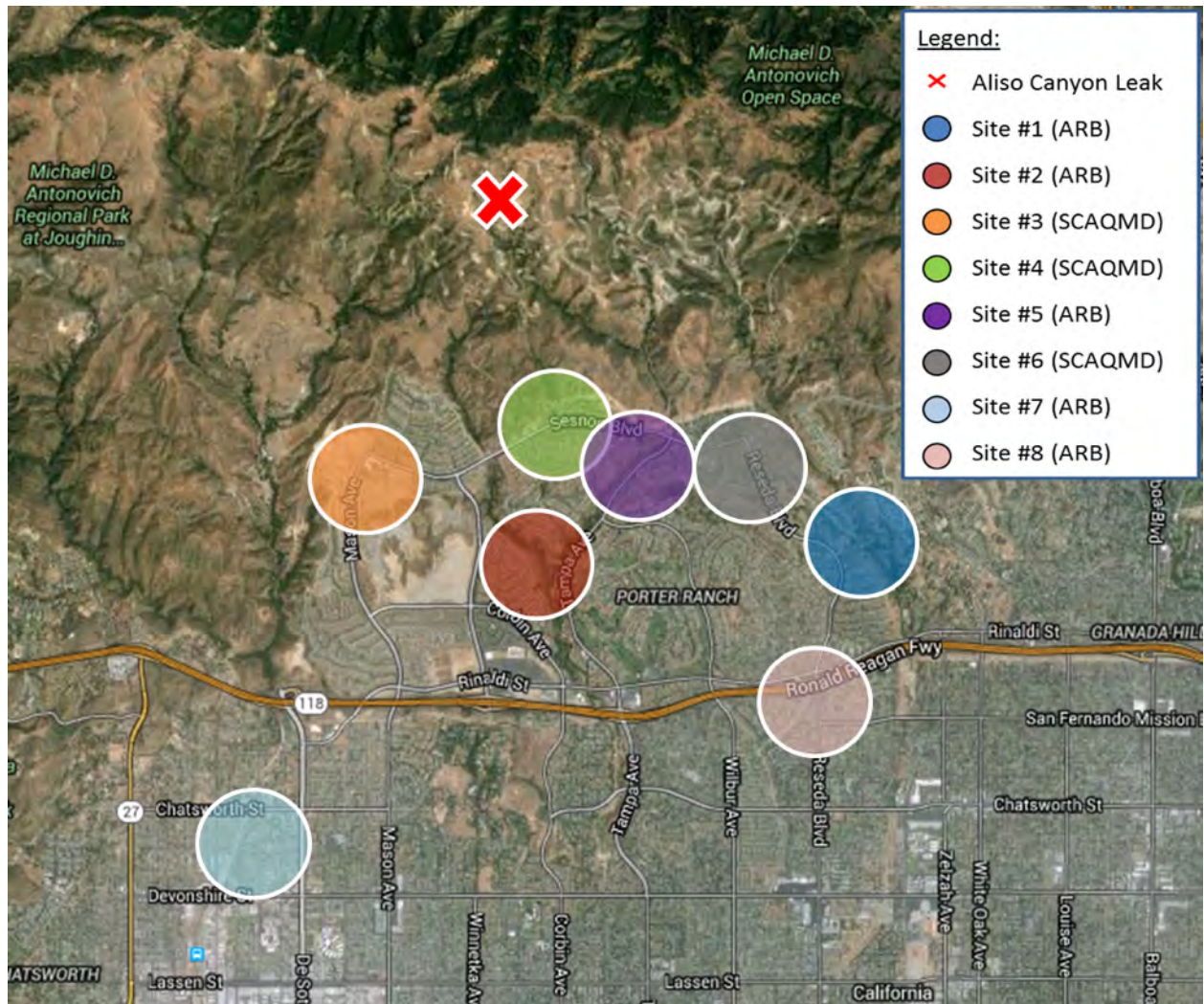


Figure 2. Map of government monitoring locations

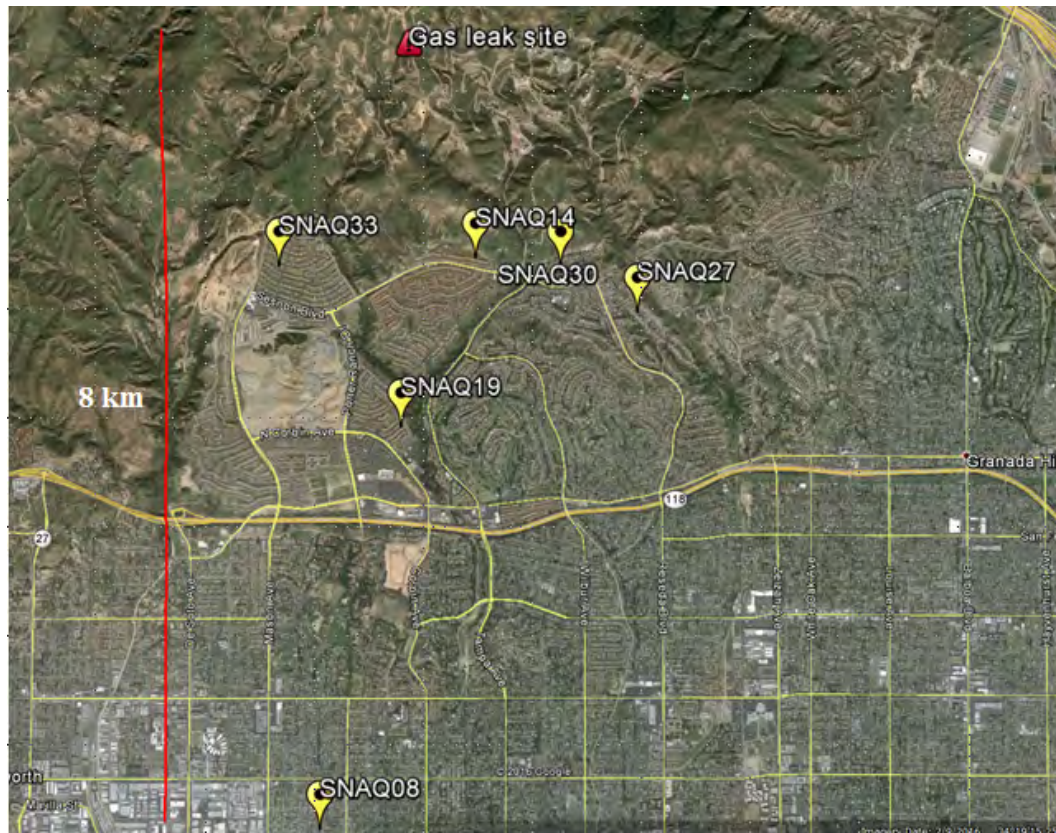


Figure 3. Map of SNAQ monitor locations

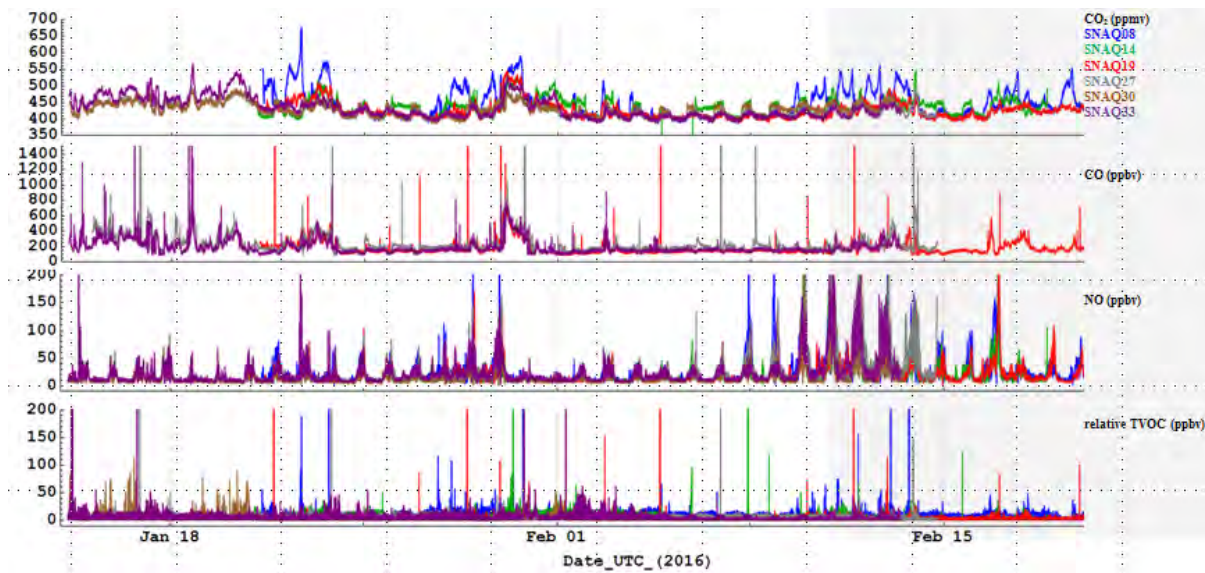


Figure 4. Time series plot of CO<sub>2</sub>, CO, NO and relative TVOCs during the deployment period.

\*The gray shading corresponds to period the leak was capped.

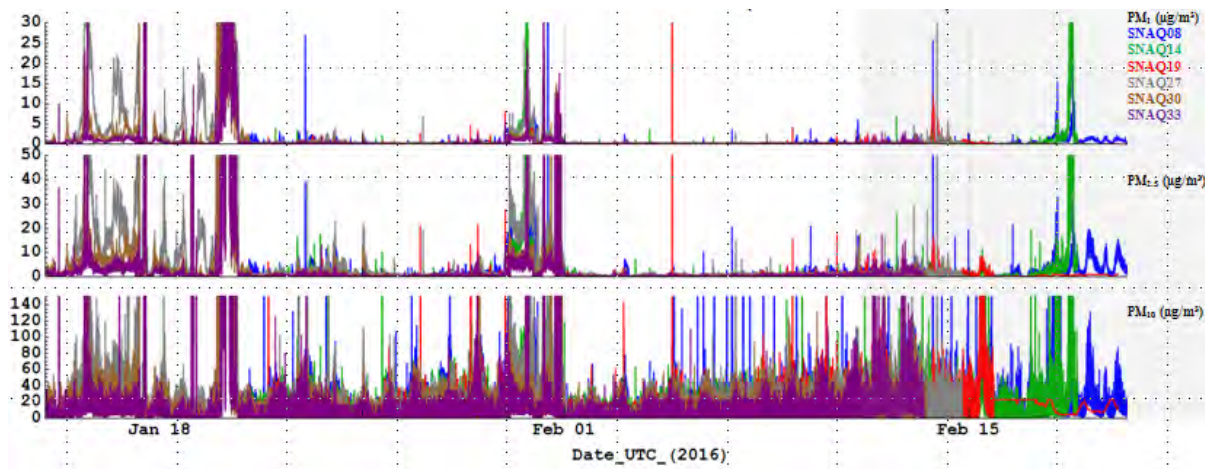


Figure 5. Time series plot of PM<sub>1</sub>, PM<sub>2.5</sub> and PM<sub>10</sub> during the deployment period. The gray shading corresponds to period the leak was capped.

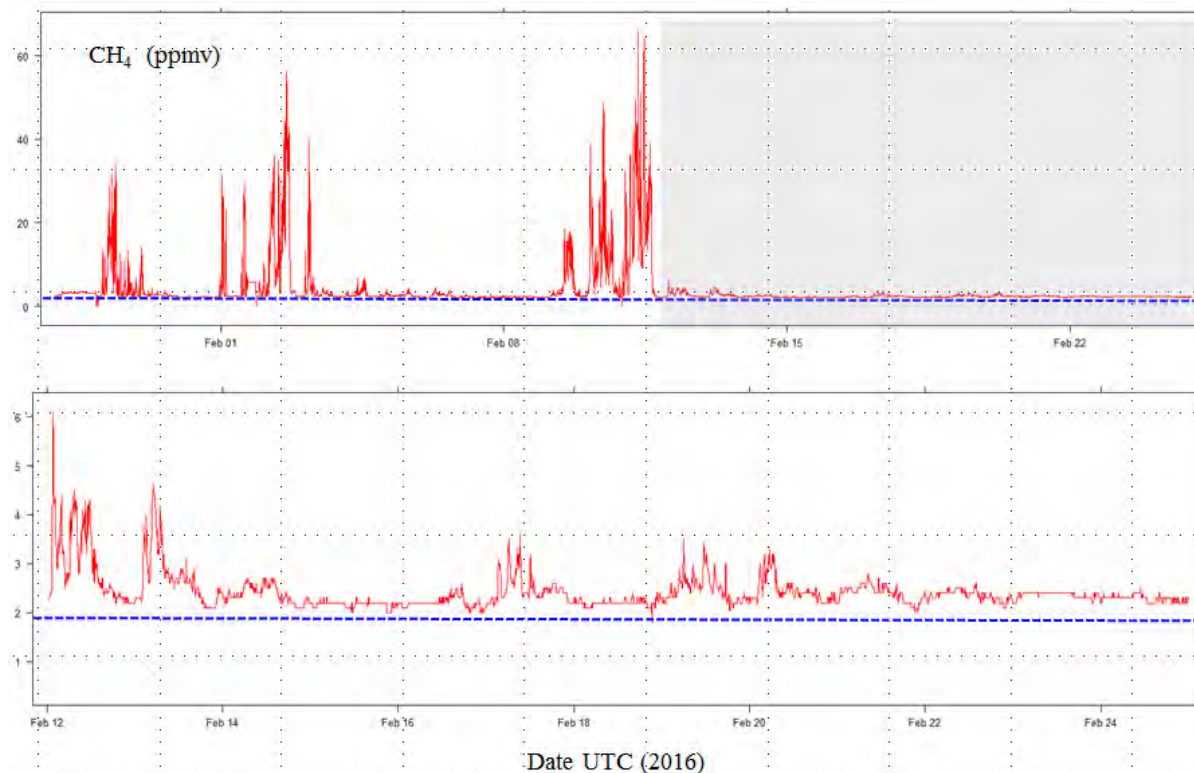


Figure 6. Time series plot of CH<sub>4</sub> in proximity of SNAQ14 (see fig 1). Top panel is from 27 January – 25 February, 2016. The gray shading corresponds to period the leak was capped, shown in higher resolution in bottom panel (12 – 25 February, 2016). Blue dashed line represents typical northern hemispheric CH<sub>4</sub> background. Note the difference in the y axis magnitude of the two plots (top is ~10 × the bottom).

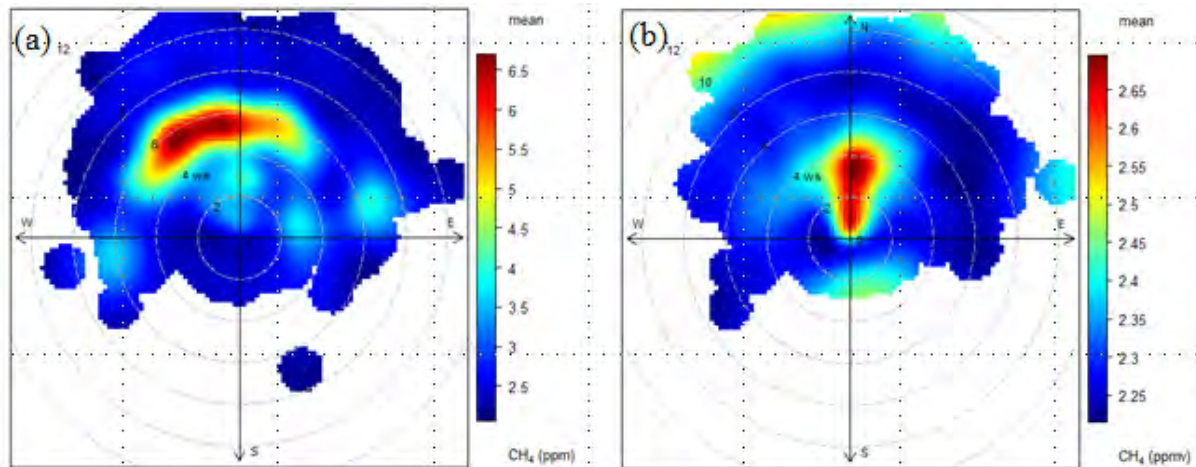


Figure 7. Polar bivariate plots of  $\text{CH}_4$  shown in figure 5. (a) 27 January – 25 February, 2016. (b) 12 – 25 February, 2016.



Figure 8. Government methane monitoring sites with official site numbers

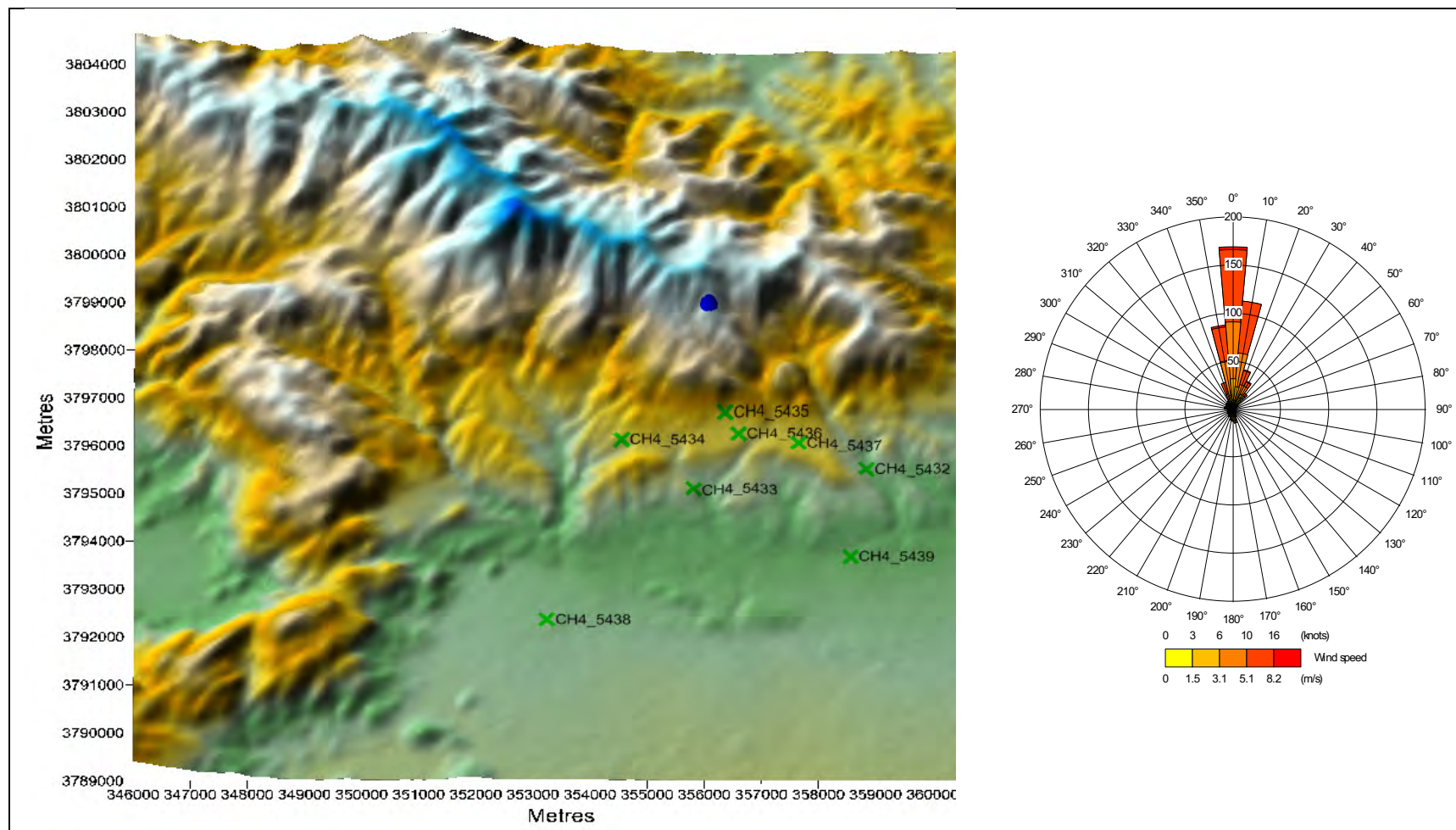
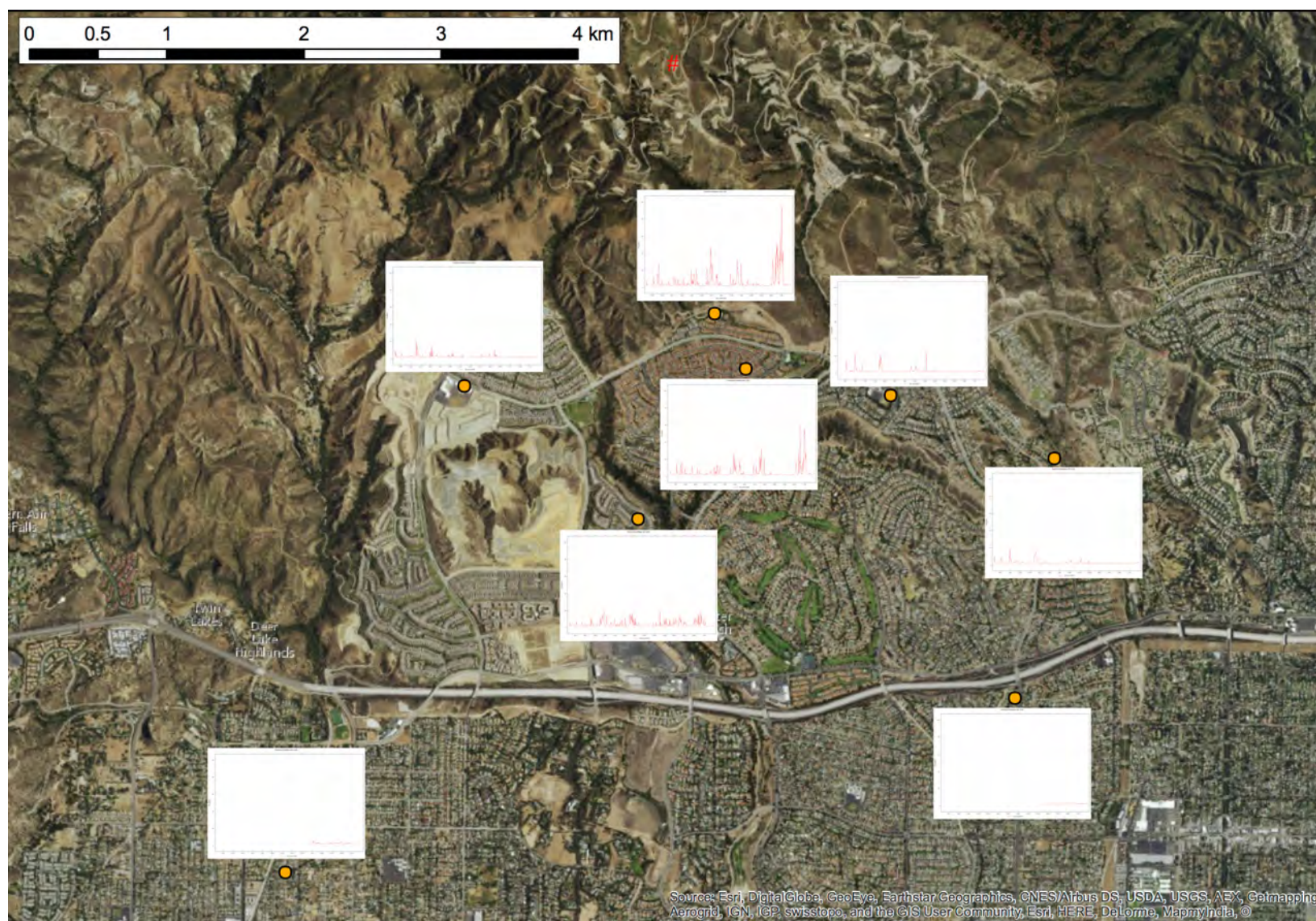
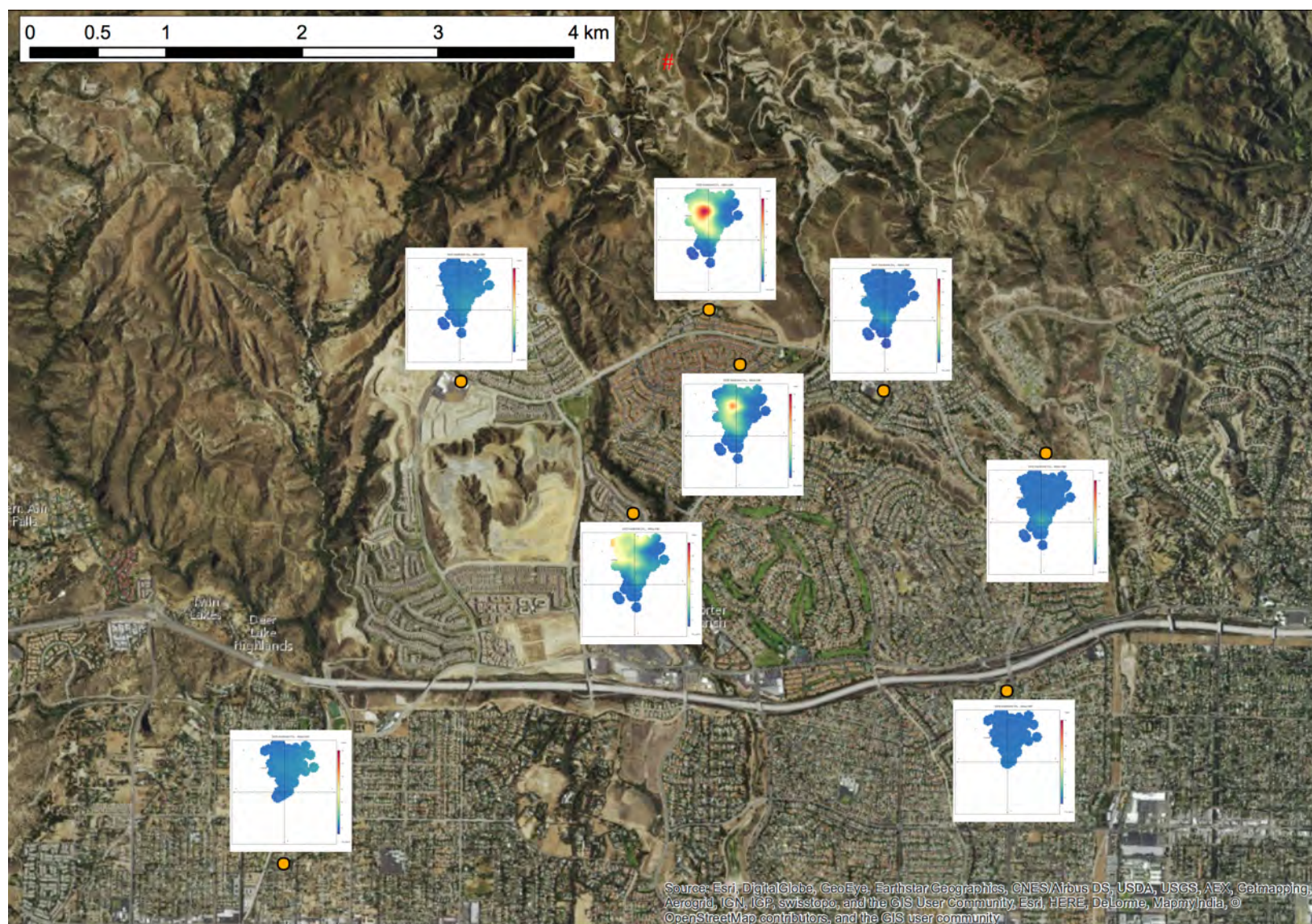


Figure 9: Modeled terrain (left) and a wind rose of the modelled meteorological data (14<sup>th</sup> January 2016 to 12<sup>th</sup> February 2016)





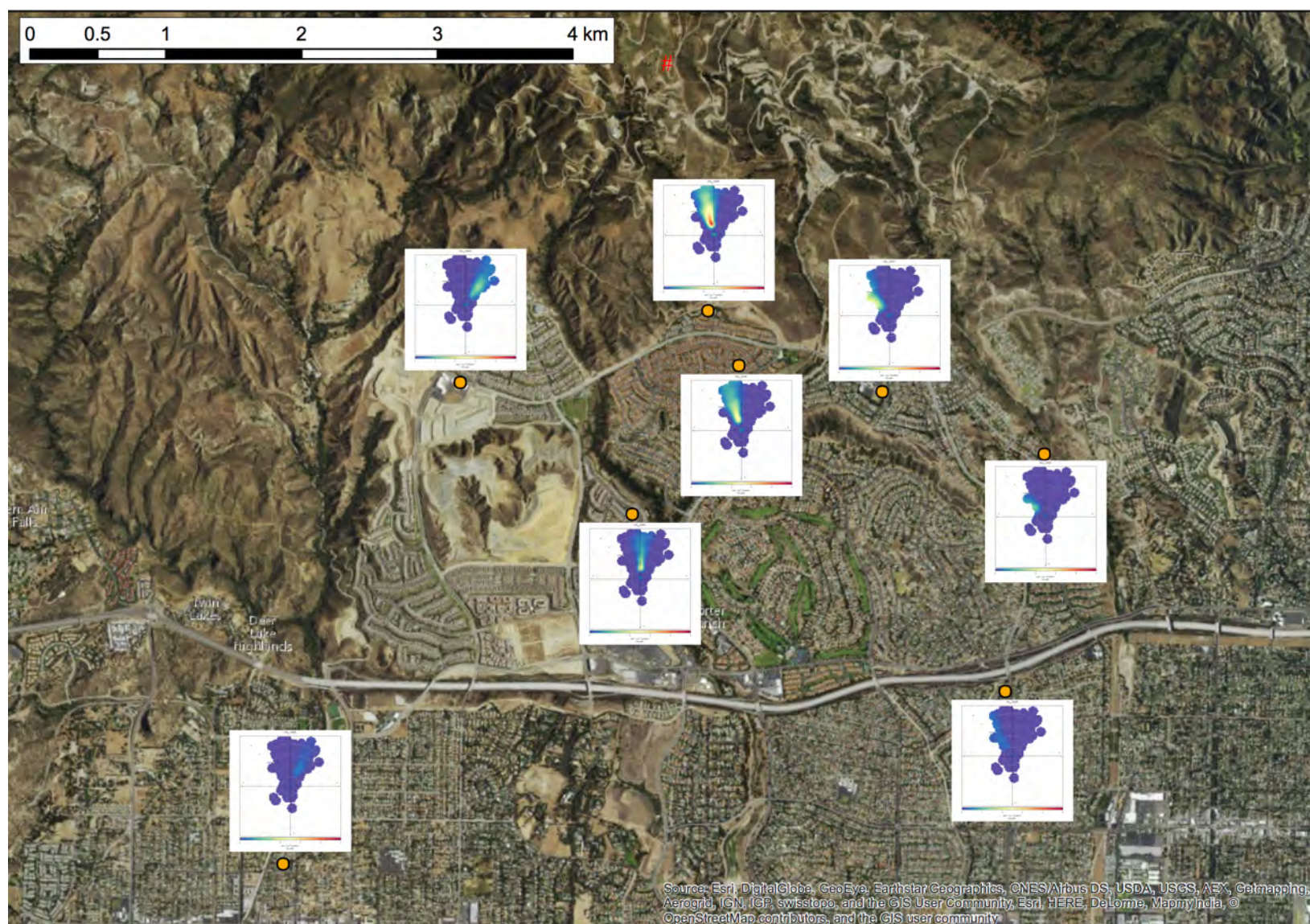


Figure 12. Polar plots of modeled concentrations for 1g/s release (5436 met data). Scale: 0 ppb – 5ppb

*Polar plots by atmospheric stability: top-left = unstable; top-right = unstable/neutral; bottom-left = neutral/stable; and bottom-right = stable*

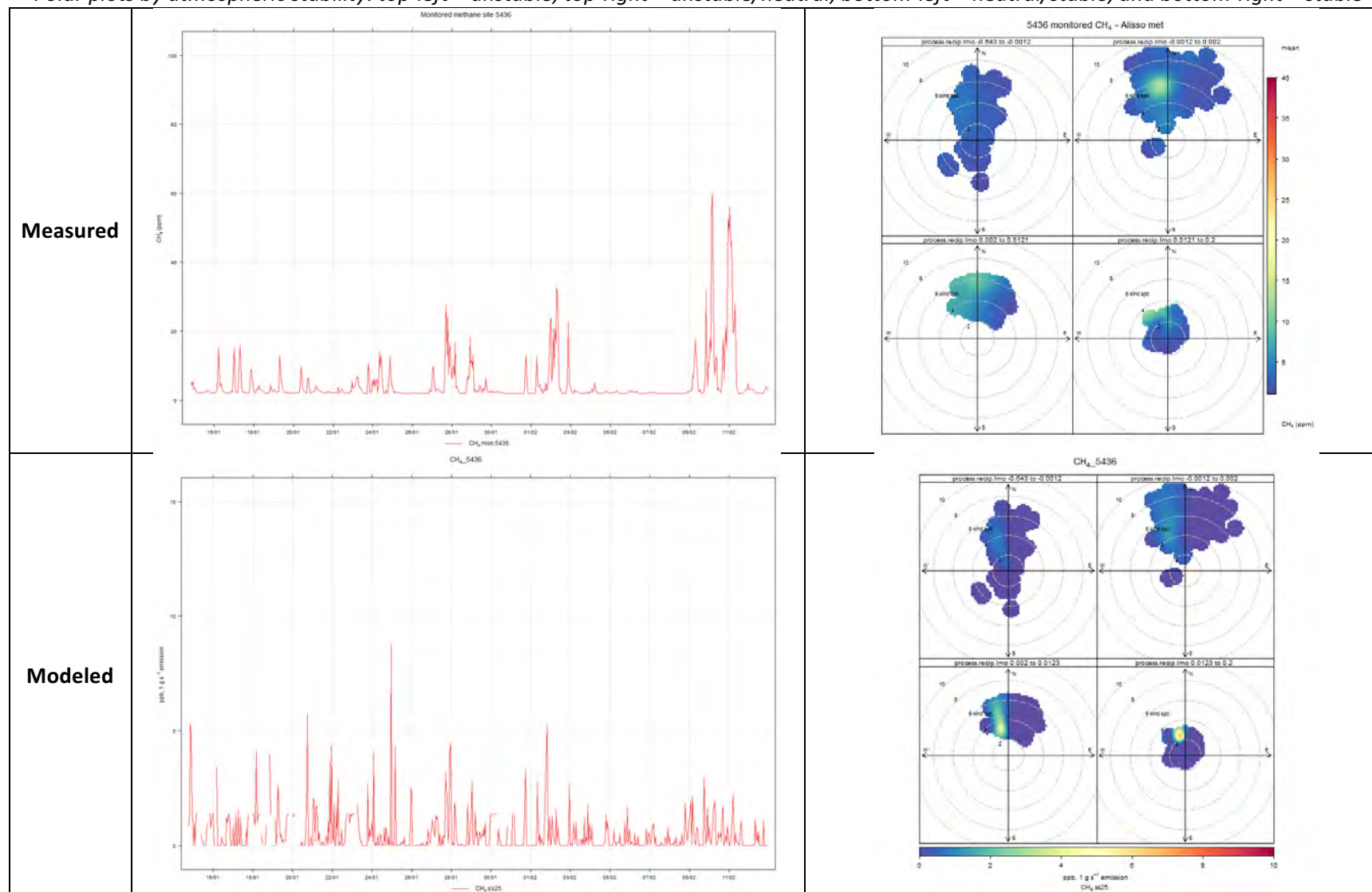


Figure 13: Time series and polar plots by atmospheric stability for site 5436

*Polar plots by atmospheric stability: top-left = unstable; top-right = unstable/neutral; bottom-left = neutral/stable; and bottom-right = stable*

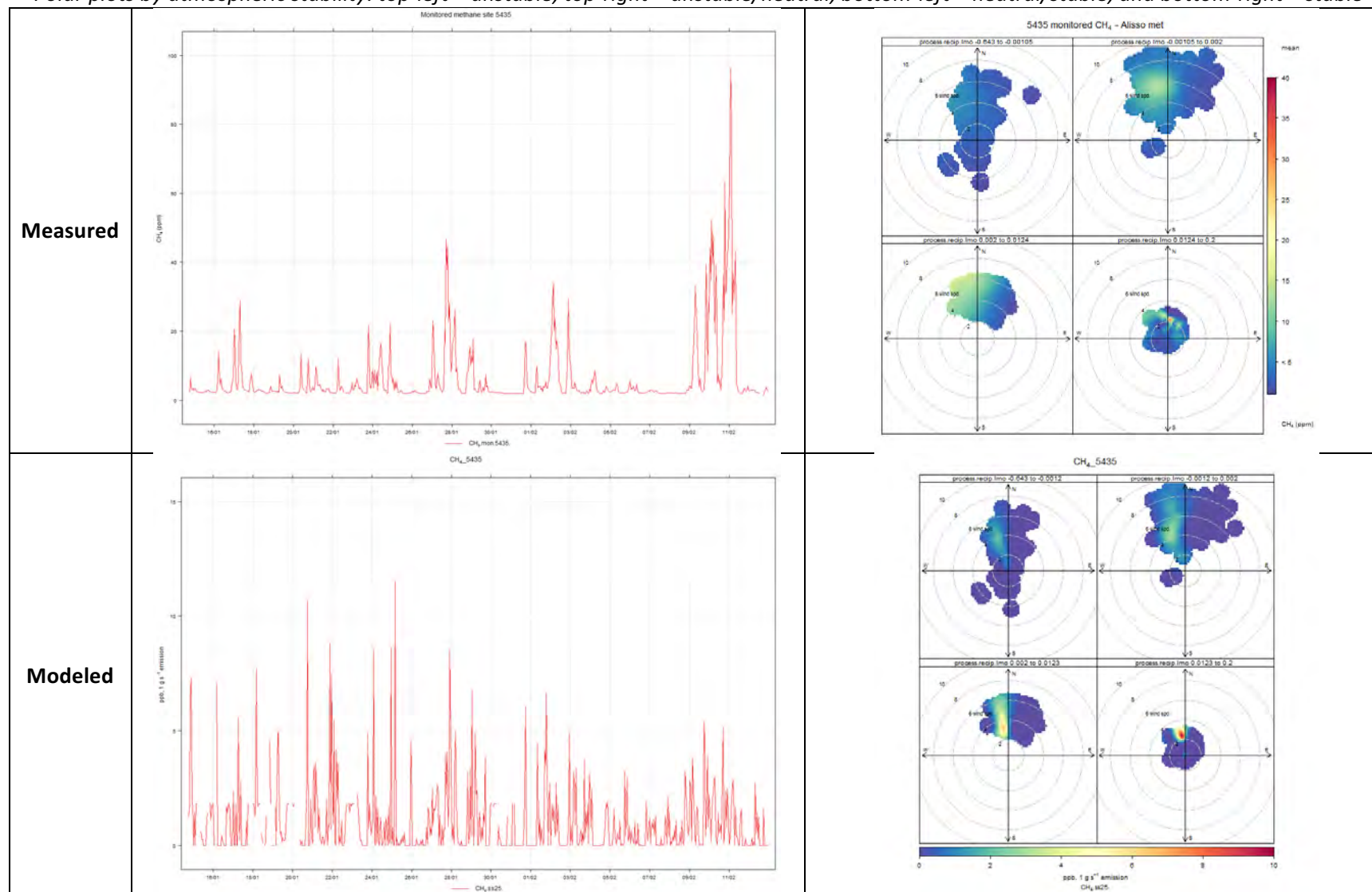


Figure 14. Time series and polar plots by atmospheric stability for site 5435

*Polar plots by atmospheric stability: top-left = unstable; top-right = unstable/neutral; bottom-left = neutral/stable; and bottom-right = stable*

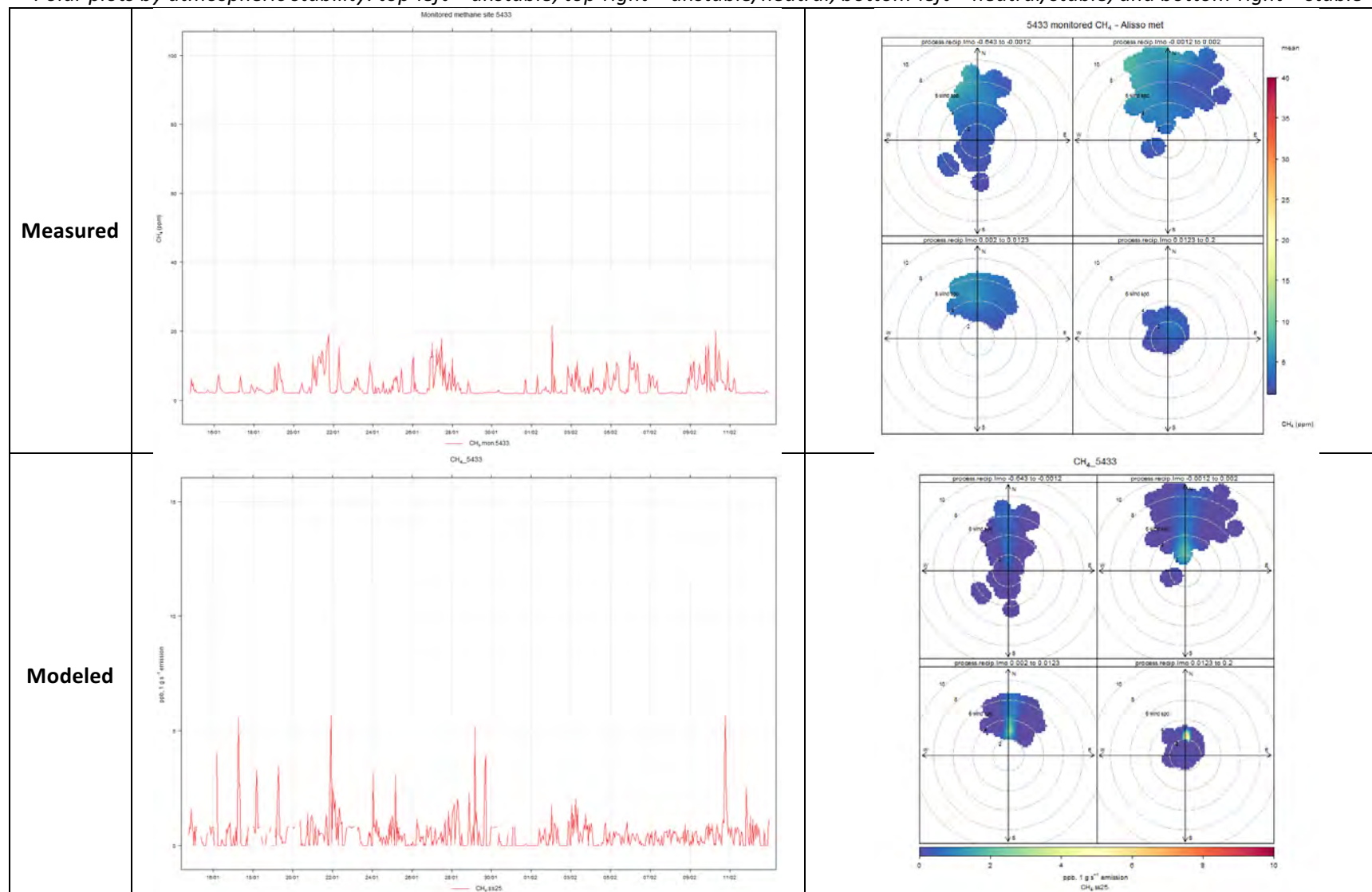


Figure 15. Time series and polar plots by atmospheric stability for site 5433

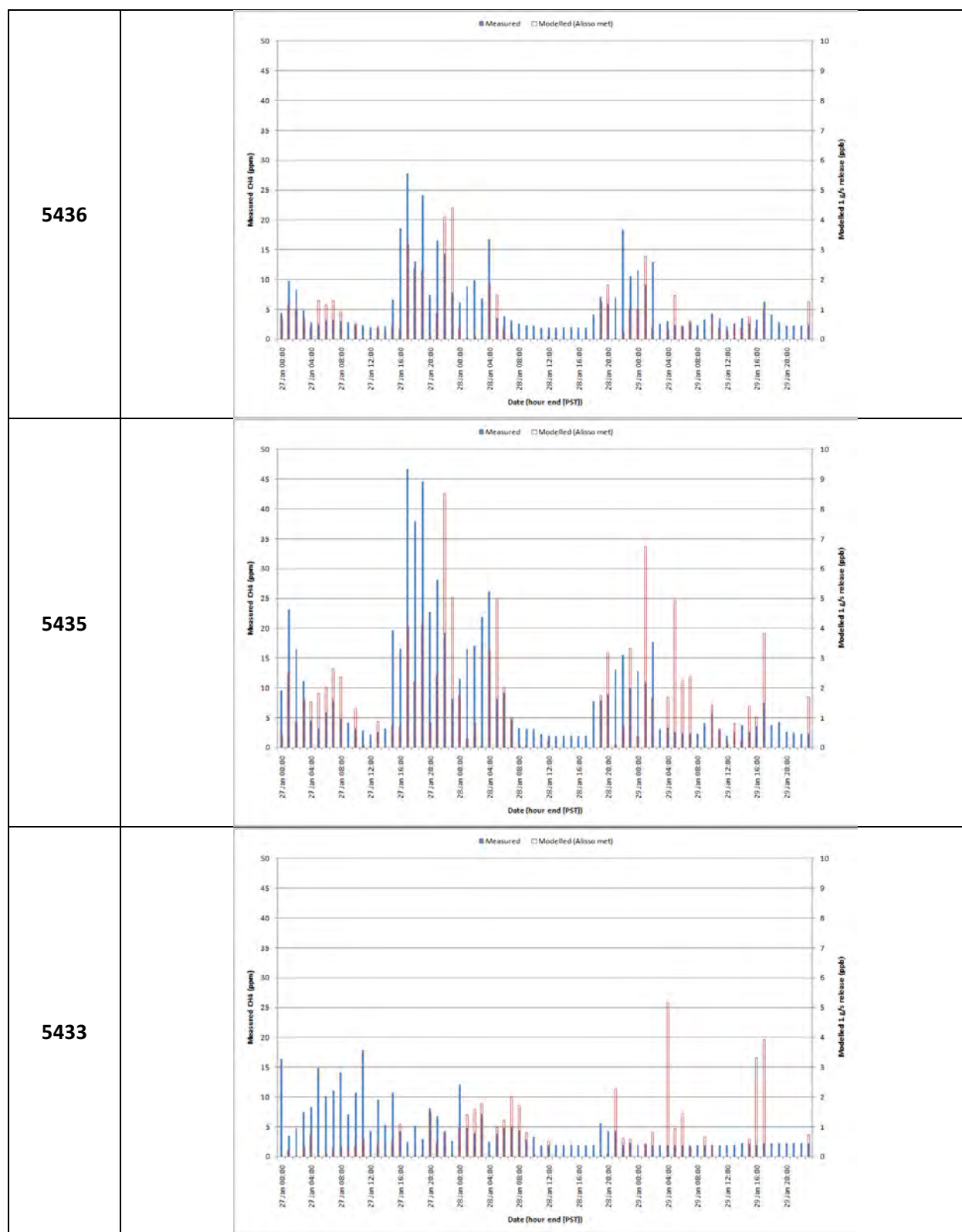


Figure 16: Measured (filled blue bars, left axis) and modeled concentrations (unfilled red bars, right axis), 27th to 29th January 2016

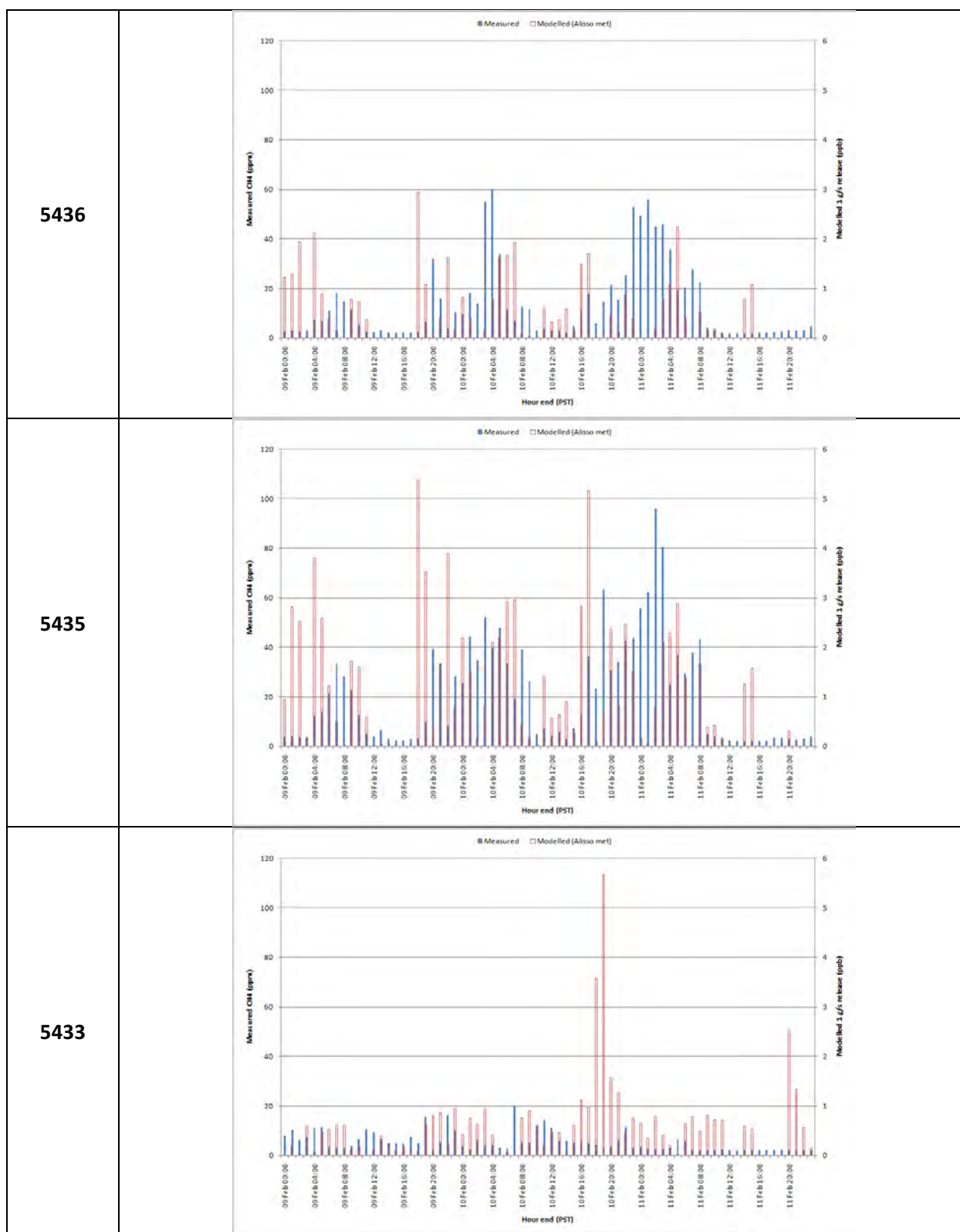


Figure 17: Measured (filled blue bars, left axis) and modeled concentrations (unfilled red bars, right axis), 9th to 11th February 2016

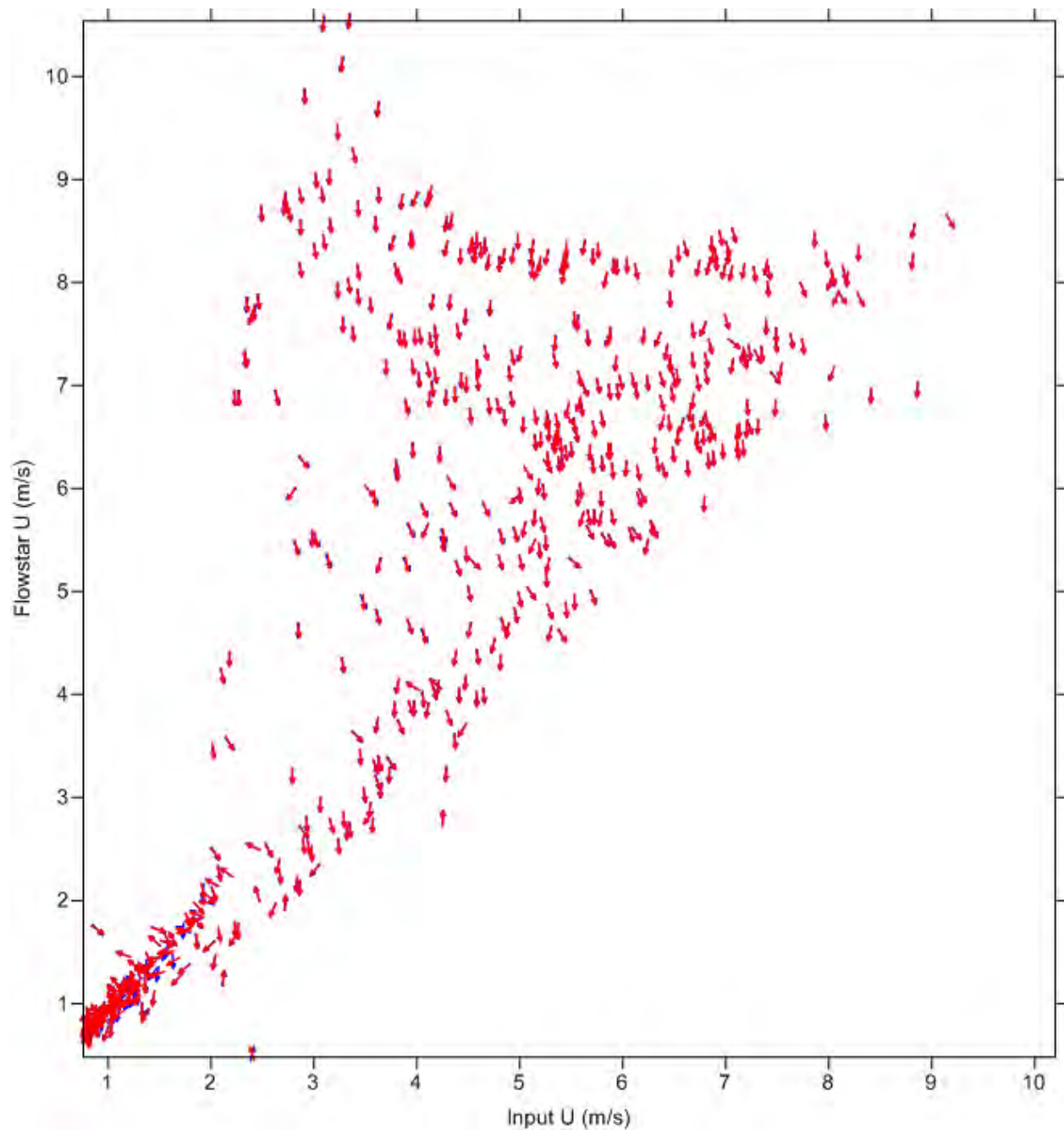


Figure 18: Scatter plot of model input wind speed (m/s) against model calculated wind speed at site 5436. The angle of the markers indicates the input wind direction (blue markers) and model calculated wind direction (red markers)

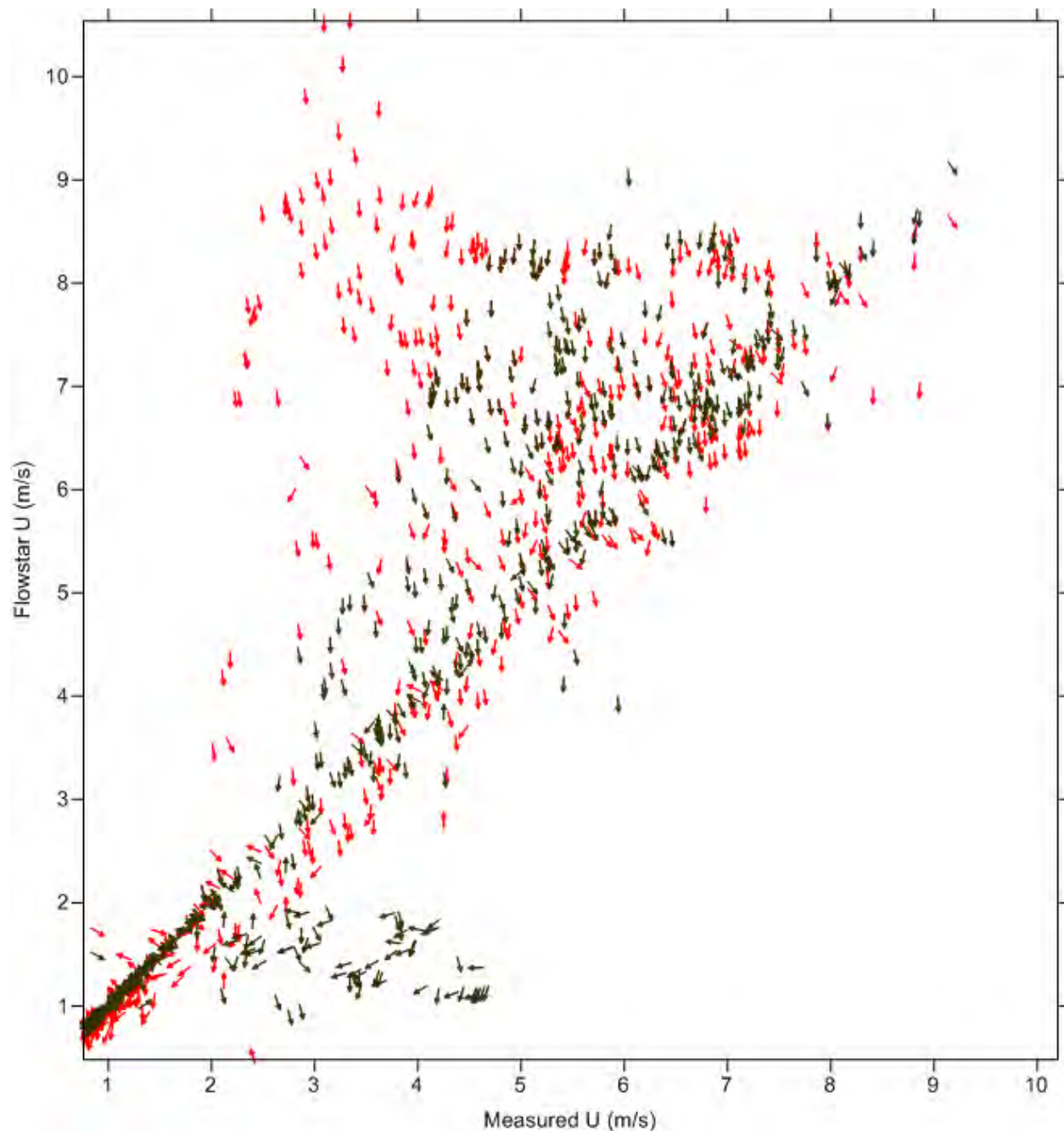


Figure 19: Scatter plot of measured wind speed (m/s) against model calculated wind speed at site 5436 for the original model (red markers) and adjusted wind speeds run (dark green markers). The marker angles indicate model calculated wind directions.

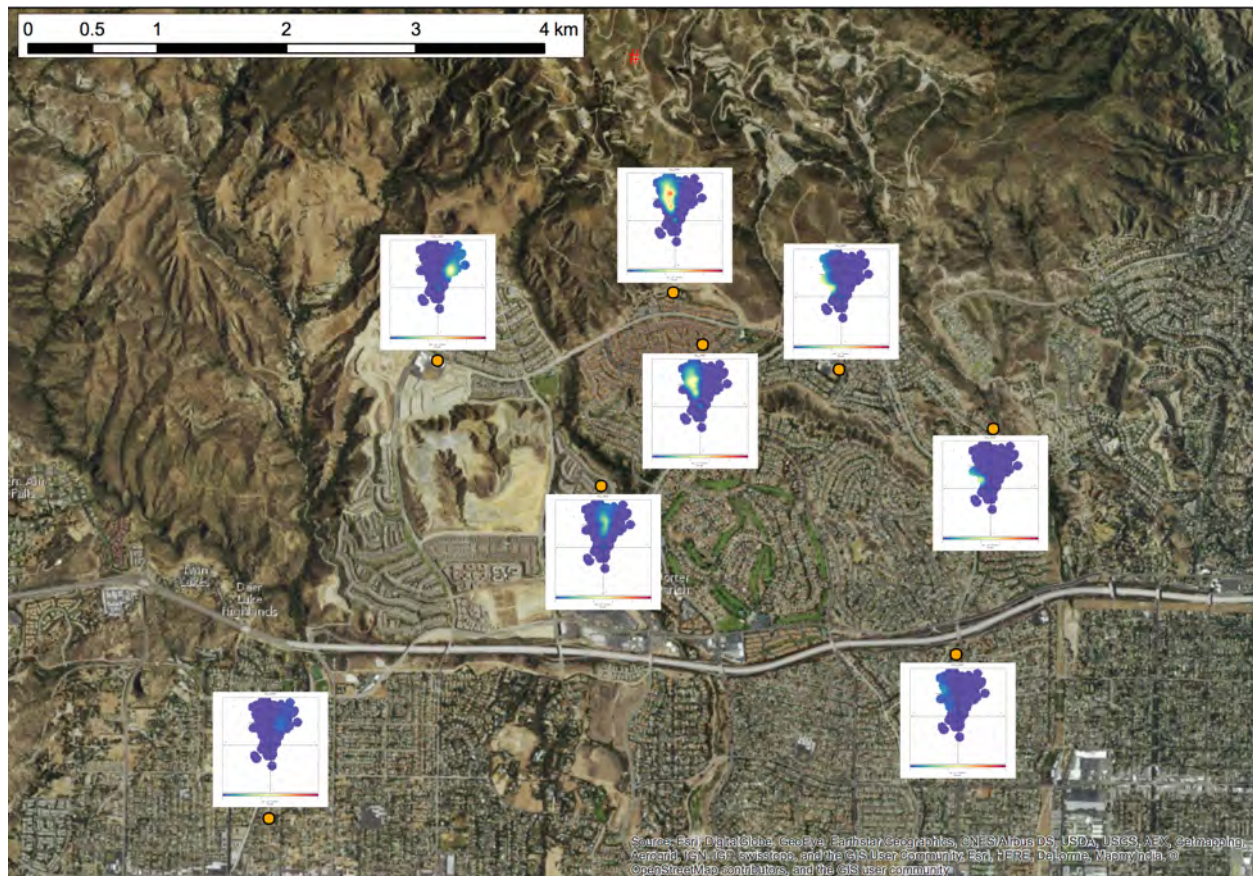


Figure 20. Polar plots of modeled concentrations with adjusted wind speeds for 1 g/s release. Scale 0 ppb – 5 ppb

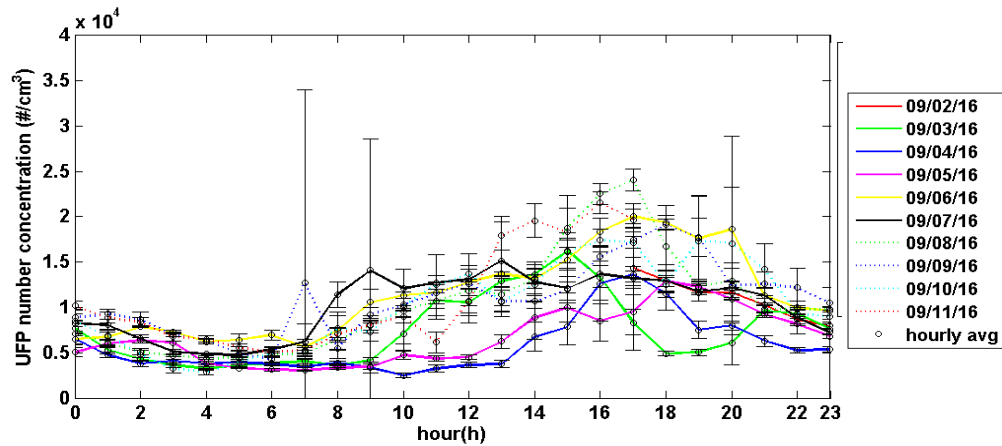


Figure 21. Hourly average ultrafine particle concentrations at the Porter Ranch Estates site during early September 2016.

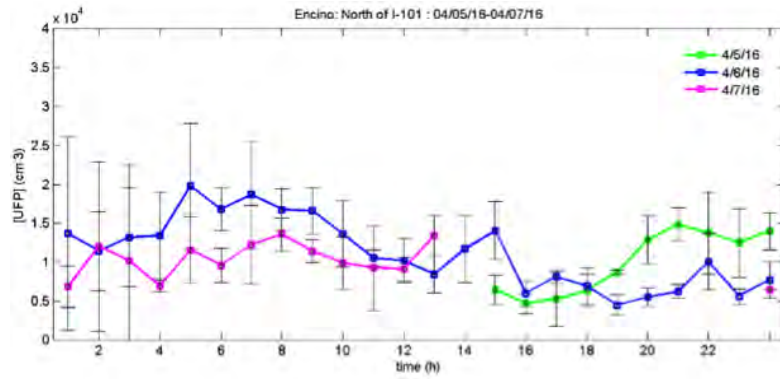


Figure 22. One minute average ultrafine particle concentrations at a site in Encino 20 m north of the 101-freeway collected during April 2016.

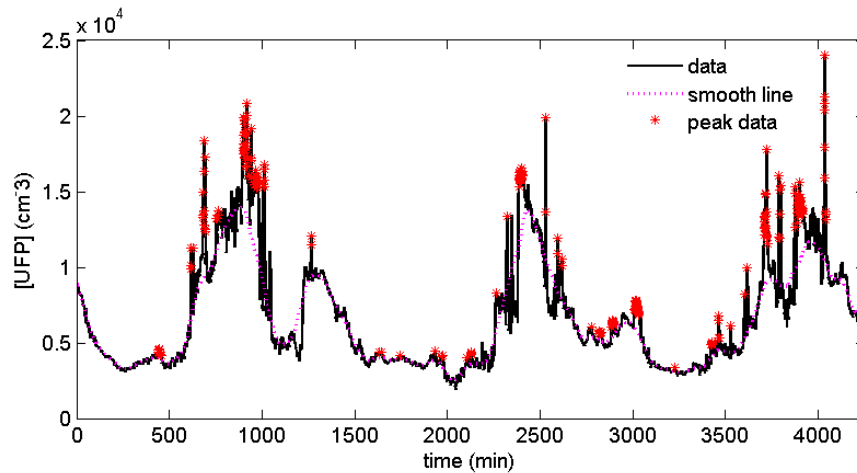


Figure 23. Filtering of peak data set for the 3/9/16-5/9/16 period. The black solid line is the [UFP] time series. The magenta dashed line is the smooth line over a 2h period and the red stars are data points falling one standard deviation above the calculated background level.

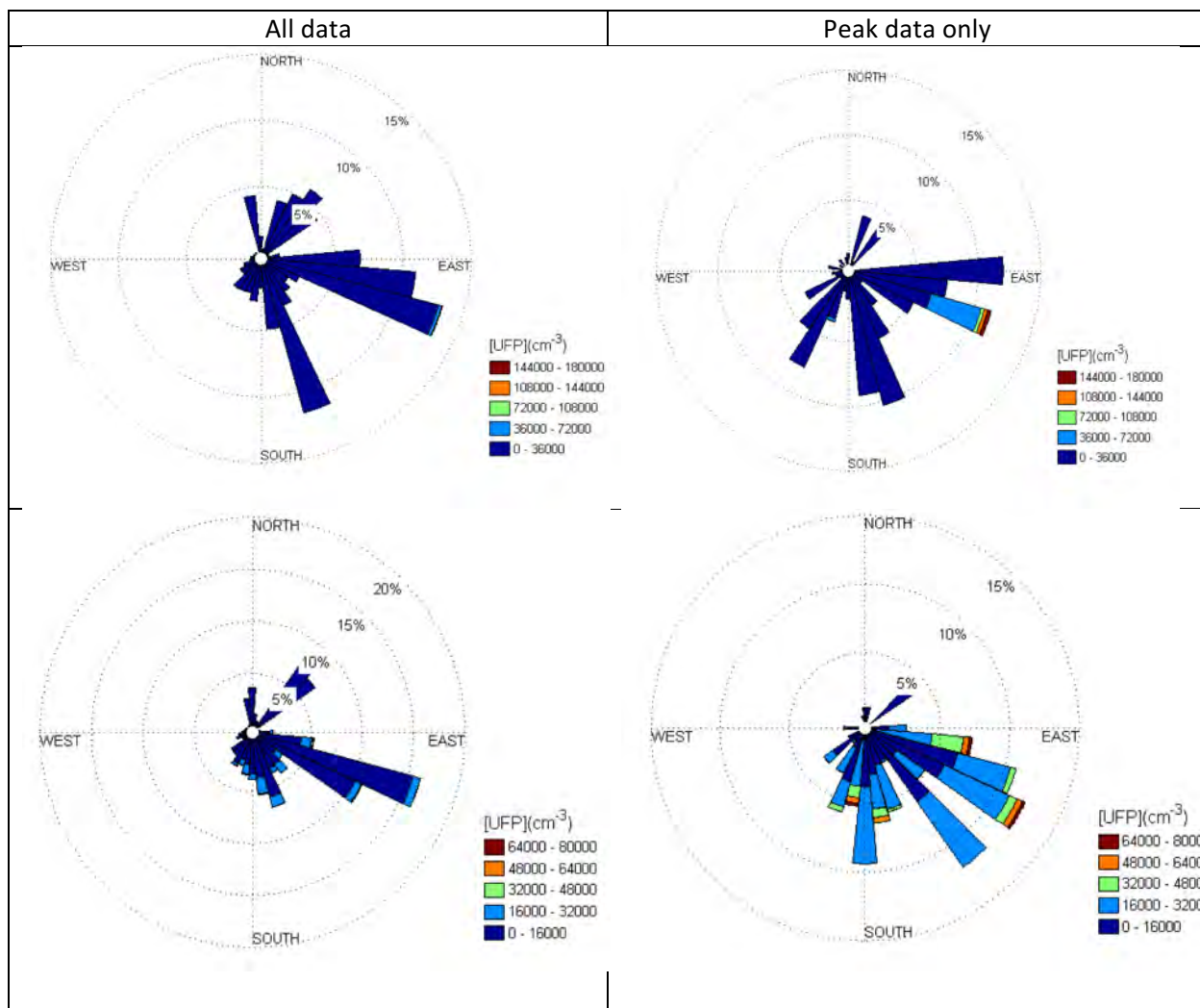


Figure 24. Ultrafine particle number concentration-wind direction roses for UFP monitoring conducted in Porter Ranch on dates at [Top row: PRE 5/27/16 – 5/31/16; Bottom row: PRE 7/01/16 – 7/05/16]. The left panels show all data, and the right panels show peak data only, defined as data more than 1 standard deviation above the local baseline (discussed above and illustrated in Figure 23). Wind data are from the Fenceline monitoring station, slightly north west and closer to the base of the mountains than the measurement site in Porter Ranch Estates.

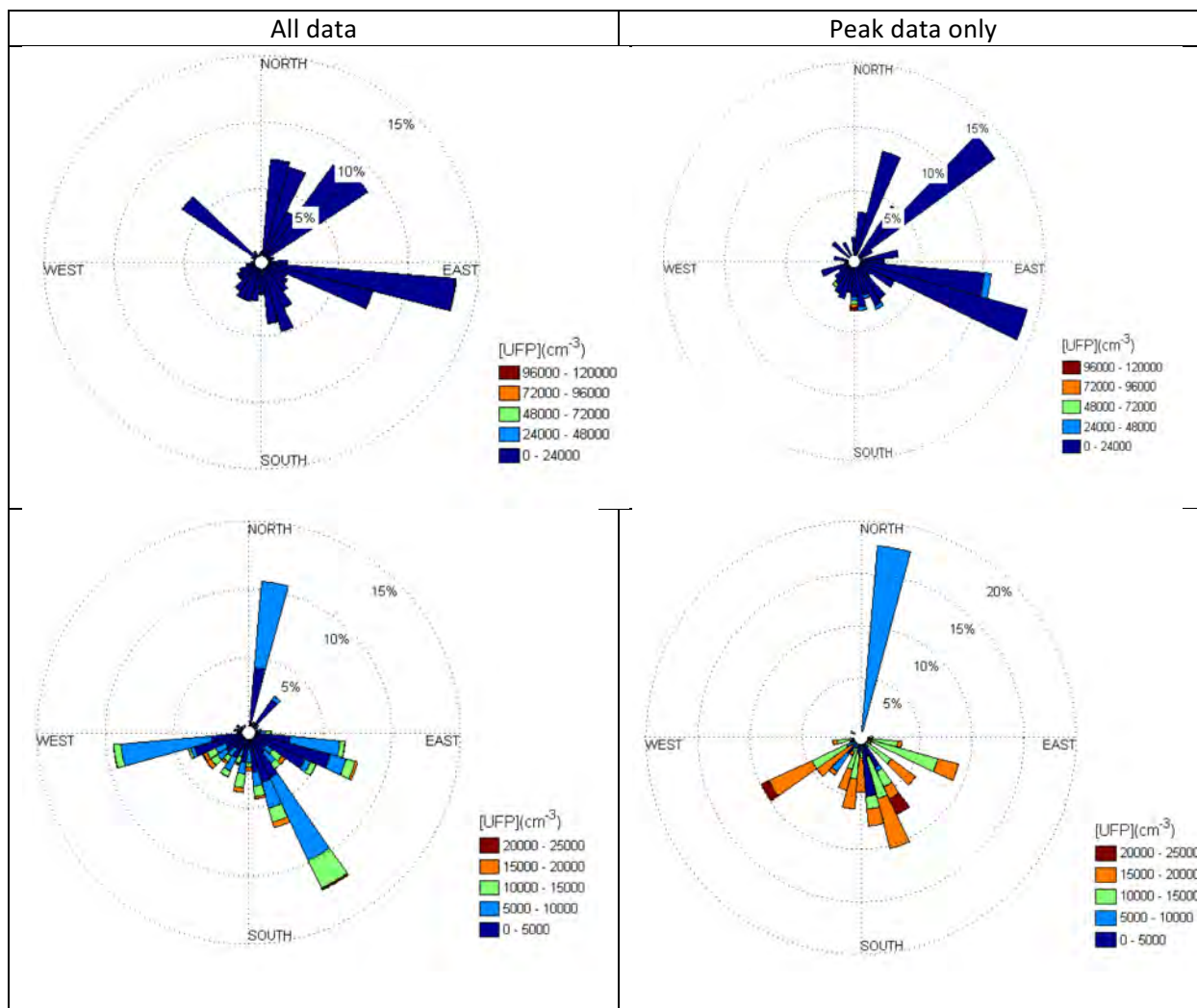


Figure 25. Ultrafine particle number concentration -wind direction roses for UFP monitoring conducted in Porter Ranch on dates at [Top row: PRE 7/11/16 – 7/15/16; Bottom row: PRE 9/03/16 – 9/05/16]. The left panels show all data, and the right panels show peak data only, defined as data more than 1 standard deviation above the local baseline (discussed above and illustrated in Figure 23). Wind data are from the Fenceline monitoring station, slightly north west and closer to the base of the mountains than the measurement site in Porter Ranch Estates.

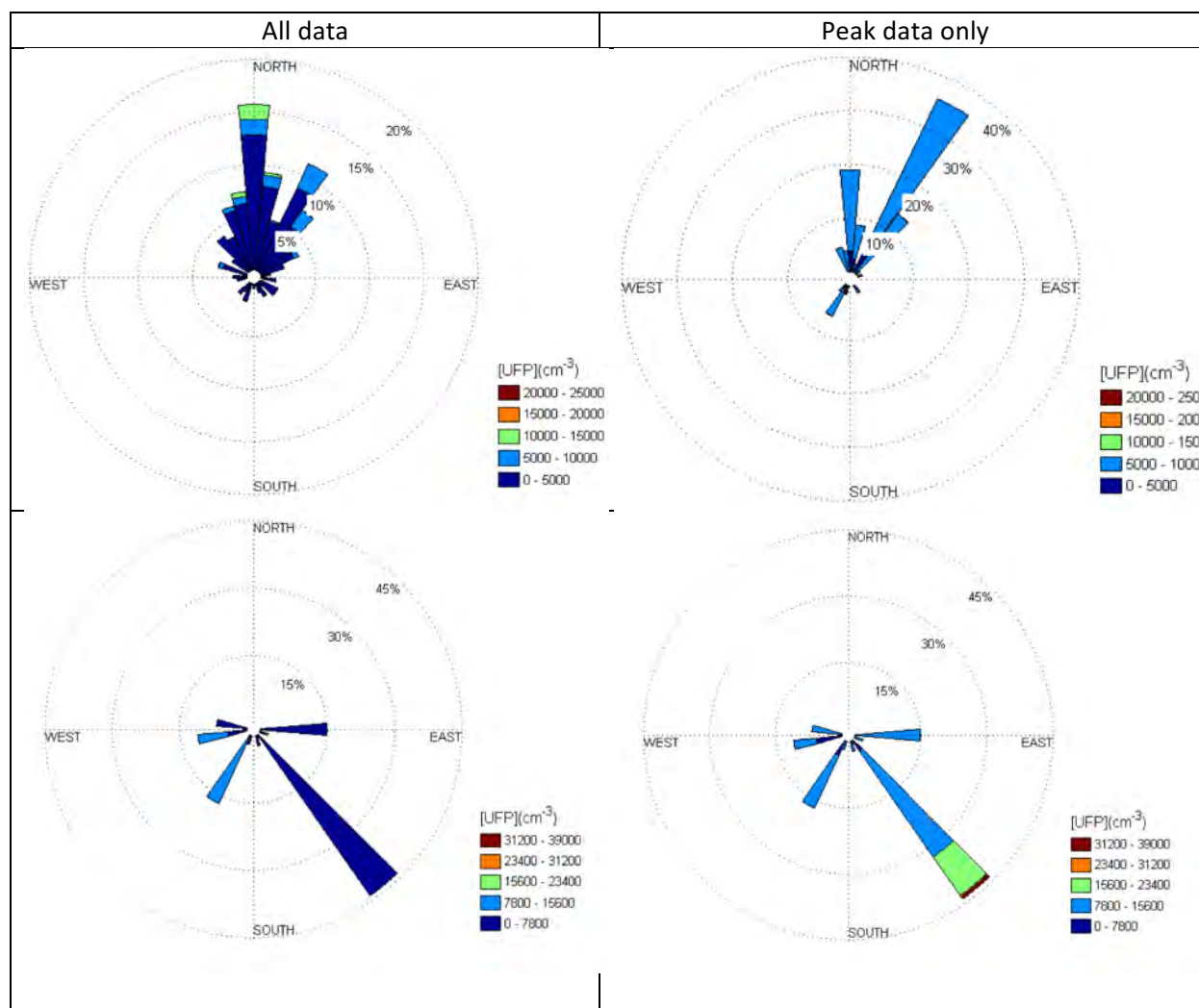


Figure 26. Ultrafine particle number concentration -wind direction roses for UFP monitoring conducted in Porter Ranch on dates at [Top row: PRE 1/28/17 – 1/30/17; Bottom row: PRE 1/30/17 – 2/2/17]. The left panels show all data, and the right panels show peak data only, defined as data more than 1 standard deviation above the local baseline (discussed above and illustrated in Figure 23). Wind data are from Chatsworth (EW9895), to the south of the measurement site, and are expected to be representative of the regional flow.

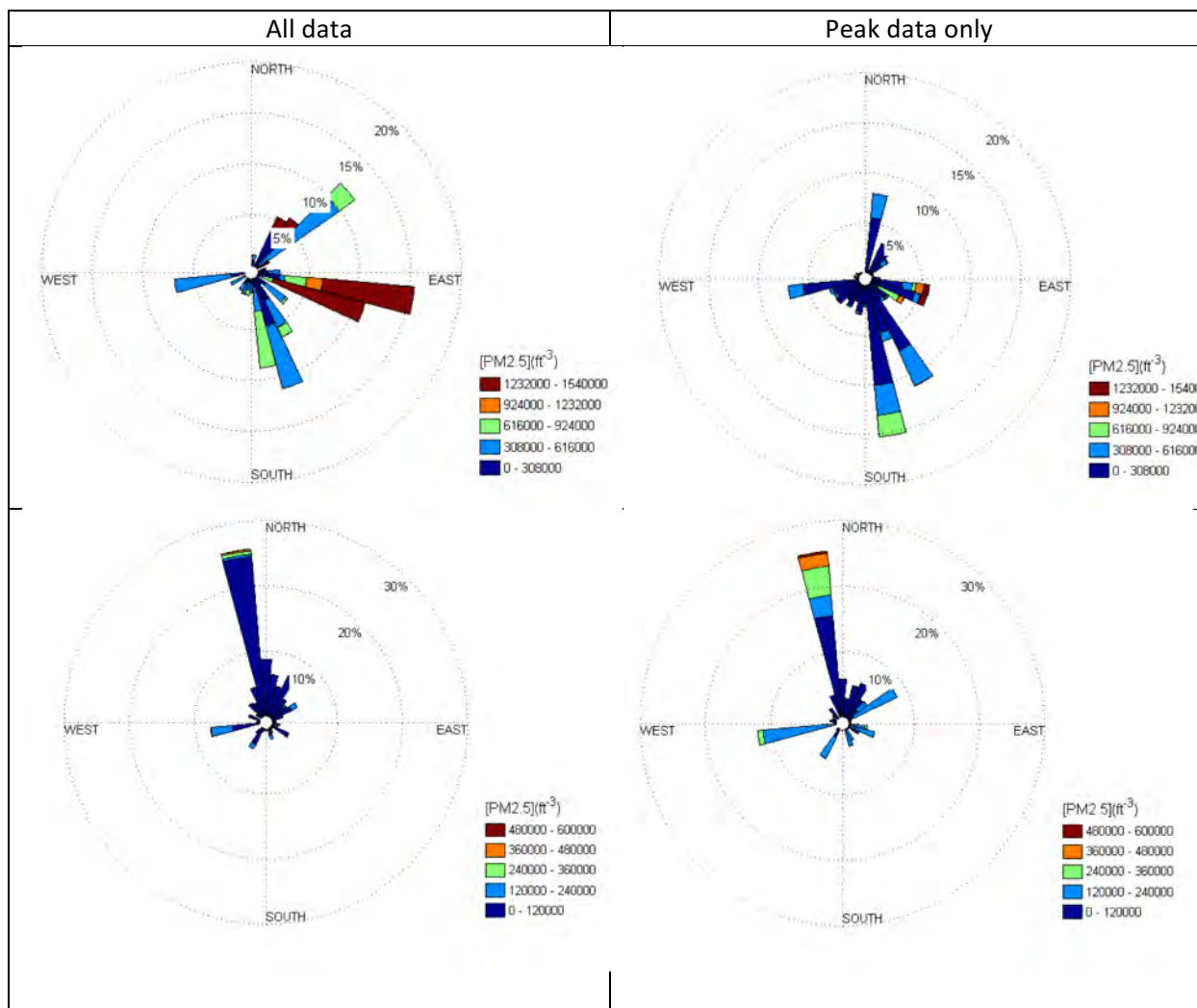


Figure 27. Concentration-wind direction roses for PM<sub>2.5</sub> (0.5 -2.5  $\mu\text{m}$ ) number concentration monitoring conducted in Porter Ranch at [Top row: PRE 9/02/16 – 9/06/16; Bottom row: PRE 1/28/17 – 1/30/17]. The left panels show all data, and the right panels show peak data only, defined as data more than 1 standard deviation above the local baseline (discussed above and illustrated in Figure 21). Wind data for September are from the Fenceline monitoring station, slightly north west and closer to the base of the mountains than the measurement site. January wind data are from Chatsworth (EW9895), to the south of the measurement site, and are expected to be representative of the regional flow.

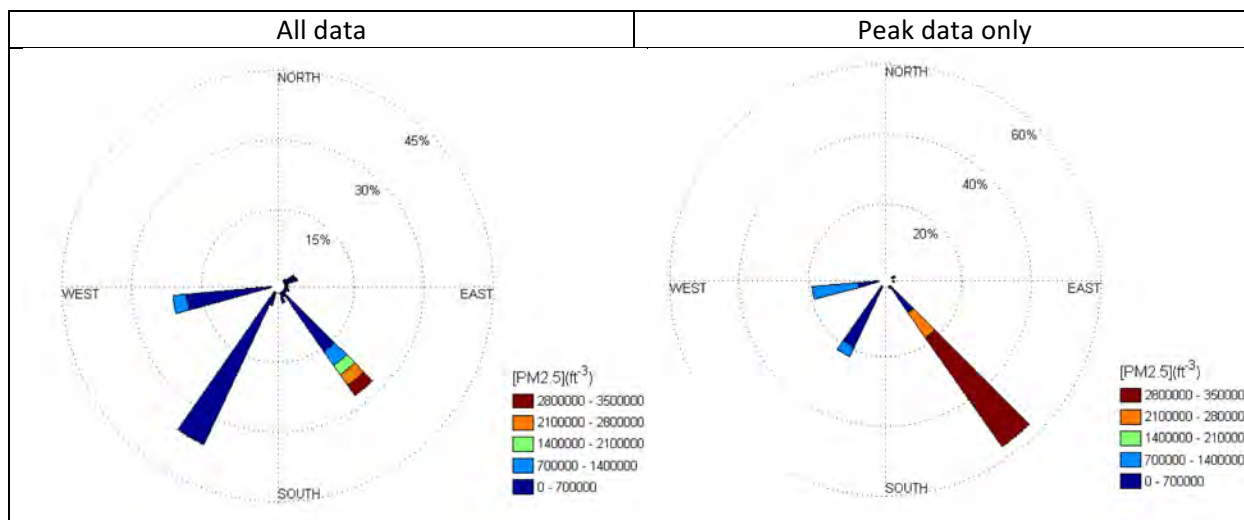


Figure 28. Concentration-wind direction roses for PM<sub>2.5</sub> (0.5 -2.5  $\mu\text{m}$ ) number concentration monitoring conducted in Porter Ranch at [H2 1/30/17 – 2/02/17]. The left panels show all data, and the right panels show peak data only, defined as data more than 1 standard deviation above the local baseline (discussed above and illustrated in Figure 1). Wind data are from Chatsworth (EW9895), to the south of the measurement site, and are expected to be representative of the regional flow.

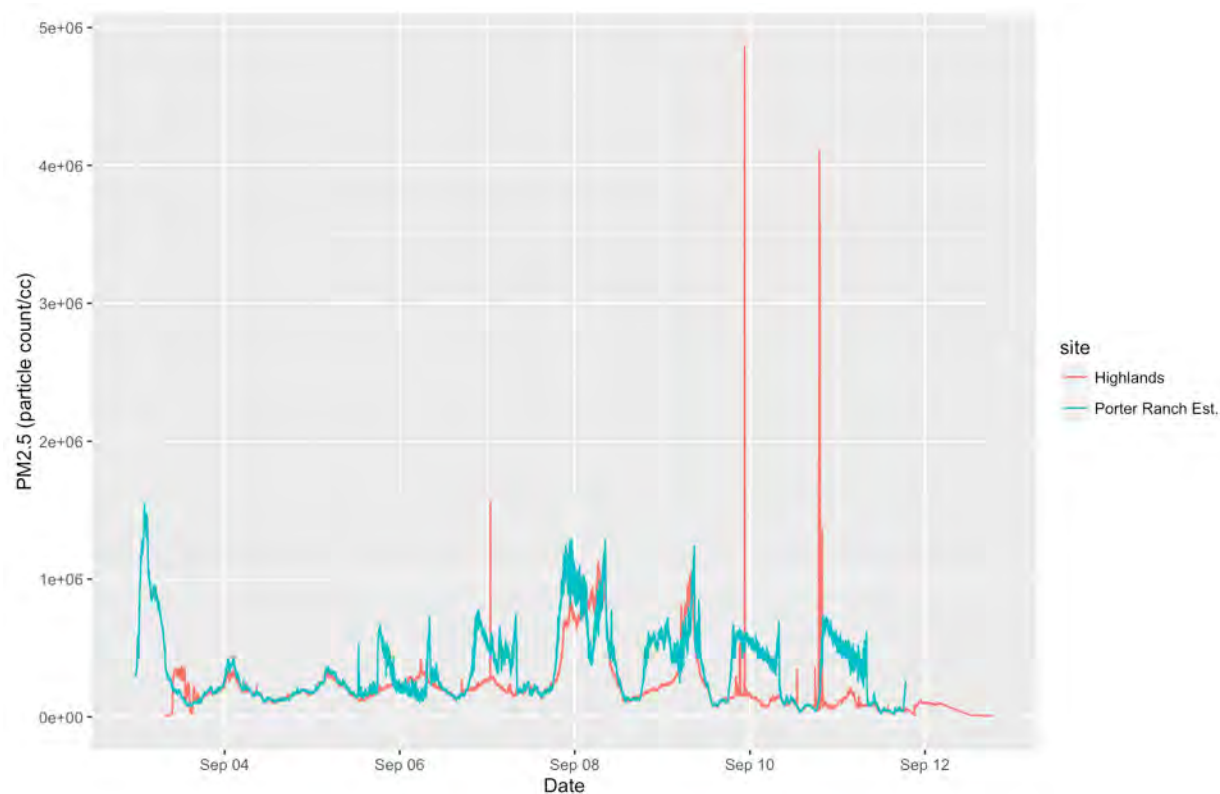


Figure 29. Time series of Dylos instrument collection early to mid-September at Highlands (H2) and Porter Ranch Estates (PRE).

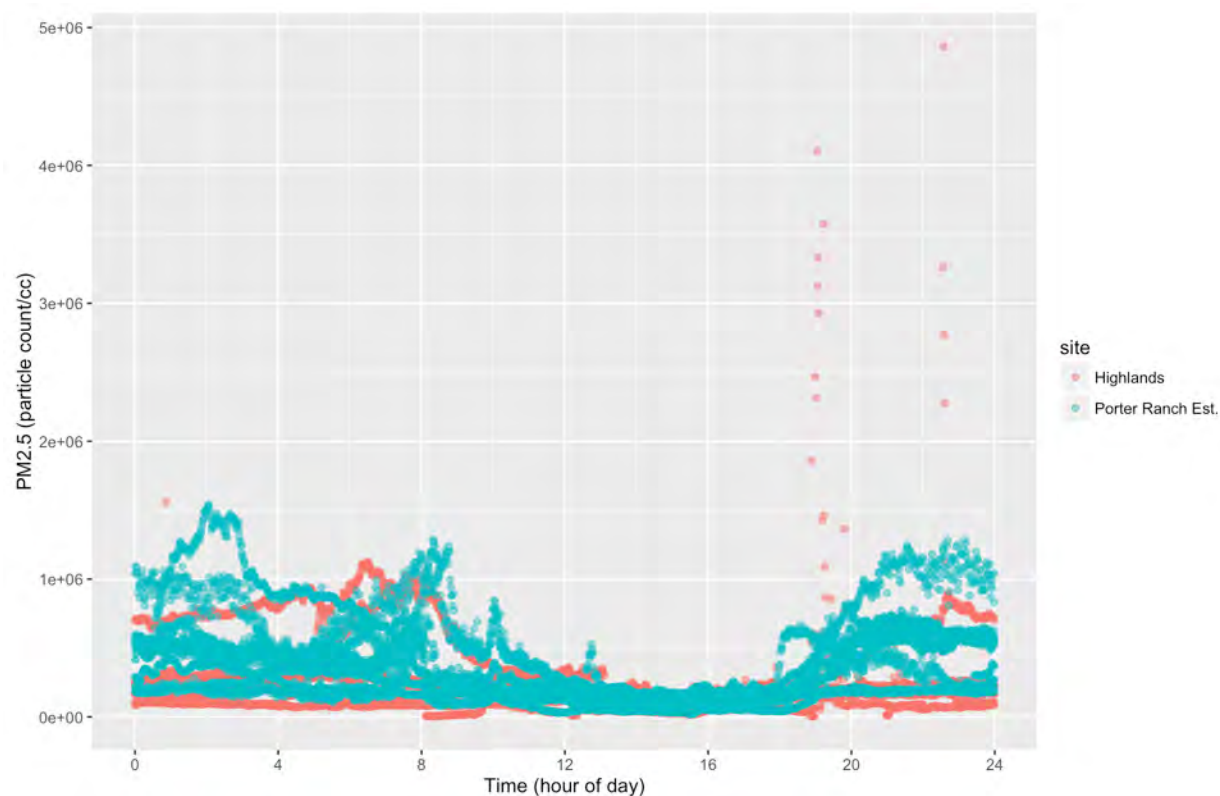


Figure 30. Dylos measurements plotted against hour of day (September 3 – 13, 2016)

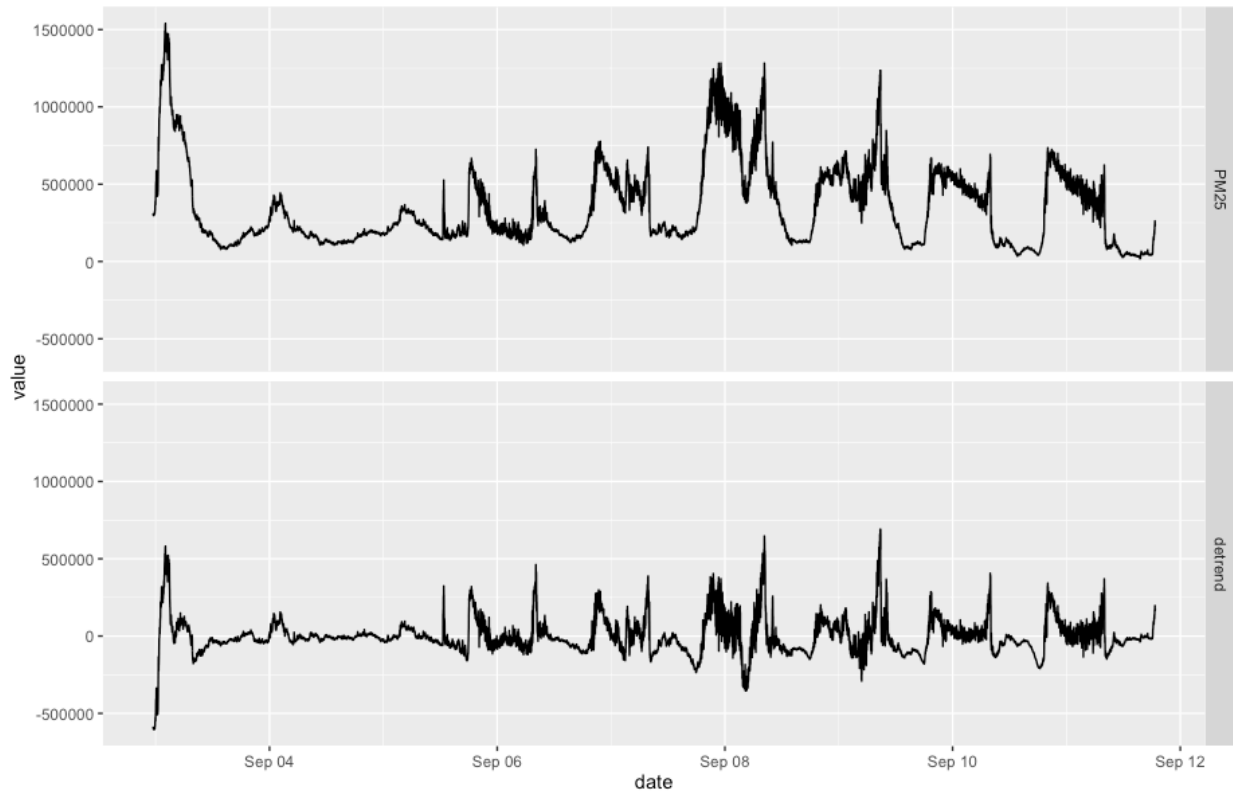


Figure 31. Unfiltered and detrended time series data at Porter Ranch Estates (PRE)

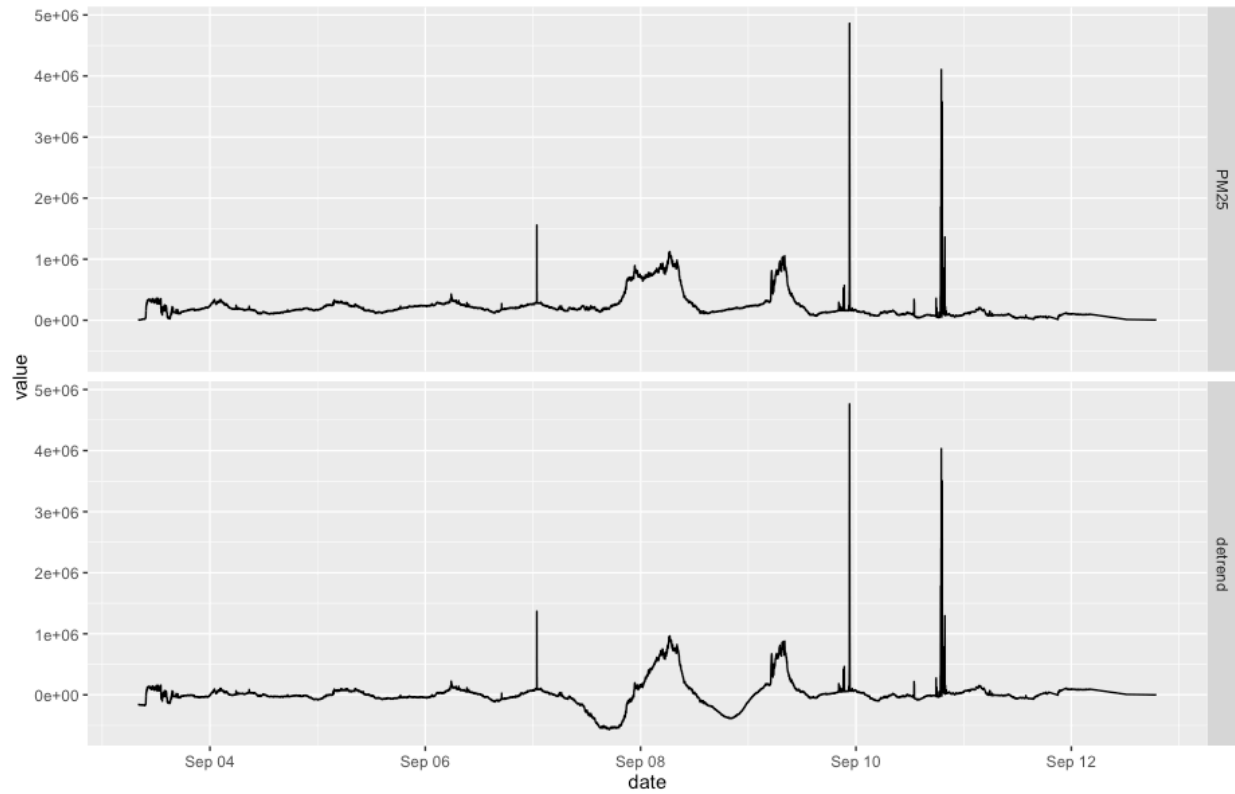


Figure 33. Unfiltered and detrended time series data at Highland Estates (H2)

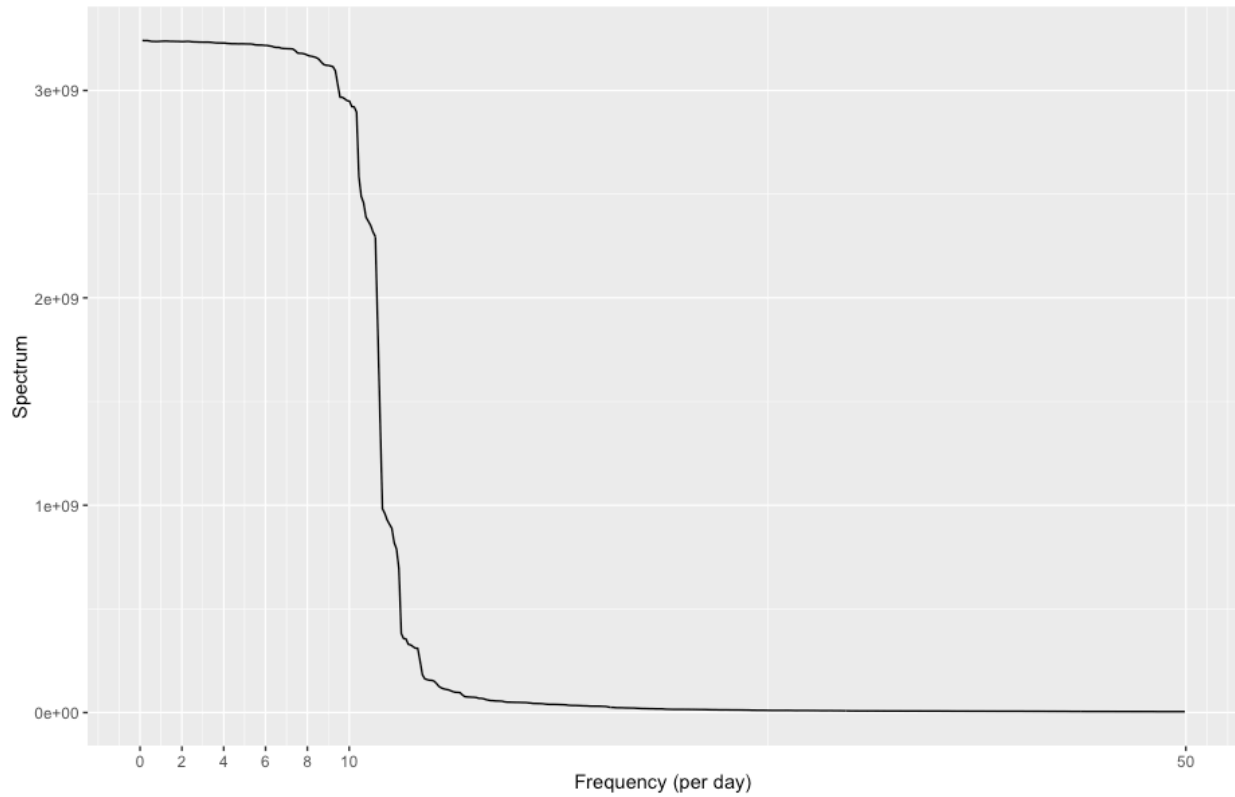


Figure 34. Spectrogram created with Fast Fourier Transform for raw data collected at Porter Ranch Estates (PRE)

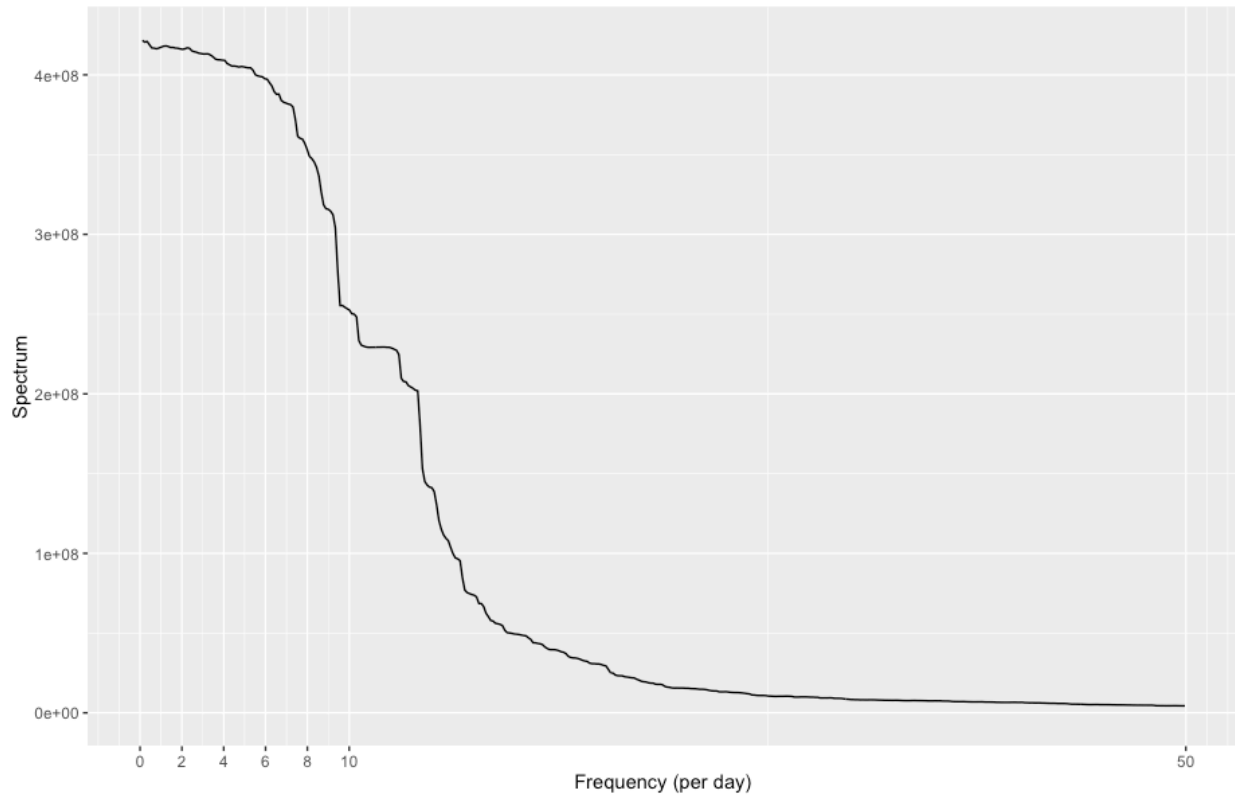


Figure 35. Spectrogram created with Fast Fourier Transform for detrended data collected at Porter Ranch Estates (PRE)

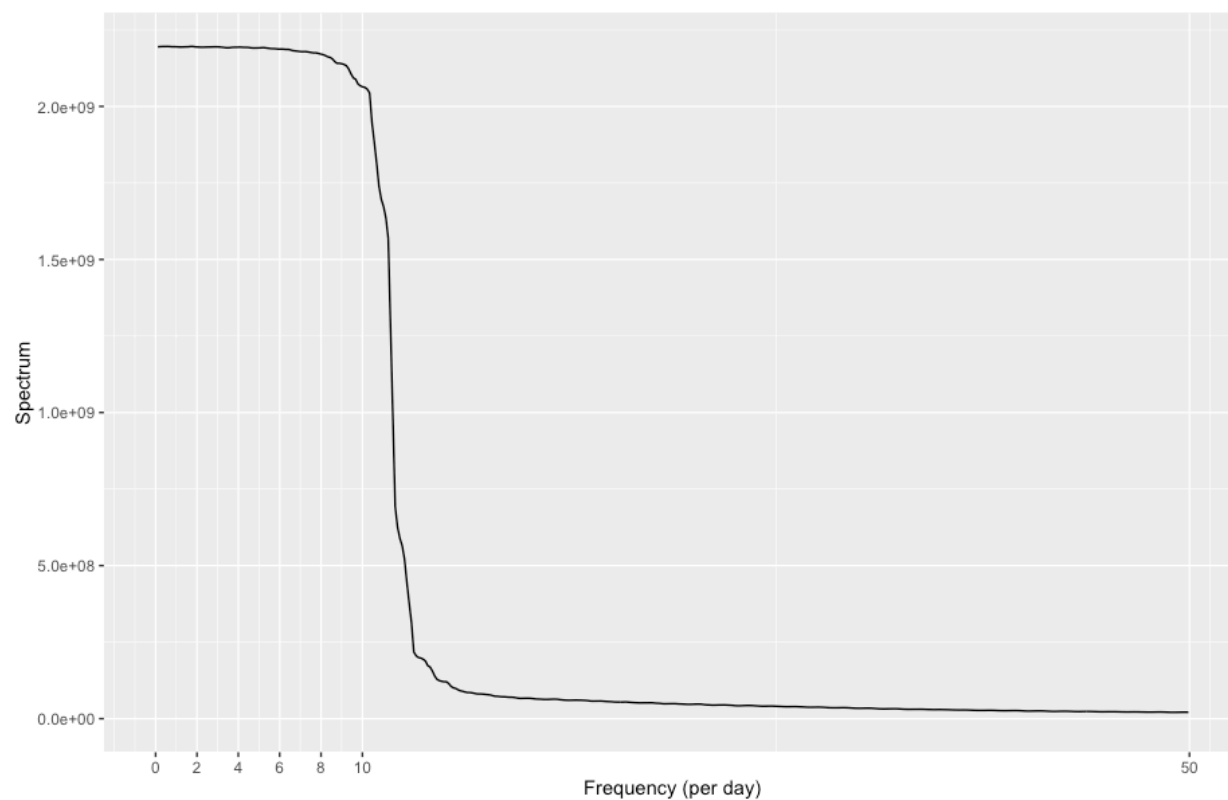


Figure 36. Spectrogram created with Fast Fourier Transform for raw data collected at Highland Estates (H2)

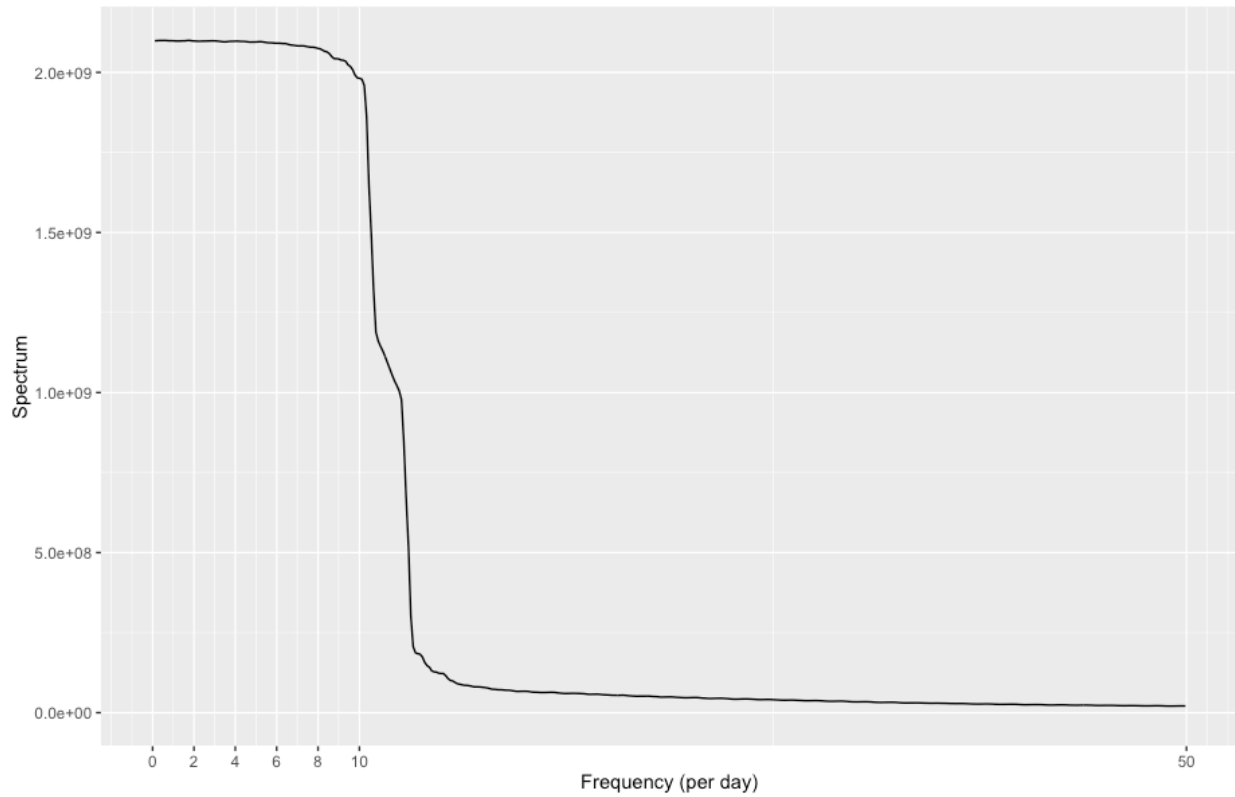


Figure 37. Spectrogram created with Fast Fourier Transform for detrended data collected at Highland Estates (H2)

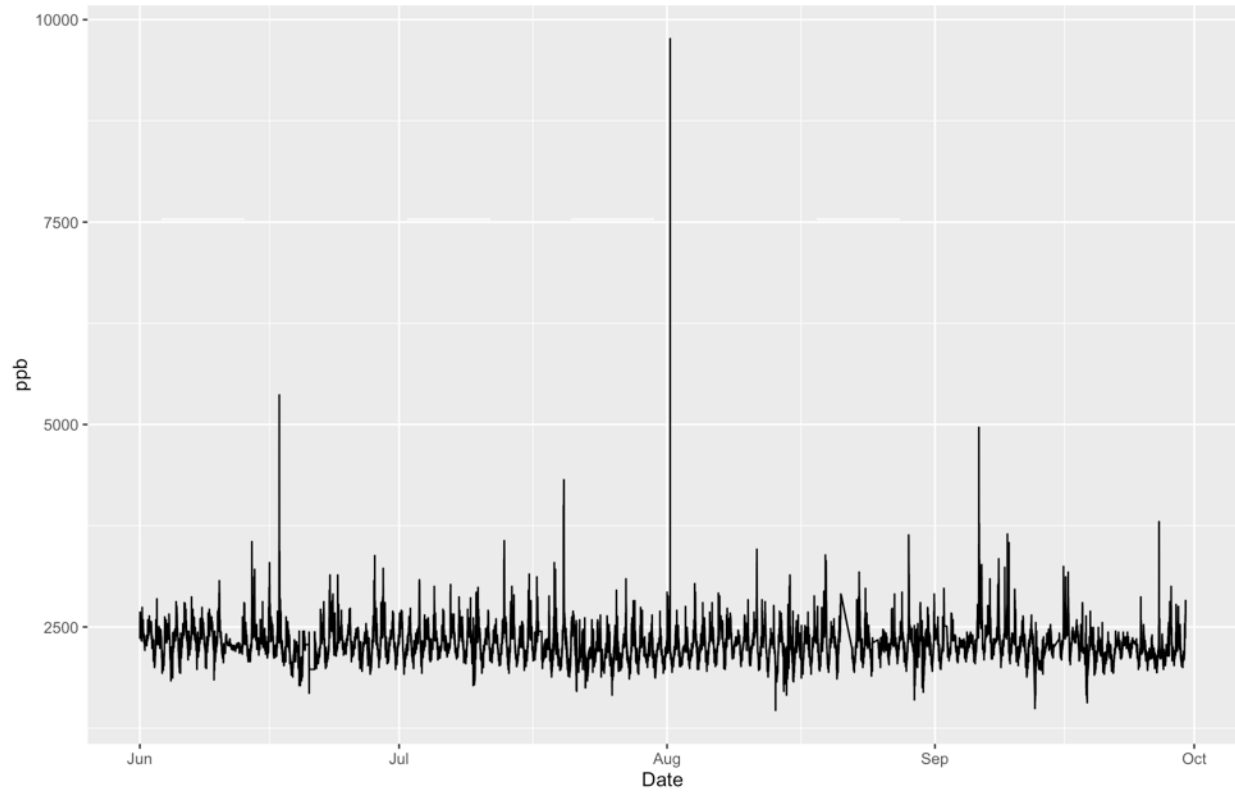


Figure 38. Time series of methane data collected at Fenceline monitoring location (June-September 2016)

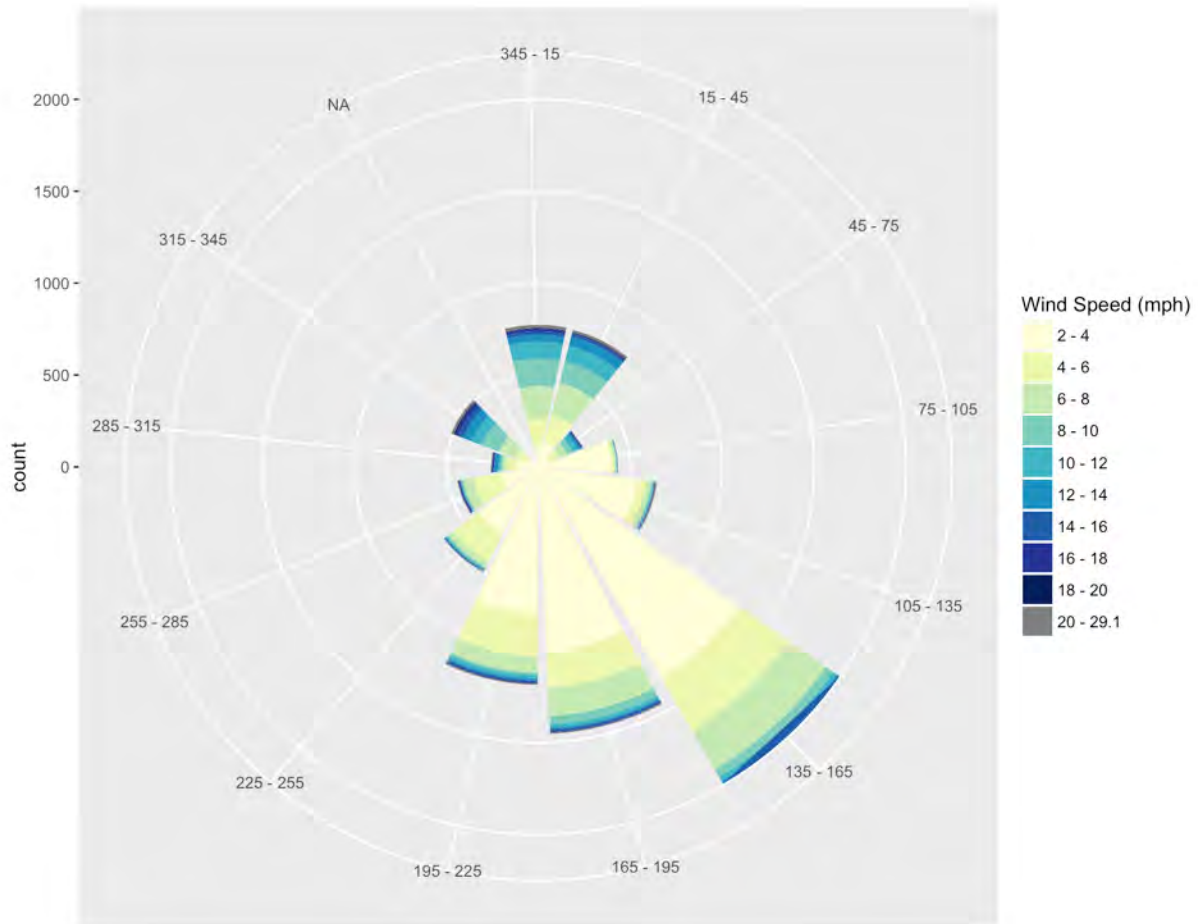


Figure 39. Wind-rose plot from Fenceline wind data June 1 – September 30, 2016

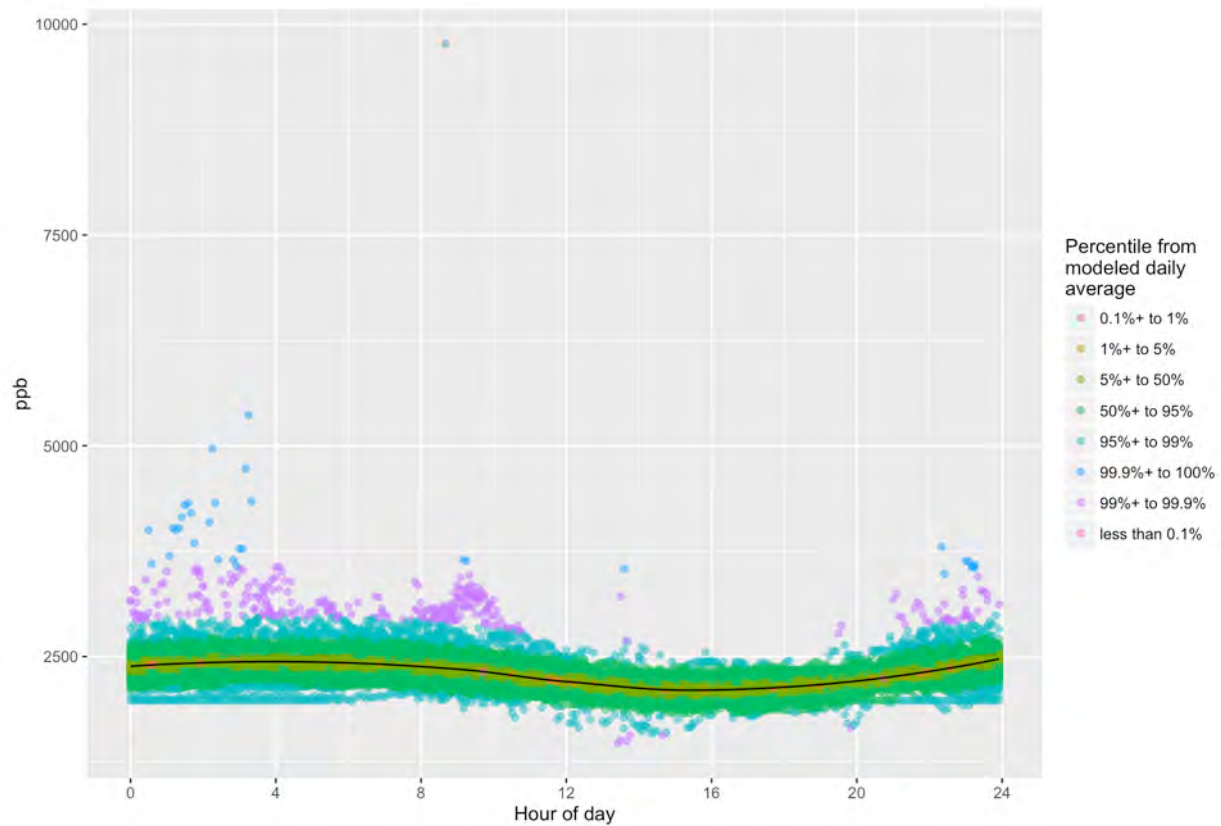


Figure 40. Plot of Fenceline methane data against time of day, color coded by estimated percentile (June 1 – September 30, 2016). Black line represents modeled average diurnal pattern used to estimate percentile deviation from the mean.

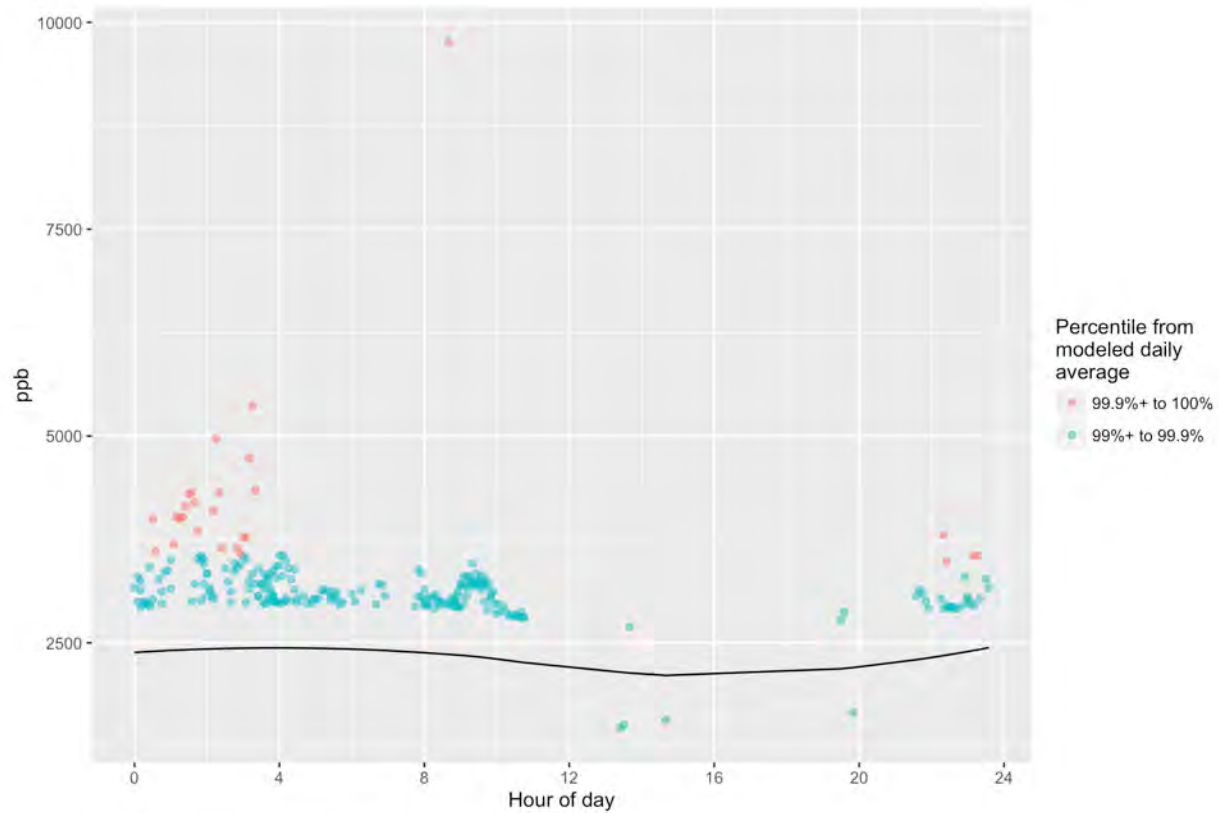


Figure 41. Plot of Fenceline outlier methane data (99%ile +) against time of day (June 1 – September 30, 2016). Black line represents modeled average diurnal pattern used to estimate percentile deviation from the mean.

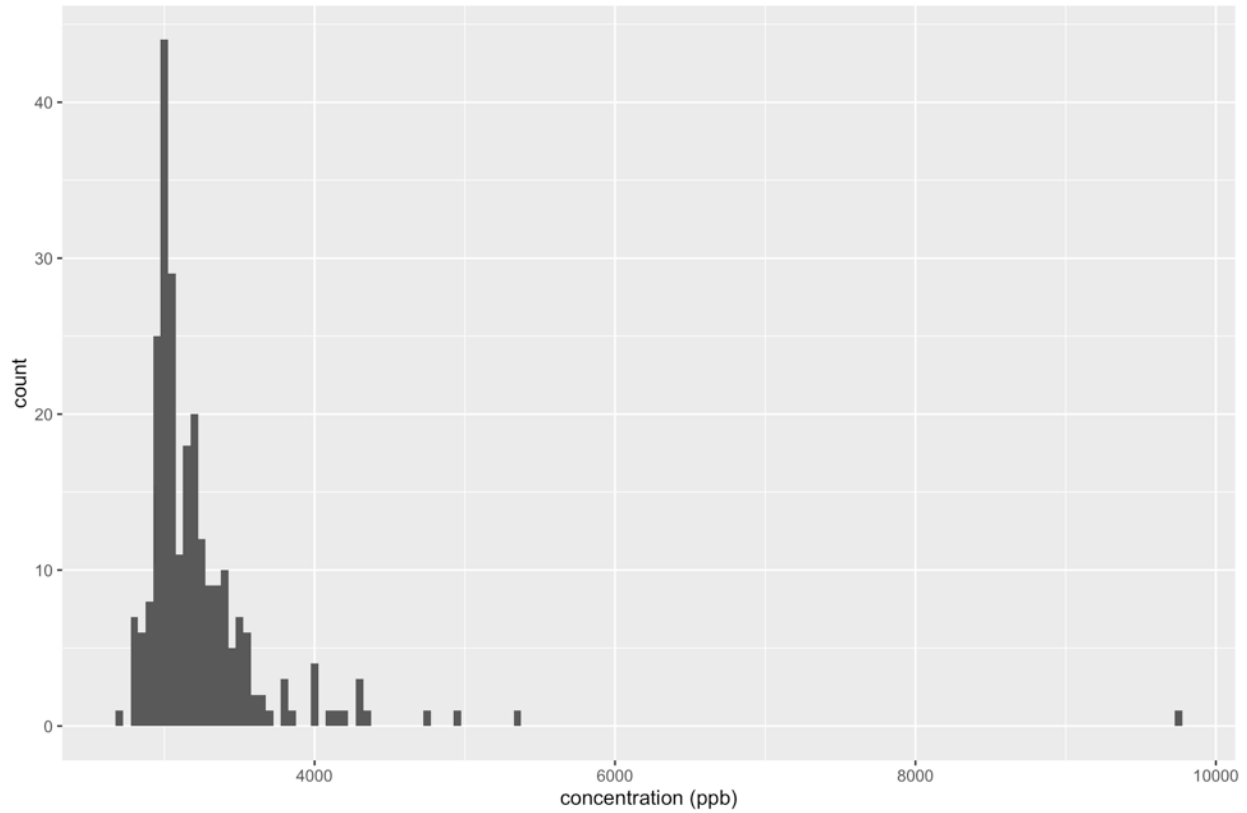


Figure 42. Concentration histogram of outliers

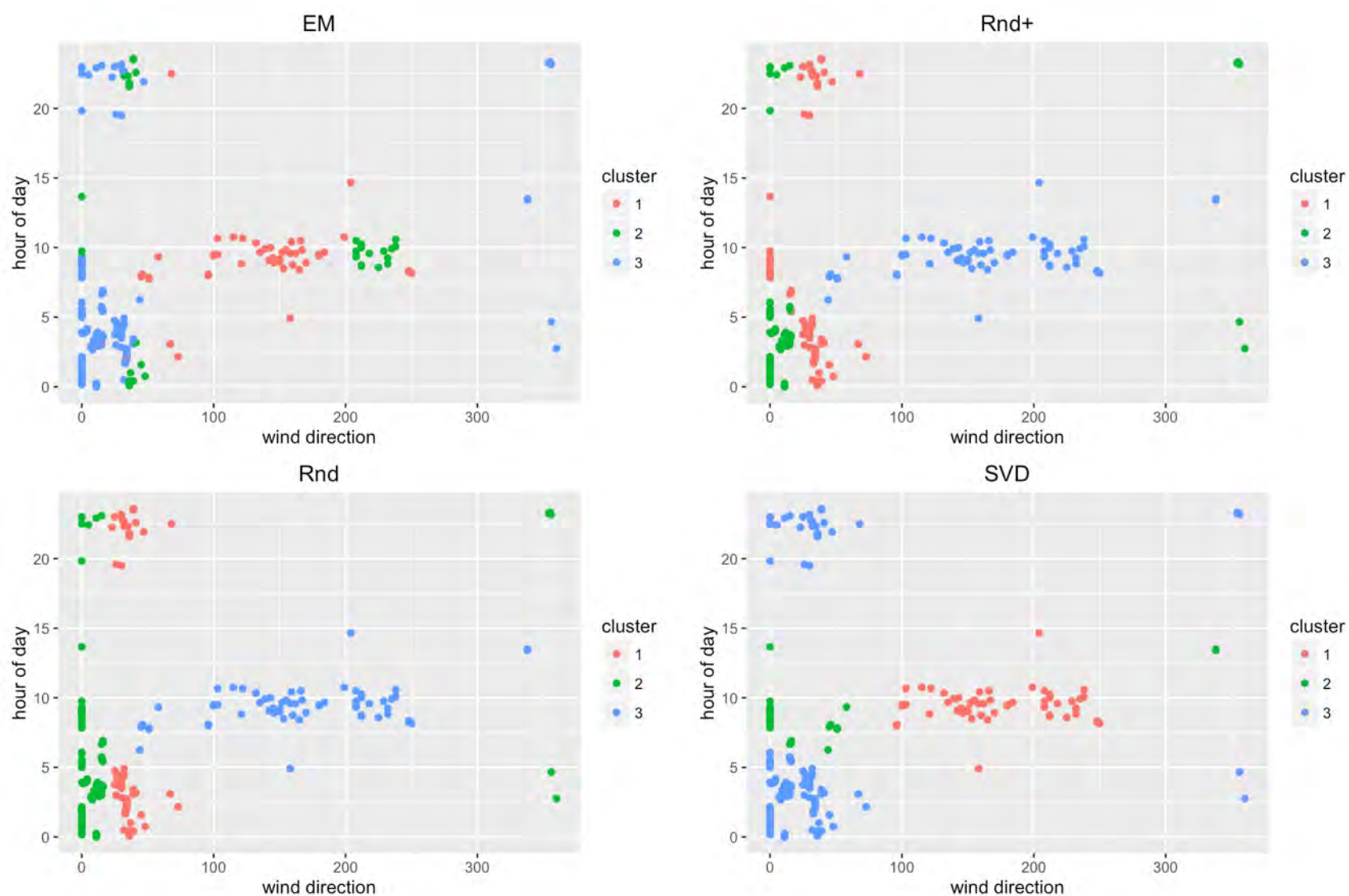


Figure 43. Results of EM Clustering on outlier methane data

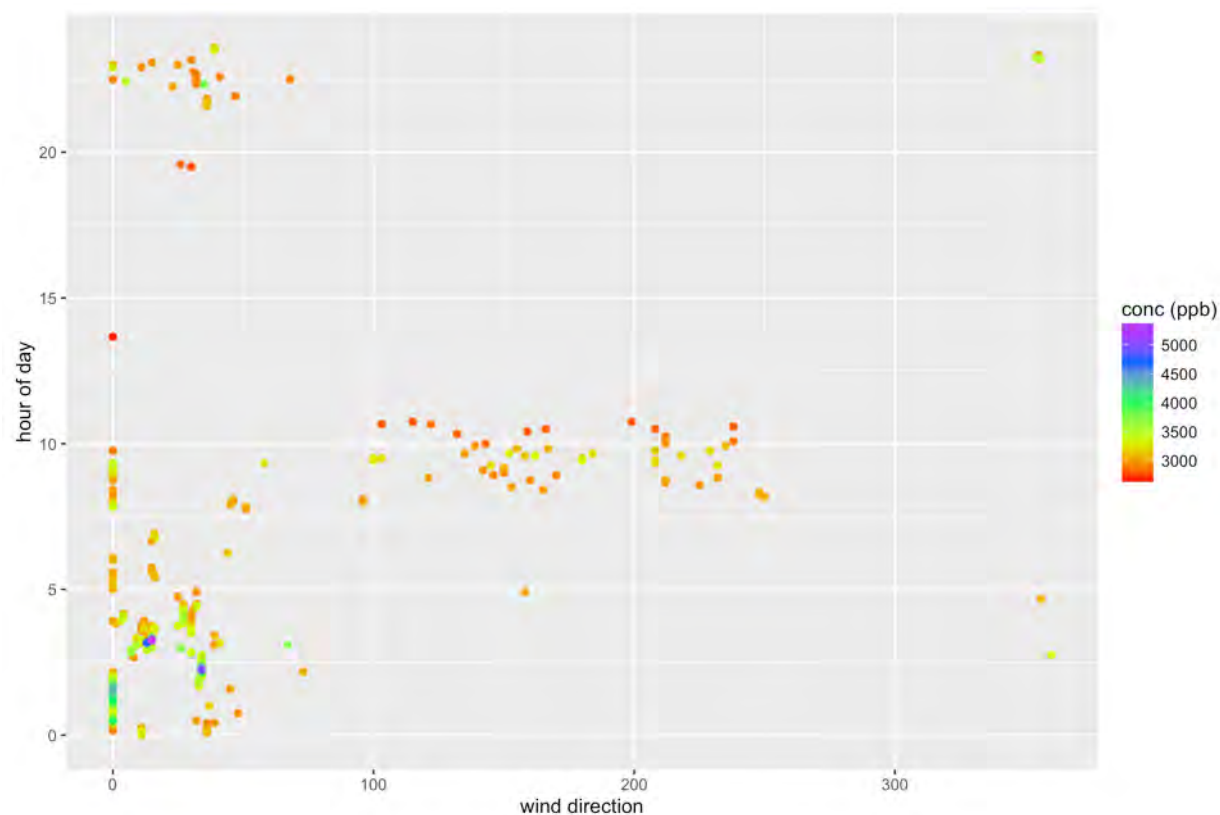


Figure 44. Outliers plotted by wind-direction and hour of day; mapped to concentration values.

## Appendix B. Supplemental Materials

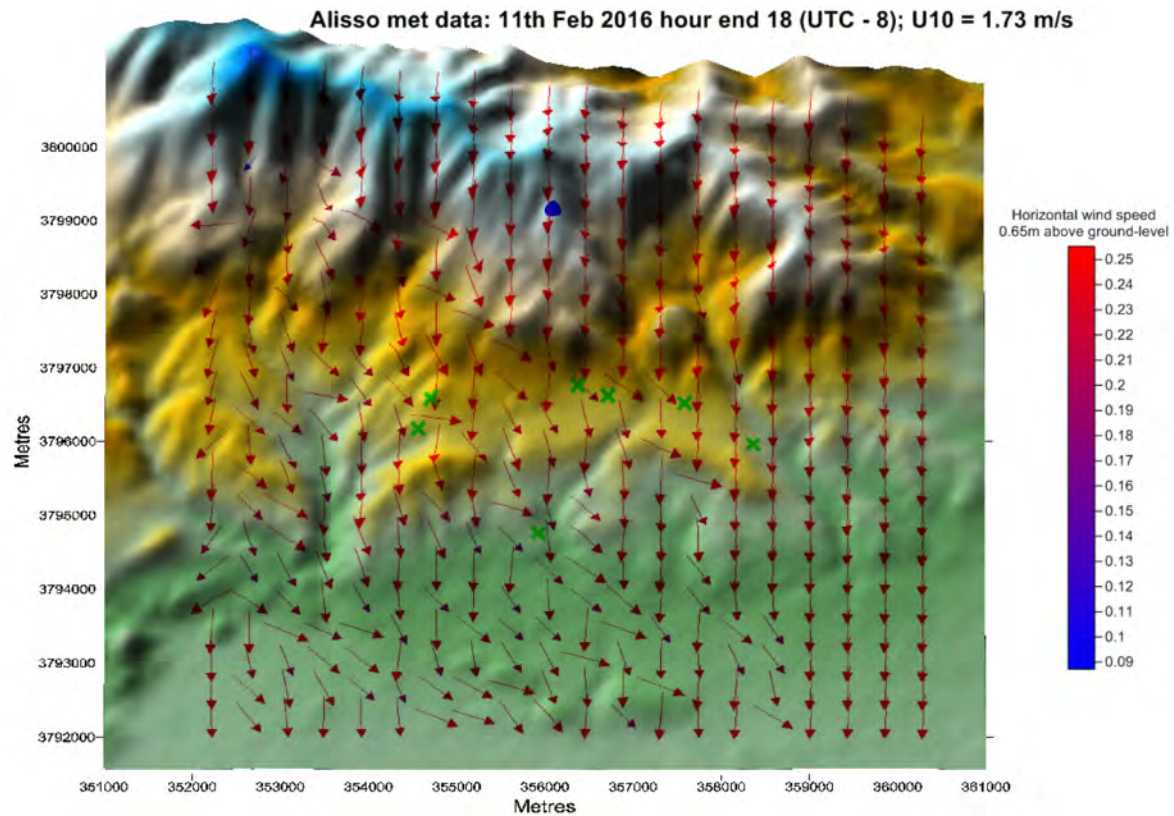


Figure B1. Single hour estimate of wind field flows produced during ADMS modeling in Aliso Canyon area.

